Universidade de Aveiro Departamento de Química
2008

Júlio César Longo

Preparation and Characterization of Functional Mortars.

Preparação e Caracterização de Argamassas Funcionais.

Universidade de Aveiro Departamento de Química
2008

Júlio César Longo

Preparation and Characterization of Functional Mortars.

Preparação e Caracterização de Argamassas Funcionais.

Dissertação apresentada à Universidade de Aveiro para cumprimento dos requisitos necessários à obtenção do grau de Mestre em Engenharia e Ciência dos Materiais, realizada sob a orientação científica da Dra. Ana Barros Timmons, Professora Auxiliar do Departamento de Química da Universidade de Aveiro e do, Professor Catedratico Karl Schulte do Departamento de Compositos da Universidade de Hamburgo (Polymer Composites Department)– Alemanha.

"Imagination is more important than knowledge, because knowledge is restricted"

Albert Einstein

o júri

presidente

Doutor Vitor Brás Sequeira Amaral
Professor associado da Universidade de Aveiro

Doutor José Luis Barroso de Aguiar
Professor associado da Universidade do Minho

Doutora Ana Margarida Madeira Viegas de Barros Timmons
Professora auxiliar da Universidade de Aveiro

Doutor Victor Ferreira
Professor auxiliar da Universidade de Aveiro

Doutor Karl Schulte
Professor catedratico da Teschnische Universität Hamburg-Harburg

Acknowledgments
Agradecimentos

The present report has been submitted in partial fulfillment of the requirements for the degree of Master of Science.
This thesis marks the culmination of my master's program at the TUHH and UA universities, and I owe thanks to a number of people for its successful completion.
I wish first to thank the mentor of this work, Professor Ana Barros Timmons, for her encouragement, advice, and constructive criticism. Sometimes she was my mother, sometimes my father, sometimes my boss but overall she was someone that I always could trust. I would like to express my gratitude to Professor Victor Ferreira for the interesting discussions and helpful suggestions during the course of this work.
I am grateful for the efforts of the Weber Cimenfix Saint Gobain represented by Eng. Luis Silva that was a partner in this project. Luis is a great example of a leader, always teaching me about the amazing world of cement mortars and all that surround it. I want to thanks too: Eng. Nuno Vieira for spend part of your time with our tests, Olga Barros, Eng. Pedro Miguel da Silva Sequeira, and Rui António da Silva Ribeiro for spending their time to teach me and help me at Weber's laboratory.
I want to thank also my colleague from the Revdimul project, Carla Lopes, for sharing her time with me.
I want to thank my EMMS' colleagues Mgbemere Henry Ekene, Lapamnouyphon Bussara and Sriyai Montira for providing me a background in this field and for my other colleagues for the time that we discuss study and help each other. They are: Eng. Jean Conceição Lorenzzi MSc, Eng. Marcos Ghislandi MSc and Eng. Fabio Bertocco. They are for me more than colleagues or friends; they are my family.
Also deserving of thanks are the members of the chemistry laboratory. I want to tank MSc. Fabiane Oliveira for our friendship and all the help that she gave me. Other important people are: Dr. Ricardo Pinto, Gil Gonçalves MSc, and Dr. Carlos Granadeiro that provided me pertinent and instructive comments.
In addition, I thank in special the EU and EMMS Program for the financial support that made this master program possible. Projecto Ideia - Revdimul (Desenvolvimento de revestimentos dinâmicos e multifuncionais is also acknowledged for some financial support during this work.

I thank my family, friends, master colleagues and all the administrative staff for their understanding and support during this master program. Their patience during those times that I was consumed with this work is greatly appreciated.
Finally, I would like to acknowledge all the people that helped me in some way and were not mentioned here.

Sincerely

palavras-chave

Argamassas funcionais, fotocromismo, nanotubos de carbono, cimento-cola, compósitos.

resumo

Pretendeu-se com o presente trabalho preparar e caracterizar dois tipos de argamassas funcionais: argamassas estruturais e argamassas decorativas obtidas a partir da incorporação de nanotubos de carbono e compostos fotocrómicos respectivamente.

Quanto às argamassas estruturais (SCM), utilizaram-se nanotubos de carbono (superficialmente modificados, ou não) como material de reforço. Neste contexto foram estudados: (i) os limites de concentração, (ii) diferentes métodos de dispersão e, (iii) estratégias preparativas que minimizam o problema da hidrofobicidade dos nanotubos quando adicionados à argamassa. Os materiais foram caracterizados por testes de solubilidade, resistência à compressão, resistência à tracção, resistência a flexão, módulo de elasticidade, capilaridade e microscopia electrónica de varrimento (SEM). Os resultados mais promissores foram obtidos após modificação superficial dos CNT, ou recorrendo à dispersão numa suspensão de TiO_2. As propriedades mecânicas das argamassas resultantes foram superiores à amostra padrão no mas as suas propriedades físicas foram mantidas similares. Tendo em conta a natureza aplicada deste projecto foi ainda feita uma breve avaliação económica sobre a utilização de CNT na indústria de argamassas. Essa avaliação apontou para a necessidade de novos estudos semelhantes ao aqui apresentado afim de minimizar as quantidades de CNTs a usar.

Em relação às argamassas decorativas (DCM) o uso de compostos fotocrómicos foi explorado. Nesse sentido, estudou-se o efeito da adição de: (i) haletos de prata, (ii) lentes fotocrómicas moídas, (iii) trióxido de tunsténio em pó e, (iv) compostos de trióxido de tungsténio e óxido de titânio. Os materiais foram caracterizados por colorimetria. Foram obtidos resultados positivos para algumas das amostras estudadas nomeadamente as que envolveram o uso de trióxido de tungsténio e compostos de trióxido de tungsténio e óxido de titânio, as quais após exposição à luz solar revelaram uma súbtil variação na tonalidade ou indício de alteração da cor. Por fim foi ainda estudado o efeito da adição de CNT a argamassas decorativas no sentido de avaliar a possibilidade de utilizar CNTs com vista a uma melhoria das propriedades mecânicas de DCM. Tal como no caso das SCM a modificação superficial dos CNT revelou-se necessária.

Deste modo obteve-se um conjunto de materiais com propriedades inovadoras, nomeadamente ópticas e estruturais, podendo dar origem a argamassas com possíveis mudanças de cor quando expostas à luz solar e argamassas com elevada resistência mecânica respectivamente.

keywords

Functional mortars, photochromism, carbon nanotubes, adhesive-cements, composites.

abstract

The present work aims at developing two different types of functional mortars: (a) Structural cement mortars (SCM) and (b) decorative mortars (DCM).
In the case of SCM, multiwalled carbon nanotubes (MWCNT) were used for reinforcement and the effect of different sample preparation variables on the mechanical properties of the ensuing composites was studied. This include: (i) concentration of MWCNT, (ii) surface modification of MWCNT and (iii) the dispersion method. The materials were characterised by solubility tests, bend resistance, strength resistance, and compressive strength, modulus of elasticity, capillarity and Scanning Electron Microscopy (SEM).

The most promising results were obtained using surface modified CNTs or dispersing them in a TiO_2 suspension. The ensuing cement mortars had improved properties when compared to the standard cement mortar and the physical properties were similar. In view of the applied research nature of this project a brief economical analysis was carried out. Such analysis points that further studies are required in order to minimise the amount of CNT to be used.

As regards DCM the addition of photochromic materials such as silver halides, tungsten oxide and of a tungsten oxide + titanium oxide composite was explored in order to yield a light responsive material which could change its colour or at least shade depending on the intensity of light. The materials obtained were characterised by colorimetry.
The results obtained for samples prepared using tungsten trioxide and composites of tungsten trioxide and titanium oxide were encouraging. Upon sunlight exposure either a subtle colour shade or colour change was observed.
Finally, addition of CNT to DCM was also studied aiming at increasing the mechanical properties of the decorative mortar. As in the case of SCM surface modification of CNT proved to be required.

Contents

List of Figures

List of Tables

List of Abbreviations

C–S–H	*Calcium silicate hydrate*
CNT	*Carbon nanotubes*
DCM	*Decorative mortars*
DRS	*Difference reflectance spectra*
FT-IR	*Fourier transform Infrared*
MWCNT	*Multi-walled carbon nanotubes*
MWCNT-oxy	*Multi-walled carbon nanotubes with surface oxidized*
MWCNT-TiO_2	*Multi-walled carbon nanotubes dispersed in a suspension of titanium oxide*
RS	*Reflectance spectrum*
SCM	*Structural cement mortars*
SWNT	*single-walled carbon nanotubes*
t	*Time (s)*
Tg	*Glass Transition Temperature (ºC)*

Chapter 1 – Introduction

In the past decades, functional mortars have been studied to explore properties different from those obtained by plain mortars. Not necessarily all the properties have to be improved in the same product, but a particular one to fit a desired purpose. In this way the functionality of the mortars has been studied in different ways such as: the mechanical, physical and aesthetical properties.

The use of mortars products is spreading more and more due its high mechanical properties required for example in:

- Bridges and roads in adverse environments and landscapes (sea, mountains and valleys),
- Water barriers for the production of electricity or storage,
- Skyrises buildings and,
- Unconventional constructions to environments like deep ocean and space.

Having the best performance among other reinforcement materials, it is expected that carbon nanotubes can remarkably enhance the performance of cement composites. Carbon nanotubes have excellent mechanical properties including high strength, low density and high stiffness. Therefore when used together with mortars, the nanotubes may act as reinforcement material distributing the stresses uniformly to the cement matrix [1]. However crucial problem arises when carbon nanotubes are used in advanced composites due to the low interfacial bonding between them and the cement matrix composites [2]. The high hydrophobicity of CNT results in bad dispersion where water is involved resulting in a product with aggregates of nanotubes and low mechanical properties (against the thought).

In this work was studied the influence of the addition of the CNT with multi-walls, known as multi-walled carbon nanotubes (MWCNT), in the mechanical and physical properties of the structural cement mortar (SCM) was studied. For this reason, the use of MWCNT was investigated using (i) different concentrations, (ii) different methods of dispersions and, (iii) surface treatments in order to obtain a composite material with enhanced properties.

The main composition of the structural cement mortar used can be on Fig. 1.1.

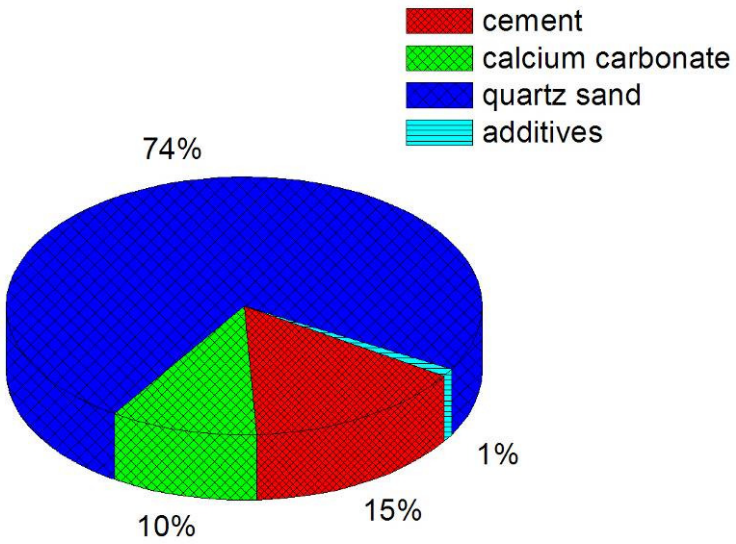

Fig. 1.1 – Main composition of SCM[1].

Different from the SCM, decorative mortars (DCM) involves using mortars in applications that are not strictly related to its mechanical properties. This type of mortars is used where the aesthetical properties are the utmost important factor. An infinity examples of such products can be found but most of products just explore the final form or the use of common dyes. For this reason the objective of this work is to study new functionalities for DCM. New approaches for functional uses such as the ability that a mortar may have to change its colour or shade according to the intensity of the sunlight giving a new style for the environment is considered interesting for the market. Moreover other applications with military purposes may also be envisaged such as the covering of bases with a product that can auto-camouflage during the day or sunlight exposure.

In this work the effect of adding photochromic materials was studied aiming at the change of the colour or shade of the decorative mortar. However, there are other possible functionalities that mortars can exhibit such as self-cleaning materials that can keep it free from the pollutants, non-bio-degradable materials and toxic residual materials in the gas, liquid and solid phase keeping its surface clean against dust and dirt. In this case, the process is governed by photocatalytic reactions involving TiO_2, a common pigment of DCM [4 to 6]. Although some of the DCM's samples studied here contained TiO_2 in appropriate concentrations and type, this kind of functionality was not studied due to the difficulties involved in the necessary measurements and time constraints.

[1] The composition of the SCM used in this work is similar to the composition of a normal cement mortar used by the company.

Decorative mortar is a semi-finished product used to cover walls. The difference between this and a structural one lies on the fact that in the composition of the former all the components (water, sand, pigment, etc …) were added in a previous step (see Fig. 1.3). This product is sold in gallons with a desired colour and after the application; the wall will have a smooth and coloured surface without the need of paint use, there is no need to water addition. In this work, photochromic properties were studied to obtain a product that could change the colour or colour shade according to the sunlight.

In this work the use of silver halides (powder and milled photogrey lenses), tungsten trioxide and a mixture of WO_3-TiO_2 was studied.

The main composition of the decorative mortar used can be seen below.

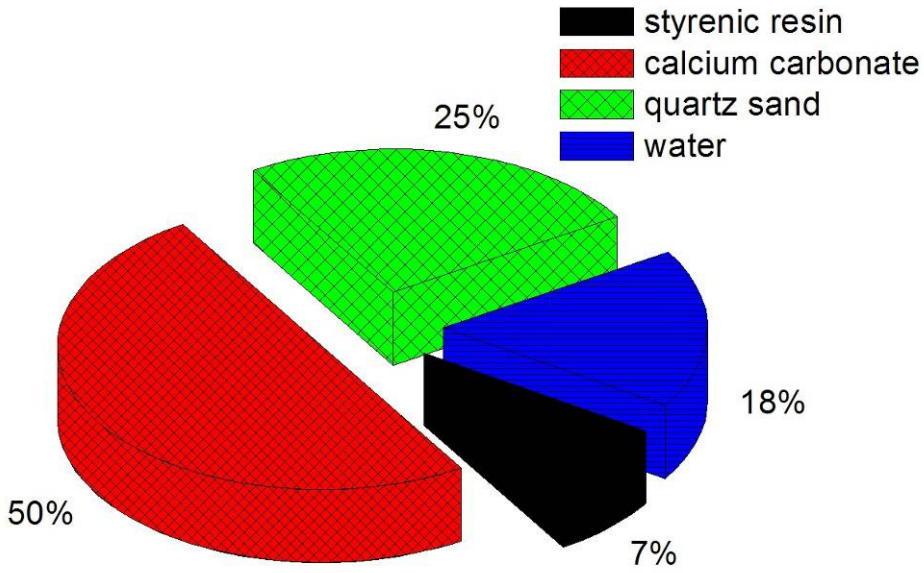

Fig. 1.2 - Main composition of DCM.

Specific work reported in the literature on SCM, carbon nanotubes, DCM and photochromism will be discussed in following chapters.

Chapter 2 – Structural Cement Mortars

Carbon nanotubes (CNT) are one of the most important areas of research in nanotechnology. Their distinctive properties and potential for valuable commercial applications ranging from electronics to chemical process control have meant that huge efforts have been undertaken on the investigation of nanotubes in the last five years. Despite this high level of research activity, very little attention has been paid to potential applications in the construction industry [7]. This work aims to fill the gap between CNT research and construction materials area.

In this chapter, attempts to improve the mechanical properties of cement pastes are by adding CNT are studied aiming at producing a new and higher-performance composite material due to the high specific strength and low density of MWCNT while its physical properties are kept similar to a standard product produced today by the company. In this way the reinforced product can be used as a fix point of masonry when the original mortar has washed away, or even in new constructions without any abrupt change on the project.

To reach an efficient cement-based composite with nanotubes, we have studied: *(i)* the effect of CNT concentration, *(ii)* different conventional dispersions methods, *(iii)* a novel dispersion method of CNT using a suspension of titanium oxide and *(iii)* the effect of surface modification of CNT.

The physical properties used to assess the resulting mortars were: (i) workability (water content), (ii) density, (iii) mass variation, (iv) retraction changes (dimensional changes) and, (iv) capillarity. The mechanical properties set to be tested in this work were: (i) bend resistance, (ii) compressive strength and, (iii) modulus of elasticity.

2.1 Literature Review

2.1.1 Structural cement mortars (SCM)

In the lasts years much effort has been done regarding technical innovations in the construction industry and improved SCM have been attracting particular attention.

Mortar and concrete and other cement-based materials are the most important construction materials. These materials consist of a mixture of fine and coarse aggregates held together by an hydrated cement binder. SCM consists of a type of mortar with enhanced properties which can be used in a wide range of construction applications such as beams, pillars and foundations, either alone or with hand-tied rebars.

Pre- or post- tensioning of concrete or SCM beams and other structures is also used to provide improved mechanical performance of structures such as tanks, beams, nuclear reactor

containment facilities and water pipes. New frontiers are now being explored such as skyrise buildings, possible space and ocean constructions and heavy bridges [7, 9]. Therefore, SCM have to be sufficiently strong to support stresses from the building structure and other situation for example domestic accidents (gas explosions). Moreover, SCM have to resist the environmental aggressions (wind, pollution) and natural accidents (seismic activity) [9].

Conventional mortar mixes are based on Portland cement, lime or plasticizer and sand, and are graded according to compressive strength. The shear strength of mortar walls, for example has to be considered during the project and design of a building structure. The cement mortar structure has to be able to absorb and release some movements coming from the masonry as well as oscillations due to thermal effects that can otherwise result in creep without cracking. The modulus of elasticity is the property behind this occurrence. As it is known, the stronger the mortar, the less it is able to adapt to changes in form. Hence, a being the balance between the strength and the elasticity of the material is recommended. The SCM must thus be able to allow any movement between the wall and the main structure. Movement takes place in all masonry materials as a result of applied stress, moisture, temperature changes and chemical reactions [9]. These effects together with the foundation movements can result in cracking. Therefore, a structure made of SCM should present an average to high modulus of elasticity.

Furthermore, movements on the building structure as the deflection of supporting beams may induce tensile stresses in the supported wall causing cracking or failure of the structure. Bend resistance characterizes the behaviour of a structural element subjected to an external load applied perpendicular to the axis of the element.

On the other hand, bending produces reactive forces inside a beam[2] as the beam attempts to accommodate the flexural load; the material at the top of the beam is being compressed while the material at the bottom is being stretched. Moreover, there are three notable internal forces caused by lateral loads that have to be considered: shear parallel to the lateral loading, compression along the top of the beam, and tension along the bottom of the beam. If the considerations made above somehow fail, non-structural walls beneath beams or slabs (which are not intended to support them) may become loaded as a result of the deflection of these elements resulting in damage to the structure [9].

For conventional uses steel is the mostly used reinforcement material. Steel is the strongest commonly-available fibre, and can be provided in different shapes sizes and lengths while for the high-performance materials, the use of fibrous materials such as carbon filaments and conventional carbon fibres as fillers in cement matrix composites are been extensively tried [2].

[2] A beam is a structural element that carries load primarily in bending (flexure). Beams generally carry vertical gravitational forces but can also be used to carry horizontal loads (i.e., loads due to an earthquake or wind). The loads carried by a beam are transferred to columns, walls, or girders, which then transfer the force to adjacent structural compression members [129].

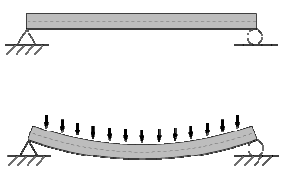

Glass fibres are inexpensive and corrosion-proof, but not as ductile as steel. Different approaches have been done using spun basalt fibres that are stronger and less expensive than glass, but do not resist the alkalinity of Portland cement. [2]. High-performance materials as graphite reinforced plastic fibres are an alternative to be used in SCM which are nearly as strong as steel, lighter-weight and corrosion-proof [2].

Improved mechanical performance is one of the benefits expected to be obtained through the application of nanotechnology to cement systems. One approach to developing better performance is the addition of nanoscale reinforcing materials, which might range from small spheres that would only act to interrupt cracking to nano-fibres or rods, which would act in a manner similar to larger scale reinforcing systems [8].

According to the Li et al. (2004, p. 1239), carbon nanotubes have a very high strength, 100 times more than that of steel whilst their specific gravity is only one sixth that of the latter. Moreover, carbon nanotubes have an elastic strain capacity of 12% i.e. 60 times higher than that of steel [2]. Furthermore, the resistance of carbon nanotubes will increase 100 times when strain changes from 0.0% to 3.2% [2].

Carbon nanotubes have the best properties when compared to more traditional fibres. As a result it is expected that they can increase the performance of cement composites [7]. First, they have significantly greater strengths than other fibres, which should improve the overall mechanical behaviour [7]. Next, CNT have much higher aspect ratios, requiring significantly higher energies for crack propagation around a tube as compared to across it for a lower aspect ratio fibre [7]. Thirdly, the smaller diameters of CNT means that they can be more widely distributed in the cement matrix with reduced fibre spacing and that their interaction with the matrix may be different from that of the larger fibres [7]. CNT, with their diameters being close in size to the thickness of the calcium silicate hydrate (C-S-H) layers hydrated cement, could show very different behaviour, including different bonding mechanisms. Finally, carbon nanotubes can be functionalized to chemically react with cement components, providing routes for other forms of interaction and control of cement system properties [7].

The most usual problems that arise in the preparation of high quality mortar composites involving CNT are: the formation of aggregates that can act as stress concentrators resulting in cracks and the lack of interfacial bonding to cement matrix, both due their hydrophobicity [2, 24, 25, 110]. To avoid this problem some surface treatments can be done. To reduce the hydrophobicity of MWCNT, oxidation using a H_2SO_4 and HNO_3 solution, may be used, leading to the formation of carboxyl acid groups on their surfaces. The presence of carboxylic acid groups enhances the reinforcement efficiency due to a series of chemical reactions along the interface [11-16]. However, these procedures are generally rather expensive and tend to break the CNT. Alternatively, the use of dispersing solutions or dispersions can also be used [130].

2.1.2 Carbon nanotubes (CNT)

Carbon nanotubes (CNT) are allotropes of carbon. Carbon nanotubes are members of the fullerene structural family, which also includes buckyballs. Whereas buckyballs are spherical in shape, a nanotube is cylindrical, with at least one end typically capped with a hemisphere of the buckyball structure. Their name is derived from their size, since the diameter of a nanotube is in the order of a few nanometres (approximately 1/50,000th of the width of a human hair), while they can be up to several millimetres in length. Carbon nanotubes are categorized as single-walled nanotubes (SWCNT), double-walled nanotubes (DWCNT) and multi-walled nanotubes (MWCNT) [7, 15].

The CNT are seamless tubes of graphite sheets with nano-sized diameter and have an ideal structure formed by carbon atoms with one dimension [20] (See Fig. 2.1). It is their shape that makes the nanometre-thick tubes so exceptional and versatile. With a thickness of between one and 50 nanometres, they look like tiny straws, but are much longer. A carbon nanotube with the thickness of a drinking straw would measure around 250 meters in length [19].

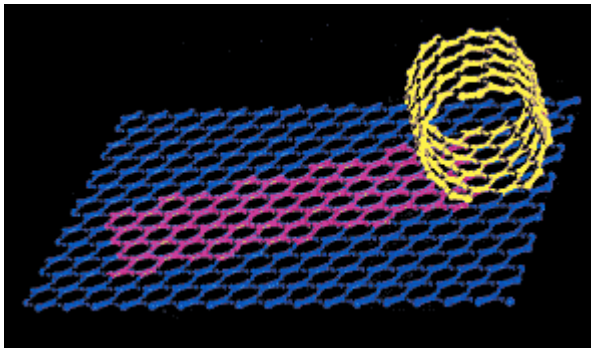

Fig. 2.1 – Formation of a SWCNT from a graphite sheet [118].

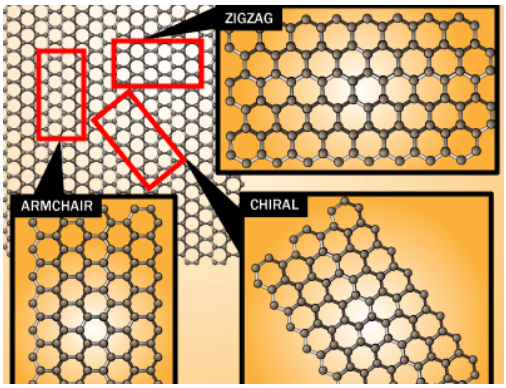

Fig. 2.2 – Chiral directions on the carbon sheet [132].

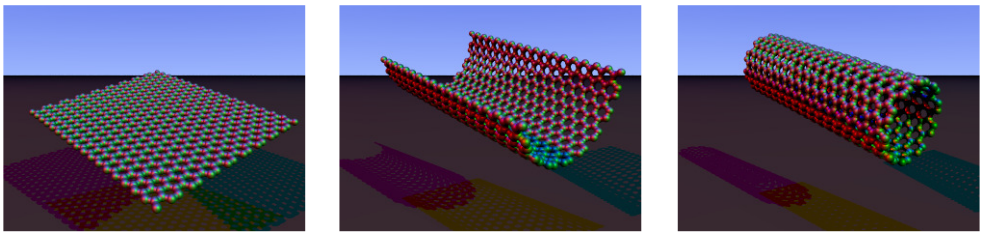

a) Carbon sheet b) Rolling process c) SWCNT

Fig. 2.3 – Process of SWCNT's formation [133].

Three different approaches have been taken so far to produce CNT: The first method discovered uses an electric arc-discharge, where a high voltage electrical current is passed through the air (or an inert or reactive gas) into a carbon electrode [7, 20]. The other methods are laser ablation, using a high intensity laser beam directed at a carbon target, and chemical vapour deposition, which uses a carbon based gas such as methane at high temperatures and sometimes pressures. In all three cases free carbon atoms are obtained and given the energy necessary to form carbon nanotubes rather than graphite or amorphous carbon [7, 20].

Although MWCNT can be produced without the presence of a catalyst, SWCNT generally require the presence of a transition metal catalyst to be formed. The catalyst is typically present in the form of nanoparticles. Individual carbon atoms are believed to enter the particle and diffuse through it to its surface, where they join to the growing tube or tubes. Depending on the shape and size of the particle and the surrounding environmental conditions, SWCNT or MWCNT will form. The final length of CNT also depends on growth conditions [7, 20].

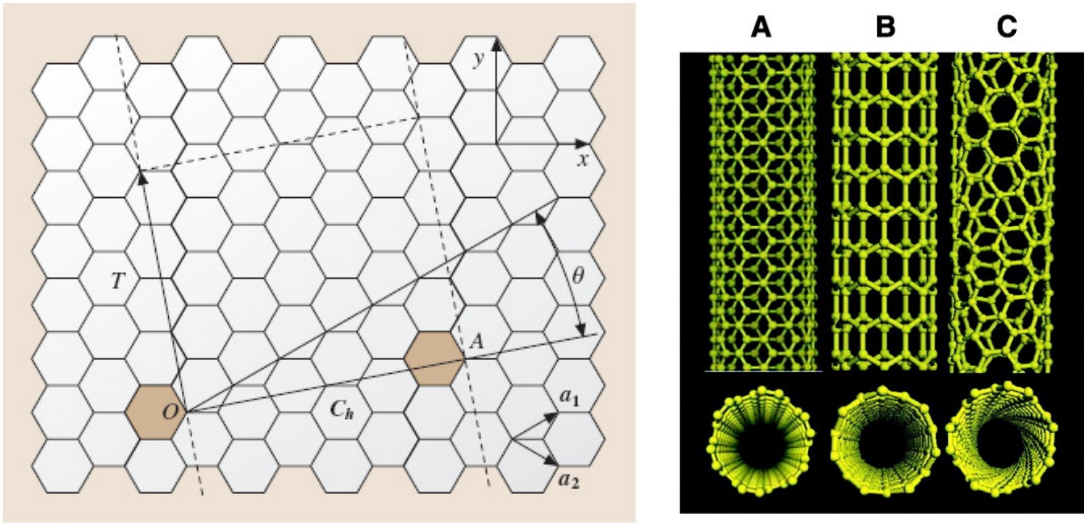

Fig. 2.4– Chiral vector of SWCNT [120] (left). At right side, examples of SWCNT: a) armchair b) zigzag and c) chiral [119].

2.1.2.1 Multiwall carbon nanotubes (MWCNT)

Multi-walled carbon nanotubes (MWCNT) consist of multiple layers of graphite rolled on themselves to form a tube shape. The easiest MWCNT to imagine is the concentric type (c-MWCNT), in which SWCNT with regularly increasing diameters are coaxially arranged (See Figs. 2.5 and 2.6). There are two models which can be used to describe the structures of multi-walled nanotubes. In the Russian Doll model, sheets of graphite are arranged in concentric cylinders, e.g. a single-walled carbon nanotube (SWCNT) within a larger single-walled carbon nanotube (See Fig. 2.3). In the Parchment model, a single sheet of graphite is rolled in around

itself, resembling a scroll of parchment or a rolled up newspaper. The interlayer distance in multi-walled nanotubes is close to the distance between graphene layers in graphite, approximately 3.3 Å (330 pm) [18].

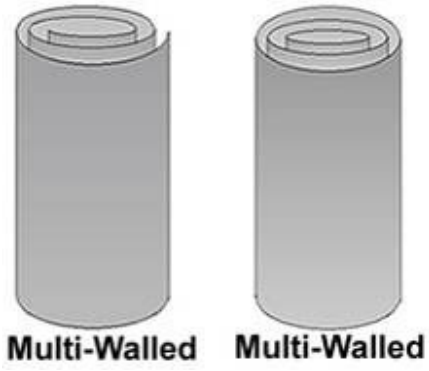

Fig. 2.5 – Types of MWCNT. Parchment model (left) and Russian Doll (right) [21].

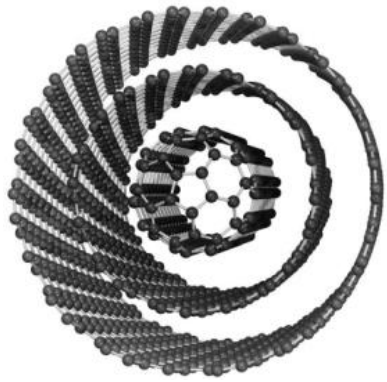

Fig. 2.6 – 3D image of MWCNT [22].

MWCNT are generally formed either by the electric arc technique (without the need for a catalyst), by catalyst-enhanced thermal cracking of gaseous hydrocarbons, or by CO disproportionation. There can be any number of walls (or coaxial tubes), from two upwards [20]. According to Prato et al. (2003, p. 4001) the production methods of CNT used currently produce impurities consisting of: *(i)* carbon-coated metal catalysts *(ii)* carbon nanoparticles/amorphous carbon and, *(iii)* structural defects, such as dangling bonds-Examples of techniques that can be used for purifying CNT include: *(i)* oxidation of contaminants, *(ii)* flocculation and selective sedimentation, *(iii)* filtration, *(iv)* selective interaction with organic polymers, and *(vi)* microwave irradiation [11].

The properties of the MWCNT depend on the perfection and the orientation of the graphenes in the tube (See Fig. 2.2). The texture depends on the processing conditions and can only be completely altered upon a severe degradation treatment (such as oxidation) [20]. As with other nanofillers, due the large surface area of this type of materials surface modification of CNT is a widely used strategy to enhance compatibility with other materials. Shaffer and Koziol (2002, p. 2074) reported on the effect of surface modification of CNT and according to them the surface treatment of CNT with strong acids introduces oxygen-containing surface groups which lead to electrostatic stabilisation in polar solvents increasing the mechanical properties [14]. Other authors [2, 24, 25, 110] believe that treated carbon nanotubes could act as bridges across cracks and voids to form a reinforcing mechanism and arrest cracking in cement matrix improving the flexural strength, compressive strength, and failure strain of cement matrix composites.

2.2 Experimental

A general cement mortar formulation (See 5.2.1) was established by the company. For each case the present study involved the following steps: (*i*) dispersion of MWCNT (described in 5.2.3), (*ii*) preparation of cement mortar paste (also called mass), (*iii*) mixture of MWCNT with the mass, (*iv*) preparation of specimens, both *ii, iii and iv* are described in 5.2.4, (*v*) 28 days of cure of the specimens in a cure room and (*vi*) physical and mechanical tests.

Initially the maximum limit of CNT to add to cement mortar was studied. Once determined the best amount, the type of dispersion method of the CNT was studied. Next MWCNT were dispersed in a suspension of titanium oxide prior to additions it to the cement paste and the resulting mortar was compared with the standard cement product. Finally MWCNT were oxidized to change their surface characteristics and then they were added to the cement mortar formulation to compare with the standard product.

The properties measured in this work were: (*i)* limit of water content to keep the same workability as the standard product, (*ii*) density, (*iii*) mass variation, (*iv*) retraction, (*v*) bend resistance, (*vi*) compressive resistance, (*vii*) modulus of elasticity and (*viii*) capillarity. The results were compared to a standard product (0% of CNT).

2.2.1 Estimation of the limit of carbon nanotubes to be used in SCM

Different amounts of MWCNT were added to the cement mortar formulation in order to determine the concentration necessary to obtain the best mechanical properties and the maximum limit of addition. The concentrations of MWCNT (by weight of cement powder) added were:

(i) 0% CNT (standard, STD),
(ii) 0,02% CNT (A02)
(iii) 0.10 % CNT (A10),
(iv) 0,25% CNT (A25),
(v) 0,50% CNT (A50),
(vi) 0,75% CNT (A75).

In all cases the nanotubes were first dispersed in an aqueous solution of Triton X405.

2.2.2 Comparison between different conventional dispersion methods of MWCNT in SCM.

The same concentration of MWCNT (0,10% by weight of cement mortar) was added to the cement mortar for each type of dispersion method test. The conditions of dispersions were:

(i) Dry mixture (Dd): the cement powder and the CNT were added in a dry mixture machine (see Fig. 5.8), and mixed for 10 minutes;
(ii) Dispersion in water (Dwt): the CNT were dispersed as described in 5.2.3 but in this case the dispersant was not used and the magnetic stirring was kept for 25 minutes;
(iii) Dispersion in water with Triton X405 dispersant (Dt).
(iv) Dispersion in water with Triton X405 dispersant and poly(acrylic acid) (Da): the CNT were dispersed as described in 5.2.3 but in this case the CNT were stirred for 10 minutes. Five minutes upon the addition of the dispersant to the suspension the poly(acrylic acid) was added to form a gel. The total time of the dispersion spent was 25 minutes;

2.2.3 Addition of MWCNT dispersed in a suspension of titanium oxide (MWCNT-TiO_2) to SCM

In this work MWCNT were dispersed in a suspension of titanium oxide in deionised water. Three samples of SCM were prepared: one standard (0% of CNT) and two using MWCNT-TiO_2. The difference between the MWCNT-TiO_2 samples regards the time used for dispersing the CNT in the TiO_2 aqueous suspension. Moreover, there was a slight difference in the amount of water used. The sample named Ti - 10 H was magnetically stirred for 24 hours and 20,5 w% of water were added. The sample named Ti - 10 was magnetically stirred for 10 hours and 19 w% of water was added.

2.2.4 Addition of MWCNT oxidized (MWCNT-oxy) to SCM

In this work MWCNT were oxidized aiming at increasing their hydrophilicity. The oxidation procedure of the MWCNT is described in 5.3.1.

MWCNT-oxy were added to a beaker containing 100 ml of water. The mixture was stirred for 24 h in order to promote a good dispersion. No presence of bundles or decanted CNT was observed after the dispersion of CNT due to the resulting affinity to water (Fig. 2.29). 0,10% MWCNT was added to cement mortar formulation.

2.3 Results and discussion

2.3.1 Basic approaches to prepare SCM containing MWCNT

In the first part of this section the use of pristine MWCNT and of simple conventional dispersion methods was studied. First the morphology of MWCNT was studied by SEM and then they were added to the SCM (SCM-MWCNT) in different concentrations using conventional methods of dispersion. The morphology of the resulting SCM was also assessed by SEM and physical and mechanical tests were carried out.

2.3.1.1 a) Morphology characterisation of carbon nanotubes

The morphology of CNT was studied by Scanning Electron Microscopy (SEM). Fig. 2.7 to 2.9 show images of neat MWCNT with diameters between 40 and 50 nm and length of tens of micra (μm), resulting in an aspect ratio up to 100–1000.

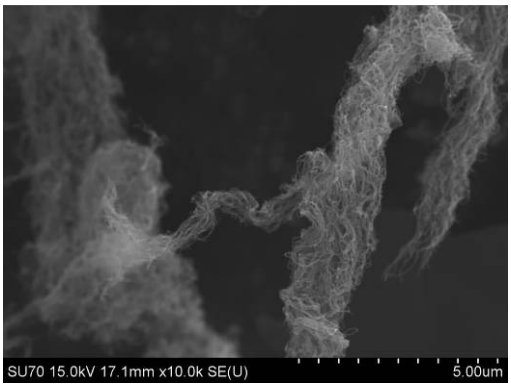

Fig. 2.7 - SEM image of MWCNT at 10.000x.

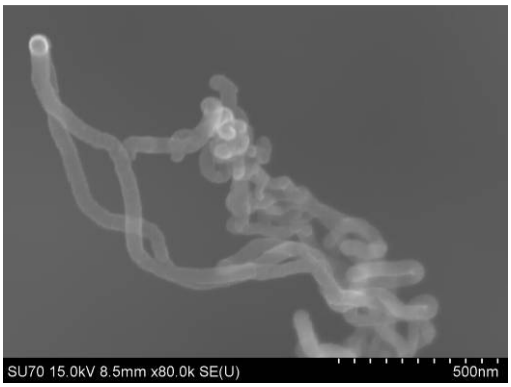

Fig. 2.8 - SEM image of MWCNT at 80.000x.

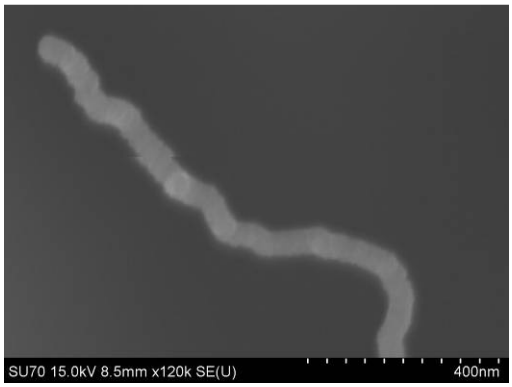

Fig. 2.9 - SEM image of MWCNT at 120.000 x. Diameter size between 40 and 50 nm and length around tens of micra.

2.3.1.1 b) Morphology characterization of SCM-MWCNT

Fig. 2.10 shows a typical SEM image of the fracture surface of a standard SCM (left side) and SCM containing CNT (right side). Using a low magnification both samples seem to have similar morphologies but the standard sample seems to have a smoother and continuous surface. When the magnification was increased (Fig. 2.11) the sample containing CNT clearly showed the presence of agglomerates. Fig. 2.12 shows a close-up view on an agglomerate spot of CNT where it is possible to see the weak interaction between the cement grains and the nanotubes. In this case the CNT seem to form a three-dimensional meshwork. In composite materials this kind of aggregates can act as inclusions reducing the mechanical properties. In all the samples containing CNT the presence of agglomerates of nanotubes was observed by naked eye. Fig. 2.13 shows specimens of SCM with CNT after the bend test.

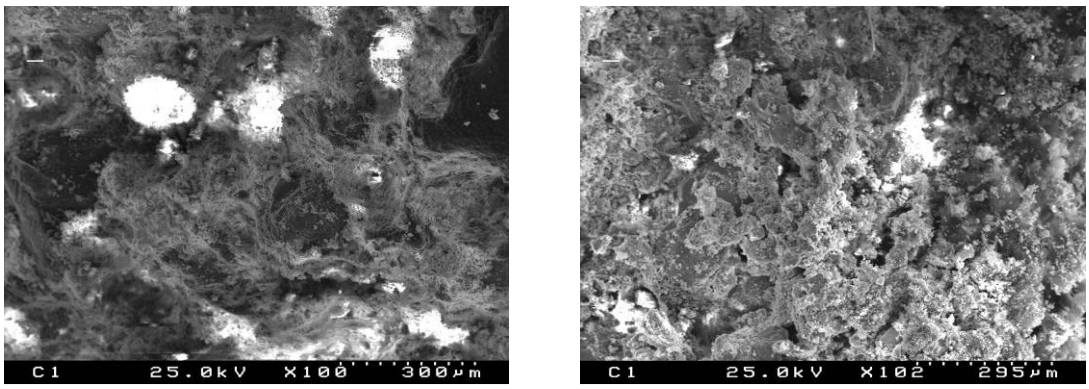

Fig. 2.10 – Images of the fractured surface by SEM of SCM standard (left side) and SCM with 0,75% of CNT (right side), both at 100x.

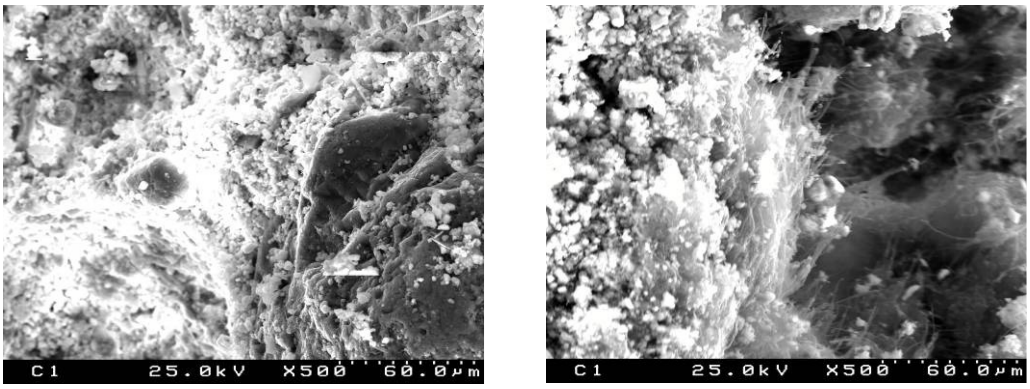

Fig. 2.11 - Images of the fractured surface by SEM of SCM standard (left side) and SCM with 0,75% of CNT (right side), both at 500 times. The latter shows the poor adhesion between the agglomerates of CNT and cement grains.

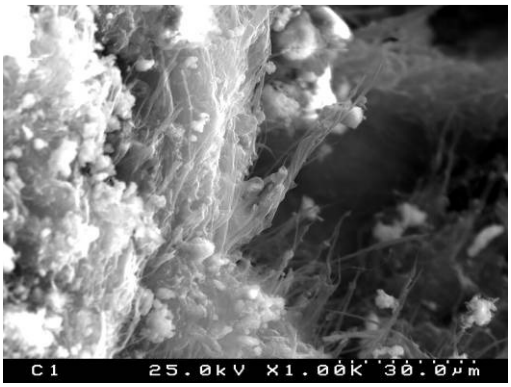

Fig. 2.12– High magnification SEM image at 1000 times. The SCM with 0,75% of CNT showing agglomerates of nanotubes.

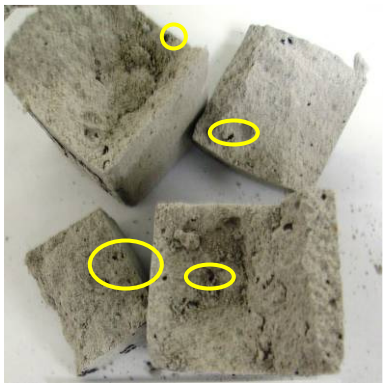

Fig. 2.13 – Image of specimens of SCM with CNT after mechanical tests showing the presence of aggregates of nanotubes that can be seen by naked eye.

2.3.1.1 c) Physical and mechanical properties of SCM as a function of CNT concentration.

Table 2.1 shows the results of the mechanical properties after 28 days curing. It is observed that increasing the concentration of carbon nanotubes, properties like density, mass variation and capillarity increased too. In contrast, the modulus of elasticity decreased. The values of all the properties increased when the concentration of CNT was 0,10% suggesting that this is the best concentration for the present formulation of cement mortar. Concentrations higher than 0,10% of CNT showed inferior values for the mechanical properties when compared to the standard (0% of CNT) product.

Table 2.1 – Physical and mechanical properties of SCM using different concentrations of CNT.

Sample	Water Ratio	Density	Retraction	Mass variation	Bend resistance	Compressive strength	Modulus of elasticity	Capillarity
0% (STD) [CNT%]*	**18 (%)**	**1,67 (g/cm^3)**	**0,64 (mm)**	**66,21 (g)**	**1,21 (N/mm^2)**	**1,65 (N/mm^2)**	**7609 (MPa)**	**5,90 ($g/dm^2.min.^{-1/2}$)**
0,02% (A02)	19	-1%	1%	28%	-21%	-3%	-3%	26%
0,10% (A10)	19	2%	11%	16%	9%	28%	-2%	3%
0,25% (A25)	22	3%	-7%	53%	-25%	-12%	-14%	46%
0,50% (A50)	25	9%	21%	87%	-25%	5%	-13%	39%
0,75% (A75)	30	9%	8%	133%	-50%	-26%	x	119%

STD specimen shows the nominative values. Results are shown in percentage compared to STD for all the samples. Measurements were made after 28 days of curing.

* Triton X405 was used as dispersant in the preparation of all samples containing CNT.

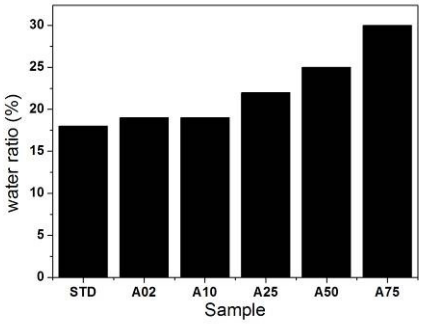

Fig. 2.**14** - Concentration of water (wt %) added to cement paste to keep the same workability.

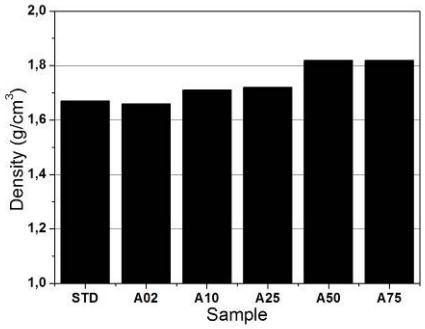

Fig. 2.**15** - Density of the samples with different concentration of CNT added.

Fig. 2.14 shows the concentration of water (w%) necessary to keep the same workability as the standard product. Workability is the ability of a fresh (plastic) cement paste mix to fill the form/mould properly with the desired work and without reducing its quality. Raising the water content will increase workability of the SCM. Excessive water however will lead to increased bleeding (surface water) and/or segregation of aggregates (when the cement and aggregates start to separate), with the resulting SCM having reduced quality [23]. A workable mortar has to present a smooth and plastic consistency, allowing it to be easily spread with a trowel and adhere to a vertical surface [9]. As it can be seen, when CNT were added to the cement paste, extra addition of water was necessary to keep the workability of the cement paste similar to the standard product. In samples with higher concentrations of nanotubes (0,50 and 0,75% of CNT) it was almost impossible to keep the same workability. This behaviour is due the high surface area of the CNT, adsorbing the water of the sample. The density of the samples (Fig. 2.15) showed an increase of the value upon addition of CNT, resulting in a product denser than the standard. This result goes in the opposite way of what was expected at the beginning of this work. We thought that due to the low bulk density of the CNT, the composite should have theorically less material (mass) per the same volume. The key for these results may be in the high area surface of the CNT providing a higher adsorption of the cement grains onto them thus resulting in more material for the same volume.

Dimensional changes and mass variation were set as the other key properties to monitor as they tend to vary during curing, mainly during the first 28 days. Such alterations can happen due to chemical reactions between the raw materials and water which promotes hydrolysis of the cement paste. Dimensional changes also take place in service following changes of moisture content. These phenomena together with the expansion of clay bricks generate movements on the building structure resulting in unacceptable cracking [9]. As regards dimensional variation, the graph of mass variation (Fig. 2.16) shows an increase of the values due to addition of CNT. All samples except A25 presented higher variation (Fig. 2.17) when CNT were added to the specimen while the retraction of the samples was similar to the standard product.

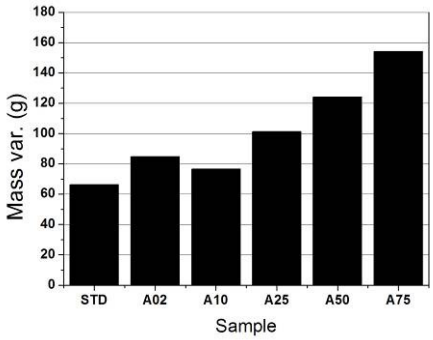

Fig. 2.**16** - Mass variation of the samples with different concentration of CNT added.

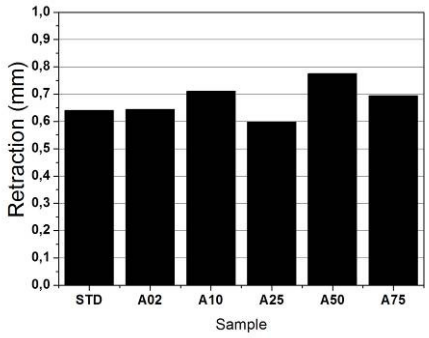

Fig. 2.**17** - Retraction of the samples with different concentration of CNT added.

Fig. 2.18 shows the values for bend resistance as a function of CNT concentration in the cement paste. The sample containing 0,10% of CNT has the value increased as expected. All the other samples had lower values than the standard. As it was cited before and showed in the SEM images (Fig. 2.13), the CNT were poorly a weak dispersed in the cement paste forming aggregates that can act as inclusions. These inclusions can act as stress concentrations reducing the mechanical properties such as bend resistance, compressive strength and the modulus of elasticity. Another reason for these negative results might be associated with the higher amount of water added containing % of CNT above 0,10%. Both CNT aggregation and an extra % of water are thought to be responsible for the results obtained for and compressive strength of the SCM.

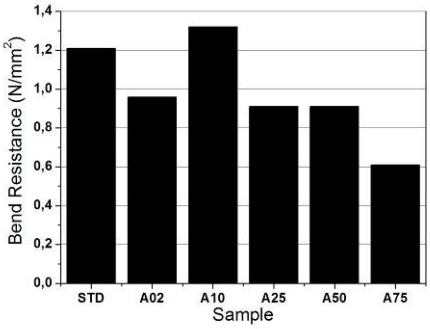

Fig. 2.**18** - Bend resistance of the samples with different concentration of CNT added.

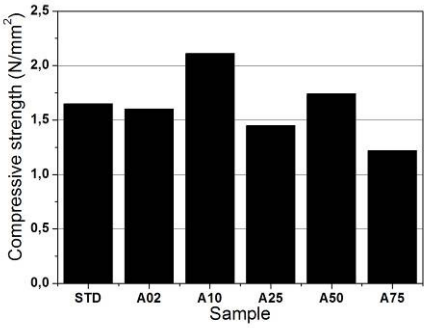

Fig. 2.**19** - Compressive strength of the samples with different concentration of CNT added.

Fig. 2.19 shows the results of compressive strength when CNT was added to cement paste. Again the best value was reached using 0,10% of CNT. The sample containing 0,50% of CNT also showed an increase of the value.

The modulus of elasticity of all samples with CNT decreased of the values (See Fig. 2.20). As is known the modulus of elasticity is the stress resistance of a material until failure divided by

its strain. Theoretically fibres increase the modulus of elasticity of a composite material due to their high strength resistance and the capacity to redistribute the global load of stresses in the matrix of this composite. Therefore, it was expected that these values would increase. Instead, a reduction was observed which can be related to the aggregation of the nanotubes, increasing the concentration of the stresses in specific spots and resulting in a general decrease of the values.

Capillarity was improved with the addition of CNT. This increase of the values is due to the fact that increasing the concentration of fine particles a higher surface area was obtained and consequently the adsorption of fluids during this test was enhanced (See 2.21). Capillarity is another important factor to prevent moisture penetration. Structures made with high porous cement mortar are exposed to environmental conditions such as rain, pollution, salts and chlorides, chemical attack and certain biological agents. The water penetrates, is entrapped in the sub-surface layers and depending on temperature can freeze on expand, which may be sufficient to initiate a crack. Salt crystallization is a physical process analogous to freezing, whereby the salt solution is carried in the mortar from the ground water or from pollutants. In warm weather the moisture evaporates and the dissolved salts crystallize in the pores below the surface of the material to form a hard skin which may then flake off to reveal a new surface. [9]. Atmospheric pollution, resulting from the burning of fossil fuels, can result in masonry being exposed to sulphur and nitrogen acids. Sulphur dioxide is a widespread pollutant which combined with water, produces sulphurous acid which attacks tri-calcium aluminate in cement mortar. Many varieties of algae, lichens, mosses and even bacteria can establish themselves on the surface of a masonry wall, penetrating in the cement mortar's pores, damaging it by producing organic acids, with similar effects to atmospheric pollution.

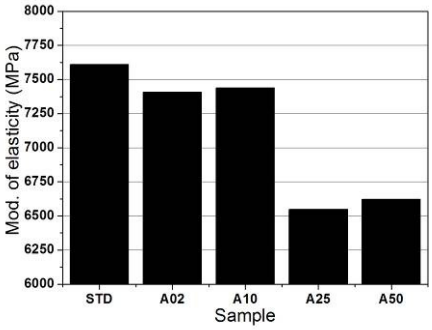

Fig. 2.**20** - Modulus of elasticity of the samples with different concentration of CNT added.

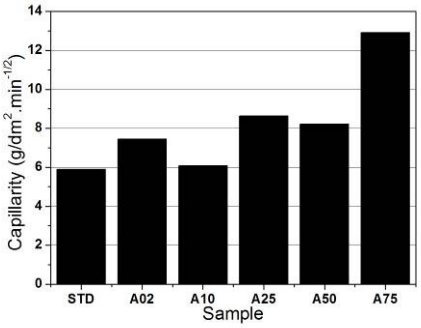

Fig. 2.**21** - Capillarity of the samples with different concentration of CNT added.

This study showed an improvement of the mechanical properties of SCM when small percentages of MWCNT were used. It seems that larger concentrations of MWCNT, (e.g. 0,50 and 0,75% of MWCNT) do not bring any improvement, thereby indicating that the optimal

concentration is around 0.10 % of CNT. In this case the main properties were increased or kept similar to the standard product.

All composite samples presented aggregation of the nanotubes during their preparation due the high hydrophobicity of the tubes. These aggregations still remain in the cement mortar cured after 28 days as observed for the specimens after the bend test. Although the interactions that occur between the nanotubes–matrix were not fully understood, as discussed above are thought to be associated with CNT aggregation. In the fact, this has been suggested in other works [2, 24, 25, 110].

2.3.1.2 Different conventional dispersion methods of CNT

According to the results of the previous section the needs to disperse the CNT prior to addition to the cement mortar formulation become evident. The sample containing 0,10% of MWCNT shows the best properties overall. For this value was added to cement mortar using different methods of dispersion in order to determinate the best method. The results obtained were compared with the standard product (STD).

As described in 2.2.2 four different dispersion methods were studied. Initially the nanotubes were dispersed in H_2O prior the addition to the SCM formulation (Dwt) due to the high hydrophobicity of CNT direct addition of these fillers without any pre-dispersion was also tested (Dd). Next the use of a commercial dispersant Triton X405 was also tested as it was done in selection 2.2.1 (Dt). Finally a slightly more complicated dispersion method was tested which also improved the use of Triton X405 followed by addition of a small amount of poly(acrylic acid) (Da). The addition of poly(acrylic acid) aimed at the formation of a gel containing the CNT to yield homogeneous composite.

2.3.1.2 a) Physical and mechanical properties of SCM using different conventional dispersion methods of CNT

Table 2.2 shows the results of the mechanical properties after 28 days curing. It is observed that the use of carbon nanotubes can enhance both the compressive and flexural strengths of cement.

Table 2.2 – Physical and Mechanical properties of SCM using different dispersion methods of CNT.

Sample [CNT%]	Water ratio (%)	Density (g/cm^3)	Retraction (mm)	Mass variation (g)	Bend resistance (N/mm^2)	Compressive strength (N/mm^2)	Modulus of elasticity (MPa)	Capillarity ($g/dm^2.min.^{-1/2}$)
0% (STD)	18	1,67	0,64	66,21	1,21	1,65	7609	5,90
0,10% (Dt)*	19	2%	11%	16%	9%	28%	-2%	3%
0,10% without disp. (Dwt)	19	5%	-8%	26%	6%	-18%	4%	-2%
0,10% + poly(acrylic ac.) (Da)*	19	5%	-503%	28%	-2%	-8%	-2%	-15%
0,10% dry mixture (Dd)	19	-1%	2%	22%	-2%	12%	2%	-39%

STD specimen shows the nominative values. Results are shown in percentage compared to STD for all the samples.

*Triton X405 was used as dispersant.

From Table 2.2 it is possible to conclude that the best results were reached using dispersions of the CNT in water with Triton X405 dispersant. In this case the physical properties were more similar to the standard product and the mechanical properties (bend resistance and compressive strength) were increased.

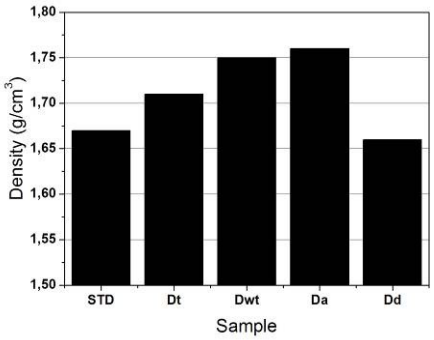

Fig. 2.22 - Density of the samples for the different dispersions methods.

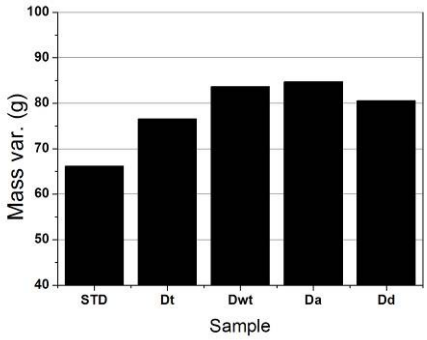

Fig. 2.23 - Mass variation of the samples for the different dispersions methods.

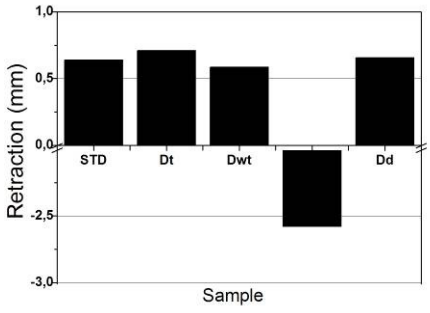

Fig. 2.24 - Retraction of the samples for the different dispersions methods.

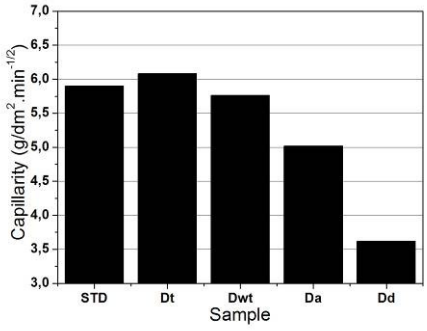

Fig. 2.25 - Capillarity of the samples for the different dispersions methods.

All the samples with exception of the dry dispersion (Dd) had the density increased when compared to the standard product (See Fig. 2.22). In Dd sample this value was smaller than the STD possibly due to the high concentration of agglomerates which generated a huge meshwork structures which can contain some air retained in the agglomerates of CNT or in voids. As result, there is less mass of cement mortar for the same volume resulting in a sample with low density.

All the samples showed higher mass variation when compared to the standard product (See Fig. 2.23). This may be due to the fact that the nanotubes retain water adsorbed on their surface which might evaporate during curing.

The retraction of the dimensions of the samples was similar for almost all samples (See Fig. 2.24). The samples where poly(acrylic acid) was added had a high increase of the dimensions (negative retraction). This may be attributed to osmotic pressure variations during the cure. Due to the high concentration of salts in the formulation the water inside the gel is expelled and consequently the dimensions were significantly reduced.

Different from the previous results which the values for the capillarity of the samples showed inferior values when compared to the standard product expected maybe due to a better dispersion in the cement mortar (See Fig. 2.25).

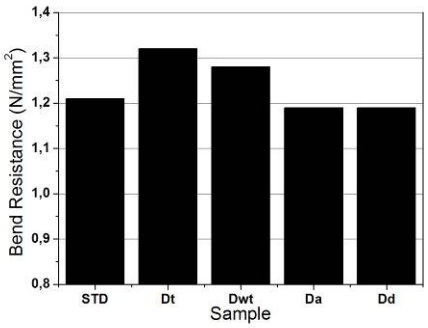

Fig. 2.26 - Bend resistance of the samples for the different dispersions methods.

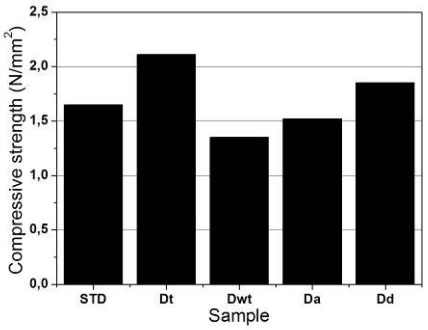

Fig. 2.27 - Compressive strength of the samples for the different dispersions methods.

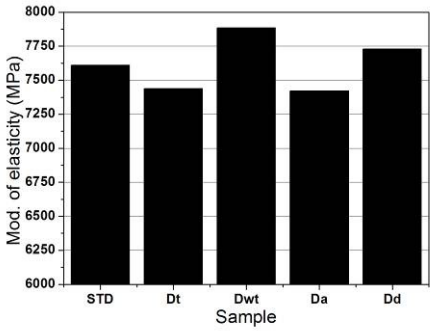

Fig. 2.28 - Modulus of elasticity of the samples for the different dispersions methods.

Figs. 2.26 to 2.28 are related to the mechanical properties of the cement mortars. Values higher than the standard products are achieved in this work indicating that the nanotubes are acting as reinforcement instead of inclusions.

Fig. 2.26 shows the results for bend resistance. Samples prepared with and without dispersant (Dt and Dwt respectively) had the value for this property enhanced when compared to the standard product. Samples Da and Dd showed inferior values. For the compressive strength (Fig. 2.27) Dt and Dd showed the best values (28 and 12% increase, respectively). Samples Dwt and Da showed smaller values than the standard product.

Samples Dwt and Dd showed higher values of modulus of elasticity than the standard product (4 and 2% respectively) as it can be seen in the Fig. 2.28, whilst the samples Dt and Da presented inferior values for this property (-2% for both).

At the end of this section the best global results were obtained for sample Dt that consists in cement mortar with 0,10% of MWCNT dispersed in water with Triton X405. In fact, this sample is the same as sample A10 in the previous section.

Therefore the alternatives studied did not bring any improvements but proved that the dispersion method of CNT have a significant influence on the physical and mechanical properties of the resulting SCM.

2.3.2 Preparation and characterization of SCM using a Novel Dispersion method of MWCNT

In view of the limited results obtained in 2.3.1.2 using conventional dispersion methods the use of neat MWCNT dispersed in a suspension of titanium oxide (MWCNT-TiO_2) in SCM was explored.

Inspired by the work of Sriyai et al developed at TUHH [130] using TiO_2 nanoparticles to improve the dispersion of the nanotubes on the preparation of MWCNT-Epoxy composite in the present work MWCNT where dispersed in an aqueous suspension of TiO_2 supplied by Degussa.

This approach differs from others works [134 to 137] where the oxidized nanotubes have been dispersed in TiO_2 suspensions to obtain photo-catalytic properties.

To assess this methodology, dispersibility tests and morphology studies were carried out on MWCNT-TiO_2 samples. The SCM prepared using MWCNT-TiO_2 were also analysed by SEM and the physical and mechanical properties measured.

2.3.2 a) Dispersibility tests of carbon nanotubes in a suspension of titanium oxide (MWCNT-TiO_2)

Dispersibility tests were carried out in order to compare the hydrophobicity of the nanotubes before and after their dispersion in an aqueous suspension of titanium oxide. Fig. 2.29 clearly shows the difference between the nanotubes (neat) and those dispersed in a suspension of titanium oxide. No decantation was observed for MWCNT-TiO_2 (right side) whilst MWCNT (neat) showed bad dispersion in water and the presence of agglomerates was visible (left side).

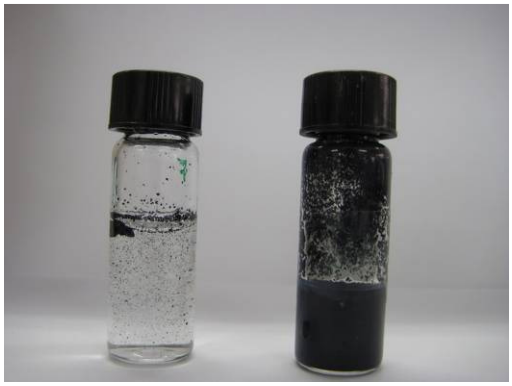

Fig. 2.29 - Dispersibility tests of MWCNT in water. Neat MWCNT (left) and MWCNT-TiO_2 (right).

2.3.2 b) Morphology of the SCM-MWCNT-TiO_2

Visual observation may result in useful information regarding the spatial dispersion of these materials. Morphology of the MWCNT dispersed in a suspension of TiO_2 was carried out by Scanning Electron Microscopy (SEM). Samples were coated with a thin layer of carbon before examination. Fig. 2.30 shows MWCNT-TiO_2 with diameter starting from 40 nm.

Fig. 2.31 is a typical SEM image of a fracture surface of the standard SCM (left side) and SCM containing MWCNT-TiO_2 (right side). Low magnification images of the samples (standard and the cement mortar with nanotubes) show similarities on their morphologies. Fig. 2.32 show high magnification SEM images of SCM-MWCNT-TiO_2. Different from the SCM prepared with untreated CNT, the MWCNT-TiO_2 are dispersed uniformly in the composite and there is no

obvious aggregation. The contact points of the MWCNT-TiO_2 in SCM were much higher than those of observed in SCM with neat nanotubes. No three-dimensional meshwork was observed. As it can be seen the treated nanotubes appear to be randomly spaced and quite distributed protruding from the cement matrix due their improved affinity to water. In this way the nanotubes can act as reinforcement distributing the stress trough the matrix. No presence of agglomerates was observed after the bend test neither.

In the Fig. 2.33 it is possible to see a grain of cement with nanotubes oriented perpendicularly to the cracking plane indicating a possible mechanism of fibre pull-out. Fig. 2.34 shows the effect of pull-out between the nanotubes and the cement matrix. It is believed that this alignment was a result of the MWCNT reorientation thus offering resistance to crack growth by spanning the crack in a direction perpendicular to the plane of the crack growth. While this type of MWCNT–matrix failure would typically be indicative of a weak interaction, in this case it is believed that the local stresses became stronger for the individual interaction nanotube–matrix. [25]. This mechanism is quite important for ceramic composites because before the fracture of the composite, the fibres are pulled-out from the cement matrix consuming energy (friction forces); as result an increase of the mechanical properties (especially bend resistance and modulus of elasticity) may be expected.

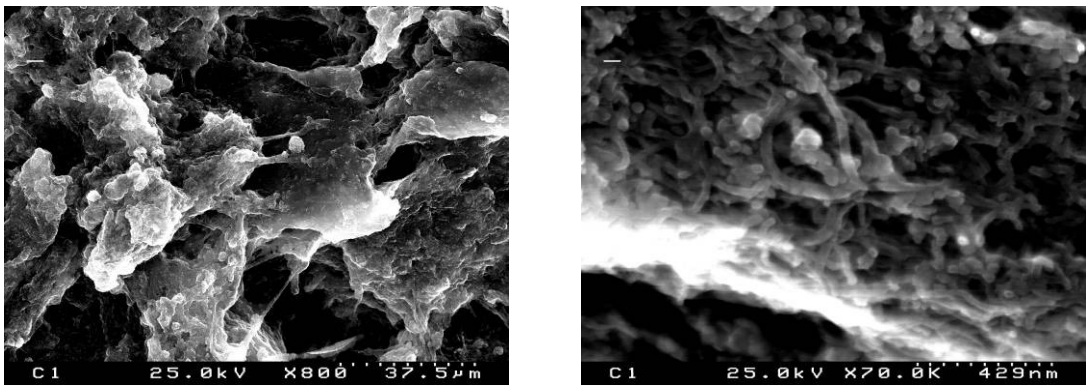

Fig. 2.30 - SEM image of MWCNT-TiO_2 at 800 times (left side) and 20.000 times (right side).

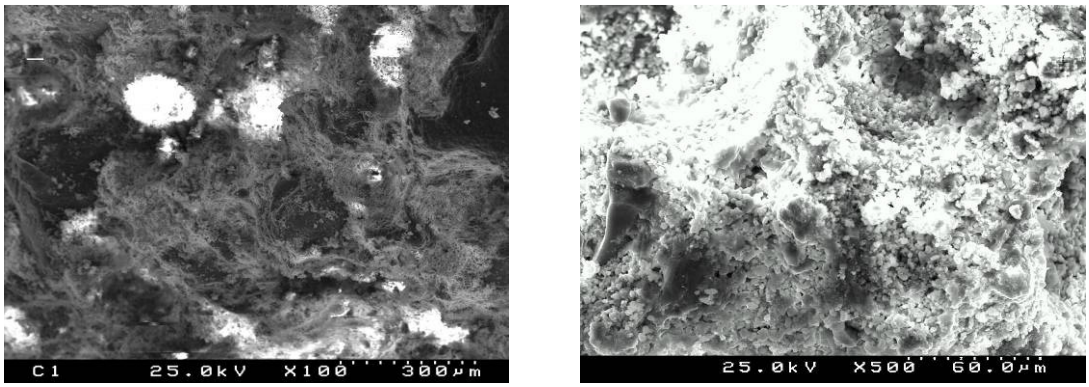

Fig. 2.31 - Comparison of the fractured surface by SEM of the standard SCM (left side) at 100 times and the SCM-MWCNT-TiO_2 (right side), both at 500 times.

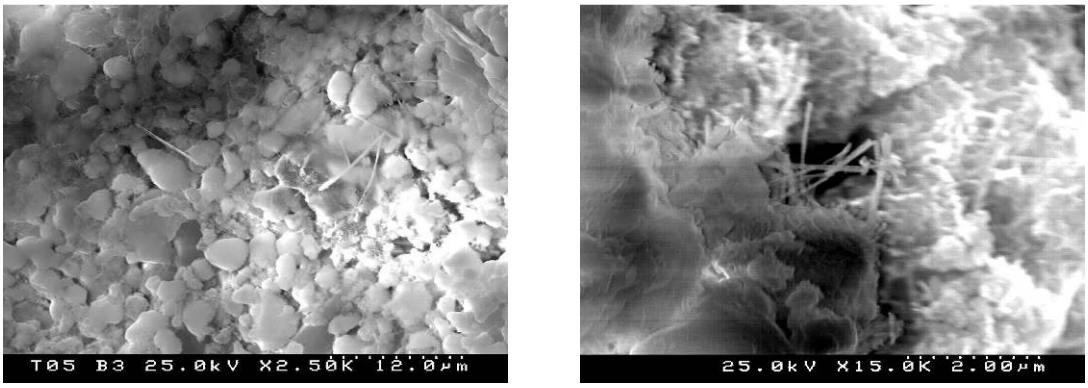

Fig. 2.32 - SEM images of the fractured surface of the SCM-MCNT-TiO_2 at 2500 (left side), and 15000 times (right side). In both images it is possible to see the good interface between cement grains and the nanotubes.

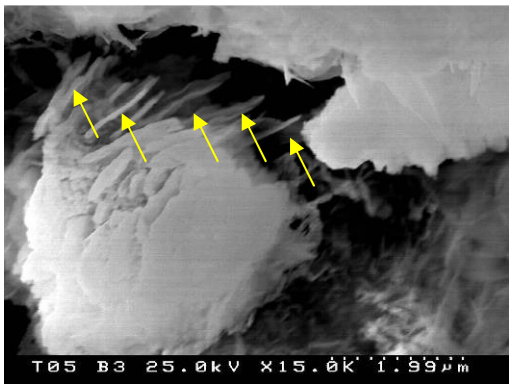

Fig. 2.33 – High magnification SEM image of the SCM-MWCNT-TiO_2 showing the CNT with orientation perpendicular to the fracture surface.

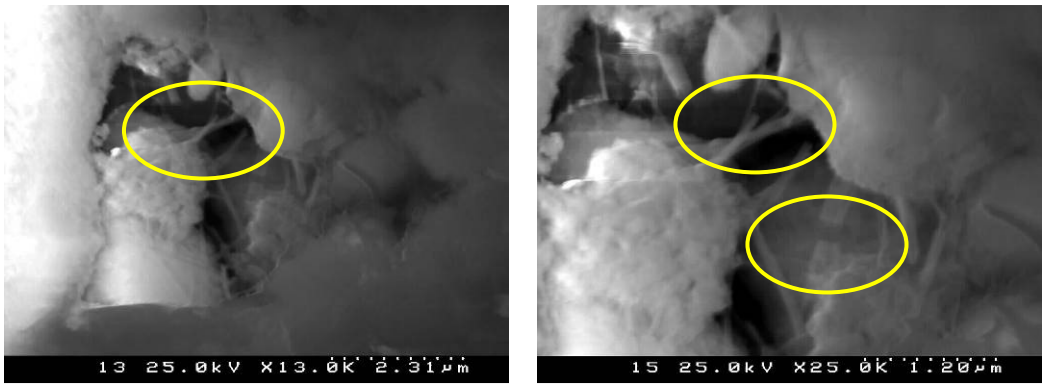

Fig. 2.34 – High magnification SEM image of a fracture surface of the SCM-MWCNT-TiO2 at 13000 times (left side) and 25000 times (right side).

2.3.10 Physical and mechanical properties of the SCM-MWCNT-TiO_2

Table 2.3 shows the results of the physical and mechanical properties after 28 days curing. The plain cement paste (STD) was taken as a reference to study the impact of the addition of

the carbon nanotubes dispersed in a suspension of TiO_2. It is observed that addition of MWCNT-TiO_2 enhanced the mechanical the properties.

Table 2.**3** - Physical and mechanical properties of SCM-MWCNT-TiO_2.

Sample	Water ratio	Density	Retraction	Mass variation	Bend resistance	Compressive Strength	Modulus of elasticity	Capillarity
0% (STD) [CNT%]	**18** (%)	**1,68** (g/cm^3)	**0,53** (mm)	**81,45** (g)	**1,08** (N/mm^2)	**1,49** (N/mm^2)	**6943** (MPa)	**7,02** ($g/dm^2.min.^{-1/2}$)
0,10% TiO_2 (Ti10)	19	10%	3%	-19%	69%	41%	49%	-19%
0,10% TiO_2 (Ti10 H)	20,5	10%	30%	1%	48%	17%	37%	-7%

STD specimen shows the nominative values. Results are shown in percentage compared to STD for all the samples.

The product obtained was well dispersed in the cement matrix resulting in mechanical properties much higher than those of the standard product. The results showed that 0,10% MWCNT-TiO_2 concentration was nearly optimal for enhancing the mechanical properties of SCM in bend resistance, compressive strength and modulus of elasticity. Sample Ti10 (19% of water) was the bend resistance enhanced by 69%, the modulus of elasticity by 49% and the compressive strength by 41%. These results were the highest in this work. This sample showed physical properties (density and capillarity) a little bit different from the standard product.

Fig. 2.35 shows the comparison of the density of the samples. As discussed before the density is increased when nanotubes are added to the cement paste due to their high adsorption of the water, resulting in a denser product. The mass variation for Ti10 H was similar to that of the STD. However, sample Ti10 the mass variation was19% smaller (See Fig. 2.36).

As regards retraction for sample Ti10 it was increased by 3% while for sample Ti10H it decreased by 30% (See Fig. 2.37). As it is well known, such high dimensions changes are not desired for mortar products since they will generate stresses on the building structure causing cracks.

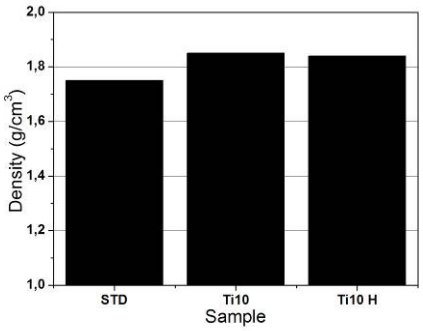

Fig. 2.35 - Density of STD and SCM-MWCNT-TiO_2 samples.

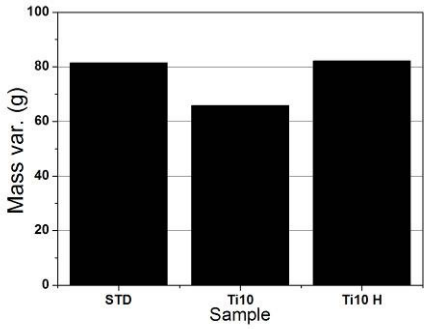

Fig. 2.36 – Mass variation of STD and SCM-MWCNT-TiO_2 samples.

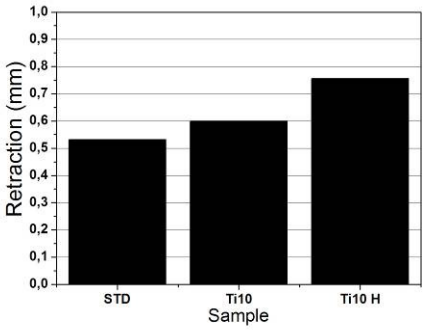

Fig. 2.37 - Retraction of STD and SCM-MWCNT-TiO_2 samples.

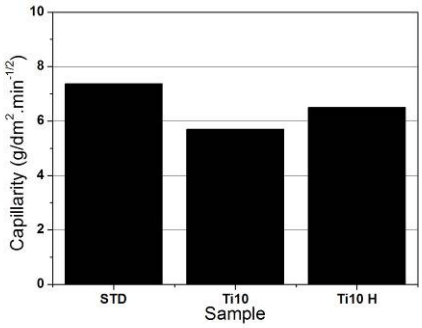

Fig. 2.38 - Capillarity of STD and SCM-MWCNT-TiO_2 samples.

The capillarity of the samples with nanotubes was much smaller than the standard product (See Fig. 2.38). For sample Ti10 the capillarity was 19% smaller than that of the STD sample while for sample Ti10 H it was 7% smaller. This effect may be due to the good dispersion of the nanotubes in the SCM, as explained before.

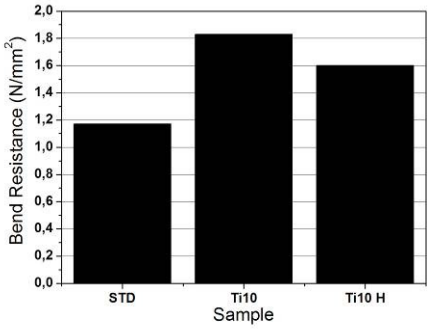

Fig. 2.39 - Bend resistance of STD and SCM-MWCNT-TiO_2 samples.

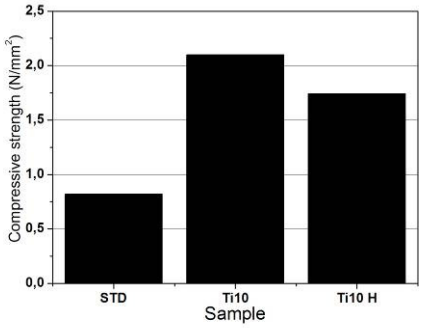

Fig. 2.40 - Compressive strength of STD and SCM-MWCNT-TiO_2 samples.

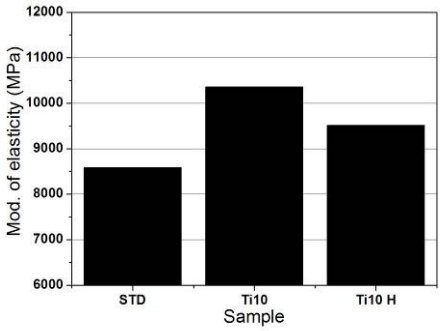

Fig. 2.41 - Modulus of elasticity of STD and SCM-MWCNT-TiO_2 samples.

Figs. 2.39 to 2.41 show the results of mechanical properties of the SCM-MWCNT-TiO_2. Values higher than the standard products are achieved in this work indicating that the nanotubes are acting as reinforcement instead of inclusions.

Fig. 2.39 shows the results for bend resistance. Samples Ti10 and Ti10 H showed high values when compared to the standard product. The former presented 69% and the latter 48% higher than the STD sample.

The results for the compressive strength can be seen in Fig. 2.40. Samples with nanotubes dispersed in a Titania suspension obtained the best results of this work. Sample Ti10 H showed an increase of 17% while sample Ti10 had an enhancement of 41% for this property.

SCM-MWCNT-TiO_2 showed higher values for modulus of elasticity when compared to the standard product (See Fig. 2.41). Sample Ti10 had an enhancement of 49% higher than the sample STD while the Ti10 H got an increase of 37%.

At the end of this section it was possible to conclude that the MWCNT-TiO_2 proved to be a powerful reinforcement for structural cement mortars increasing significantly the mechanical properties of the plain cement mortar. All the mechanical properties were higher than the standard product.

The results obtained for the physical properties were different from the plain cement. The products with the addition of nanotubes are denser, more compact and presented less mass variation than the standard product.

The fact that all mechanical properties were enhanced, as opposed to the results obtained for SCM with neat MWCNT may be due the better dispersion of the nanotubes in the cement. According to Sriyai (2008, p.62) the affinity between TiO_2 nanoparticles and MWCNT is due to the opposite charges of their zeta potential. In fact, according to her, “it seems likely that the negatively charged titania nanoparticles have a tendency to be attracted by the positively charged surface of the MWCNT” [130].On the other hand, the TiO_2 nanoparticles being polar seem to be responsible for the better dispersibility of these fillers in the cement matrix.

The conjunction of the extremely strong tensile properties with a strong nanotube-matrix bonding (due to their high surface area/volume ratio) suggests that some of the nanotubes would have their long axis orientated perpendicular to the plane of incipient cracks, providing these good results.

Sample Ti10 H showed much higher retraction of the dimensions than the STD product which makes it inappropriate to be used in the same conditions without changes in a possible project design. On the other hand sample Ti10 showed a high difference on the value of the capillarity (-17%) when compared to plain cement.

The sample Ti10 is the most indicated for the reinforcement of the SCM due to high values found for the mechanical properties and considerable similarity of the physical properties when compare to the standard product. Another positive fact is that MWCNT’s dispersion with a suspension of TiO_2 is relatively easier, faster and cheaper than the oxidation process which will be discussed next. Moreover, it can be adapted for industrial production scale.

2.3.3 Preparation and characterization of SCM-MWCNT-oxy

In view of the results obtained using neat MWCNT where bundles of MWCNT were observed due the hydrophobicity of CNT (See Figs. 5.4 and 5.6) it was decided to treat the surface of these nanomaterials. Hence, further to previous works carried out in our laboratory regarding the preparation of polymer based composites and carbon fibres [131] as well as the work of Shaffer and Kizol (2002, p. 2074), the effect of surface modification of CNT was investigated.

2.3.3 a) Solubility tests of oxidized multi-walled carbon nanotubes (MWCNT-oxy)

Solubility tests were carried out in order to compare the hydrophobicity of the nanotubes before and after oxidation. Figure 2.42 clearly shows the difference between the nanotubes before and after oxidation. Sample MWCNT-oxy (right side) showed good affinity with water and no decantation was observed.

Fig. 2.42 – Solubility tests of MWCNT in water. Neat MWCNT (left) and MWCNT-oxy (right).

2.3.3 b) Morphology of SCM-MWCNT-oxy

Morphology of MWCNT-oxy was carried out by Scanning Electron Microscopy (SEM). Samples were coated with a thin layer of carbon before examination. Fig. 2.43 shows MWCNT-oxy with diameter starting from 75 nm.

Fig. 2.44 is a typical SEM image of a fracture surface of the standard SCM (left side) and SCM-MWCNT-oxy (right side). Analyses of the dispersion of the MWCNT-oxy were made in order to verify the interactions between the carbon nanotubes and the cement matrix. Low magnification of the images show samples with similar morphology but the sample with nanotubes seems to have more porous.

Fig. 2.45 and 2.46 show high magnification SEM images of SCM-MWCNT-oxy. Different SCM-CNT, in SCM-MWCNT-oxy the CNT are dispersed uniformly in the composite and there is no obvious aggregation. The contact points of the MWCNT-oxy in SCM were much higher than those of the neat CNT in SCM. No three-dimensional meshwork was observed. As it can be seen the treated nanotubes appear to be randomly spaced and quite distributed protruding from the cement matrix due to their good dispersion during the preparation of the samples. As result the nanotubes may act as reinforcement distributing the stress through the matrix. In fact no agglomerates were observed after the bend test.

Still in Fig. 2.45 (right side) it is possible to see the effect of pull-out between the nanotubes and the cement matrix. In this image is possible to see some fracture surfaces with nanotubes bridging the crack. In this case, when the crack extends through the material an additional energy must to be spent to pull the fibres out of the matrix. Therefore, the increase of the values of the bend and compression resistance may be expected.

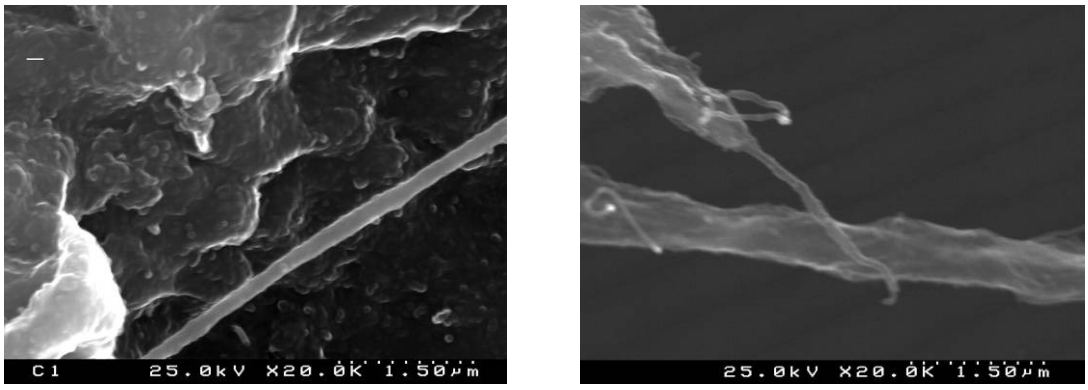

Fig. 2.43 - SEM image of MWCNT-oxy at 20.000 times.

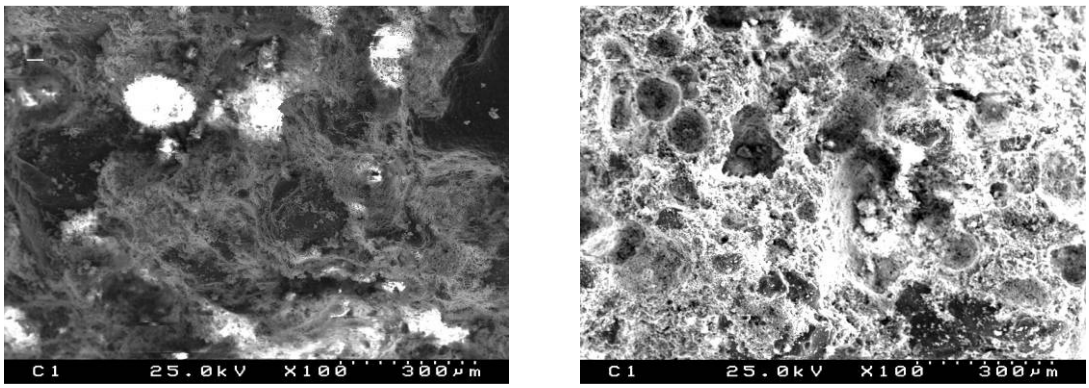

Fig. 2.**44** - Comparison images of the fractured surface by SEM of the SCM standard (left side) and the SCM-MWCNT-oxy (right side), both at 100 times.

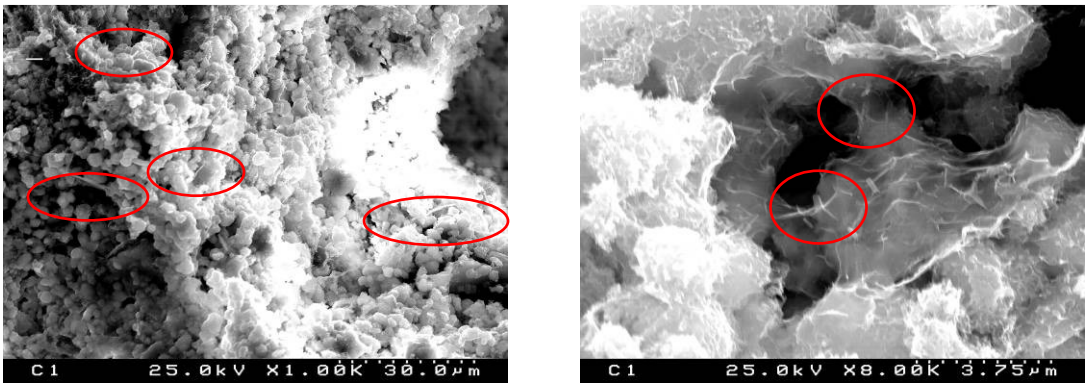

Fig. 2.45 - SEM images of the fractured surface of the SCM-MWCNT-oxy at 1000 (left side), and 8000 times (right side). In both images it is possible to see the good interfaced interaction between cement grains and the nanotubes.

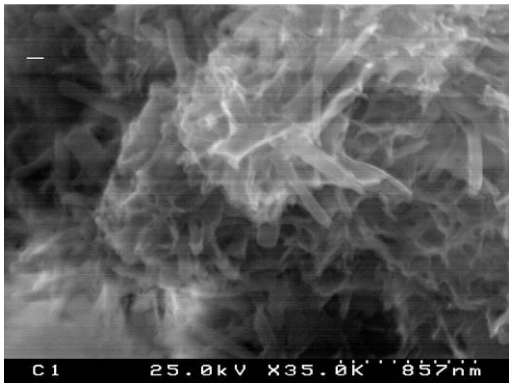

Fig. 2.46 - High magnification SEM image of the SCM-MWCNT-oxy.

2.3.3 c) Physical and mechanical properties of SCM-MWCNT-oxy

Table 2.4 shows the results of the physical and mechanical properties after 28 days curing. It is observed that the physical properties (except the mass variation and capillarity) had an increase in the values due to the addition of treated carbon nanotubes. This means that it is possible to use the SCM with MWCNT-oxy for the same purpose as the standard product, however with possible enhanced mechanical properties.

Upon addition compressive strength increased by 22% when compared to standard sample and the modulus of elasticity that increased by 20%. The most significant result was observed for the compressive strength which increased by 35%.

Table 2.**4** – Physical and mechanical properties of SCM-MWCNT-oxy.

Sample	Water ratio	Density	Retraction	Mass variation	Bend resistance	Compressive strength	Modulus of elasticity	Capillarity
STD [CNT%]	**18** (%)	**1,75** (g/cm3)	**0,74** (mm)	**79,63** (g)	**1,30** (N/mm2)	**1,56** (N/mm2)	**7973** (MPa)	**7,04** (g/dm2.min.-1/2)
0,10% oxi	19	5%	5%	-4%	22%	35%	20%	-15%

STD specimen shows the nominative values and the sample with MWCNT-oxy has the results shown in percentage compared to the former.

Fig. 2.47 shows the concentration of water necessary (w%) to keep the same workability in both products. The sample with oxidized nanotubes needed extra addition of water than the standard one, but when it is compared with the samples using 0,10% of nanotubes without treatment surface, the amount of water used was the same.

The density of the SCM-MWCNT-oxy was 5% higher than the standard product (See Fig. 2.48). This value is similar to those obtained for SCM-MWCNT (0,10%) and smaller than those containing 0,50% CNT and 0,75% CNT for which an increase of 9% was registered.

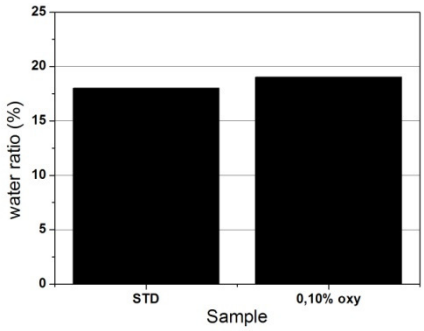

Fig. 2.**47** – Water content added to cement paste to keep the same workability.

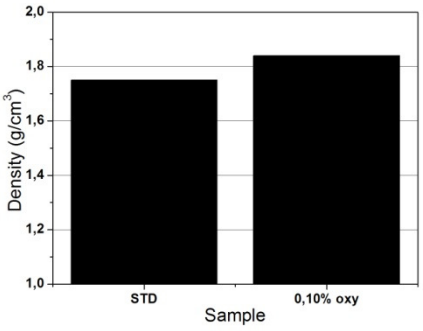

Fig. 2.**48** - Density of STD and SCM-MWCNT-oxy.

Figs. 2.49 and 2.50 show that the sample with MWCNT-oxy has a higher dimensional retraction and smaller mass variation compared to the standard; this means that the product with the nanotubes oxidized is more compact, the result reflect the good dispersion of the nanotubes adsorbing the cement grains on their surface. Even more these values can be considered similar.

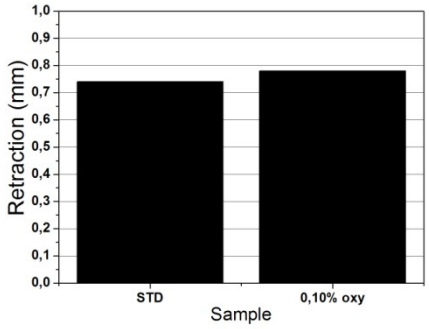

Fig. 2.**49** - Retraction of STD and SCM-MWCNT-oxy.

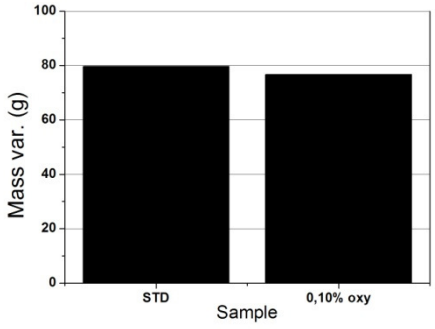

Fig. 2.**50** - Mass variation of STD and SCM-MWCNT-oxy.

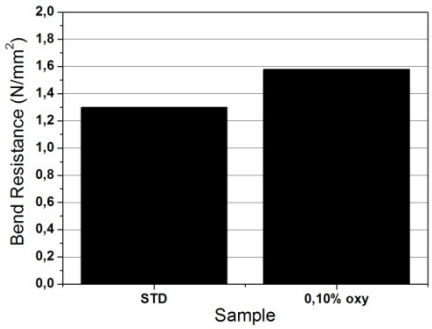

Fig. 2.**51** - Bend resistance of STD and SCM-MWCNT-oxy.

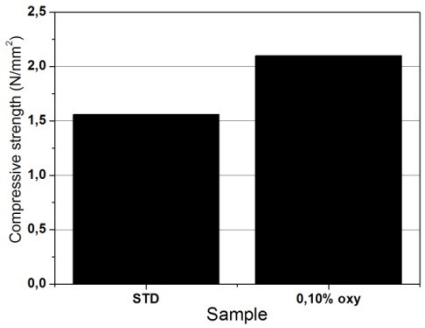

Fig. 2.**52** - Compressive strength of STD and SCM-MWCNT-oxy.

The product prepared using oxidized nanotubes showed an increase by 22% for bend resistance (Fig. 2.51). Therefore, this product can be used for example in structural beams which require high bend resistance and compressive strength. Addition of oxidized nanotubes led to an increase of 35% of compressive strength (See Fig. 2.52). This value was the highest when compared with those using neat MWCNT. The possible bridge coupling effect of carbon nanotubes showed in Fig. 2.45 (right side) seems to promote the load-transfer across voids and cracks resulting in significant increase of this property.

According to Geng et al. [2], this enhancement is due to the improvement of material microstructure. Interfacial interactions between surface-modified nanotubes and hydrations (such as C–S–H and calcium hydroxide) of cement produce a high bonding strength, and increase the load-transfer efficiency from cement matrix to the reinforcement. The chemical reactions between the carboxylic acid groups on the surfaces of carbon nanotubes and the calcium silicate hydrate (C–S–H) or $Ca(OH)_2$ from the cement powder seems to emphasize the interaction between the CNT and the cement. Fig. 2.53 illustrates the reaction proposed by Gent et al.

Different from other samples prepared using neat nanotubes (except those dispersed in a suspension of TiO_2) addition of oxidized nanotubes had an expressive increase (20%) of the modulus of elasticity (See Fig. 2.54). In samples where neat nanotubes were used, the results oscillate from -20% to 4% for the same property. Such variations were attributed to the bad dispersion of the reinforcement in the cement matrix.

As shown by SEM (Fig. 2.32 and 2.33) the interaction between the oxidized nanotubes and the cement matrix was far better than that observed for samples prepared using neat CNT (except those dispersed in a suspension of TiO_2). Hence in this case the nanotubes seem to act as fibres sharing the stress uniformly through the matrix yielding higher values for the modulus of elasticity.

As regards the capillarity, it increases when fine particles are added to cement mortar the capillarity increases due to their high area surface. However, in the present study, the capillarity (Fig. 2.55) decreased by 15% when compared to the standard product. In fact, this had already

been reported by Li et al. (2005, p. 1245) who argued that addition of carbon nanotubes reduces pore size distribution acting as the filler of voids and thus, decreasing the capillarity of cement composites. As result, these samples become much more compacted.

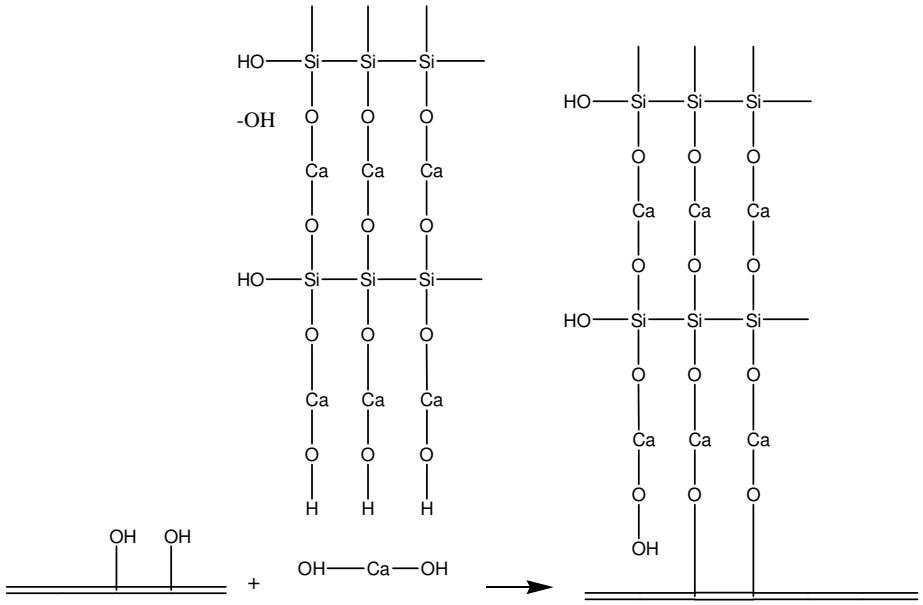

Fig. 2.53 - Reaction scheme between oxidized nanotube and calcium silicate hydrate (C–S–H) or $Ca(OH)_2$ from the cement hydrated [2].

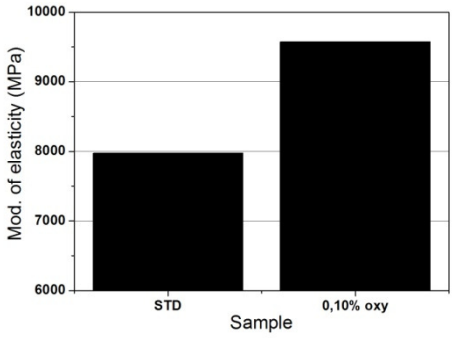

Fig. 2.54 - Modulus of elasticity of STD and SCM-MWCNT-oxy.

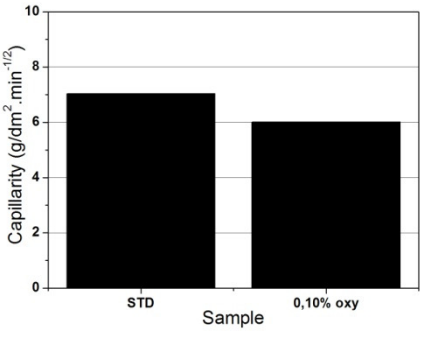

Fig. 2.**55** - Capillarity of STD and SCM-MWCNT-oxy.

This study showed an improvement of the mechanical properties when percentages around 0,10 w% of MWCNT were used.

After the bend test, no aggregates were present in the samples prepared with MWCNT-oxy. The positive results obtained using MWCNT-oxy can be due to their high hydrophilicity which yields a better dispersion (no decantation or aggregation) during sample preparation. Moreover, the presence of polar groups on the MWCNT-oxy promotes the interfacial interaction between the nanotubes and the cement paste yielding more homogeneously dispersed materials.

Cement composites are porous materials, with massive numbers of capillary pores and micro voids. The more the pores and voids the lower the strengths. Addition of oxidized nanotubes reduces the number the size of pores [2]. Thus the composites become compacted, which will lead an increase of compressive strength. The possible effect of crack-bridging (across cracks and voids) increases the compressive strength of the composite by distributing the tension uniformly through the ceramic matrix [2].

In this case it is clear that oxidized nanotubes are acting as reinforcement in accordance with other works [2, 7] the results obtained were positive even using a small concentration of nanotubes (0,10%).

2.4 Brief economical analysis regarding the use of CNT in SCM

This section was made to give an idea of the average costs of using CNT as reinforcement in cement mortars. The nanotubes used in this work were purchased from Nanocyl. The prices were estimated based on average prices taxed by companies and costs transportation (from Belgium to Portugal). These values have considered purchases in high amounts over 1kg of CNT.

The oxidation of the MWCNT was carried out at UA however the estimated cost for MWCNT-oxy based on the price of by other companies.

The estimation for the costs of MWCNT-TiO_2 were based on prices for neat nanotubes plus averages costs of raw materials (especially TiO_2 nanoparticles) as this suspension is not commercially available. Table 2.5 shows the average costs of CNT to SCM.

Table 2.5 – Average prices of CNT (€/g).

CNT	Price (€/gram)
MWCNT	5,5
MWCNT-oxy	7,7
MWCNT-TiO_2	6,6

The values per kilogram of SCM (without water) were also calculated and are summarised in Table 2.6. These values have considered the average costs of the nanotubes cited on Table 2.5 plus dispersant (Triton X405) or poly(acrylic acid) when necessary. The prices estimated did not take in account the costs of workman hours, equipments or the process involved.

Table 2.6 – Costs of SCM with addition of CNT for the samples studied in this work (wt % of cement powder).

Sample	Cost (€/ wt % of cement powder)
A02	1,15
Ti10	6,60
Ti10 H	6,60
0,10% oxy	7,70
Dwt	5,50
Da	5,71
Dd	5,50
A10/Dt	5,55
A25	13,80
A50	27,55
A75	41,30

As it can be seen in the Table 2.6 the cost of the adding CNT to SCM are much higher than the price of cement powder (around 0,20 € per kg). Samples using more than 0,10% of CNT (by weight of cement powder) are in fact impossible to be used at industrial scale. As a suggestion, further tests should be done aiming at lowering the concentration of CNT using MWCNT oxidized or dispersed in titanium oxide.

2.5 Conclusions

Carbon nanotubes are one of the most important materials under investigation for nanotechnology applications. Construction industry applications of CNT range from composite materials through to high strength structural components. Cement and concrete CNT composites have particularly strong potential, since CNT act as a near ideal reinforcing material and have diameters similar in scale to the layers in calcium-silicate hydrate [7].

Current research has shown that it is possible to distribute CNT across cement grains using oxidation (surface treatment) and dispersion in a titanium oxide suspension. The key for the improvement of the SCM's mechanical properties is the dispersion of the nanotubes in the cement matrix. The answer to provide a good interaction between the reinforcement and the matrix is the affinity of the CNT to water.

The use of neat MWCNT proved to be difficult due to their poor dispersion in the cement paste resulting in aggregates and a non-uniform distribution of the bundles within the matrix which causes a decrease in some mechanical properties. Overall, the samples containing neat nanotubes, even using dispersant or poly(acrylic acid) or dry dispersion, have shown worse mechanical properties than the plain cement paste due to the intrinsic hydrophobicity of the nanotubes and their impact on the hydration process. Increasing the concentration of nanotubes did not lead to any improvement. In fact, samples with lower concentration of nanotubes showed better mechanical properties those samples with high concentration. Therefore, when

the % of nanotubes are increased in the mixture a bad dispersion is obtained (more agglomeration and less uniform distribution throughout the matrix), thus impairing the mechanical performance [2, 24, 25, 110].

Within the range at concentrations studied the optimum limit for the addition of CNT to cement mortar seems to be 0,10% (w%) of the cement powder. However it is suggested that further studies should be carried out aiming at establishing the optimum values of carbon nanotubes oxidized and dispersed in a suspension of titanium oxide to confirm this value. Dispersion experiments with oxidized carbon nanotubes showed that the surface treatment using HNO_3 led to good affinity towards water. The same behaviour was found using MWCNT-TiO_2. When dispersing the nanotubes oxidized or dispersed in a suspension containing titanium oxide a different trend is observed resulting in an increase on the mechanical properties of the product, in opposite to those using neat MWCNT. As the optimal concentration CNT (0,10 w%) was determined using of neat nanotubes, it is expected that using nanotubes oxidized or dispersed in a suspension of titanium oxide the limit of addition be lower.

Nanotube pull-out from the matrix is possibly the predominant mode of overload failure which seems reasonable because the interfacial (MWCNT-cement mortar) shear strength is believed to be smaller than the nanotubes' tensile strength.

The use of MWCNT-TiO_2 is the most indicated to be used in cement mortars when compared with all the other samples tested in this work due its easy way and time consumed for dispersion. Furthermore this dispersion method can be easily adapted for industrial production scale. No prior studies of the addition of MWCNT dispersed in a suspension of titanium oxide in cement mortar were found in the literature. Hence, it is difficult to compare this work with others. In fact, not much has been found in literature in connection with the use of any type of CNT in cement products.

Limitations to the present study include the use of just two or three specimens for each sample type generating dispersion on the results and difficulties to accurately interpret them. Therefore, it is suggested that in future smaller specimens should be prepared in order to obtain a higher number so that Weibull analytical methods, for example, could be used to obtain more reliable results. Nevertheless the present results can be considered as a base for new procedures and further studies.

Although beyond the scope of this study, it is important to refer that the risks involved with the addition of CNT to cement mortar must be assessed. In fact, it is possible to find in the literature a lot of works [121 to 124] on the toxicity of both nanotubes and also TiO_2 nanoparticles. O'Brien and Cummins state that "two major areas should be concerned, that are, human health issues and environmental issues. With regard to human health issues there are many pathways to human exposure: inhalation, ingestion, and dermal infiltration" [124]. Genotoxicity and carcinogenesis are also possible effects [124]. According to Köhler and Som [122] and also Helland et. al. [121] carbon nanotubes seem to be able to accumulate in the food chain and ecosystems causing progressive damages to the environment and living beings.

Finally, the high price of the CNT makes their use almost impossible today for industrial production scale but the good results obtained opened new possibilities for future applications if the price of the nanotubes keeps on falling as expected as a result of technological developments.

Chapter 3 – Decorative Mortars (DCM)

The aim at this work was to enhance the aesthetical properties of decorative mortars by adding inorganic photochromic materials, to yield materials that could change their colour or colour shade according to sunlight exposure. We report on investigations of the photochromic effect of pigments focussing on decorative mortar samples. Results are compared to those of the corresponding standard products upon sunlight exposure under the same conditions. For this purpose the addition of: (i) silver halides, (ii) milled photochromic eyeglass lenses, (iii) tungsten trioxide and, (iv) two mixtures of tungsten trioxide and titanium oxide nanoparticles was studied.

A summary of the most important theoretical concepts regarding decorative mortars (DCM) will be presented as well as for photochromism including possible photochemical processes and the colorimetry technique used to analyse the colour of the samples.

In the following sections, we focus on the addition of photochromic materials to the mortar paste (with or without titanium oxide). The photochromic properties were measured using the CIELAB Colour System. Samples were exposed at the same period of the day (3 or 4 pm) and the same period of the year (in March) to sunlight without the use of any other illuminant. The analyses of the results have been done by comparing the DRS values of the samples before and after sunlight exposure. In our work it is considered that a sample shows photochromic effects when the DRS values are an order of magnitude higher than those of the standard sample (containing 0% of photochromic compound) submitted to the same conditions of sunlight exposure.

3.1 Literature Review

3.1.1 Decorative Mortars

Decorative mortars are mortars whose role is not strictly related to structural elements. The advancements in mortar stains and dyes, textures, and patterns have made it the most versatile, durable and cost-effective material in the construction market [9].

One of the biggest advantages of using decorative mortars relates to the durability of the materials which, upon appropriate selection, may be expected to remain in service for many years with relatively little maintenance. From the architectural point of view, mortar offers advantages in terms of great flexibility of plan form, spatial composition and appearance of external walls for which materials are available in a wide variety of colours and textures.

For certain applications that require low tensile strength of mortar and the aesthetical is the main function of the mortar, DCM is the key.

DCM can be used among other things for: (i) walls, floors, worktops and buildings facades and (ii) repairing old facades by covering surfaces made of mortar, concrete, or even other materials.

Since decorative mortars are used in thicker layers, they have to present at least to following characteristics: (i) good adherence to the material of the base of the wall, (ii) provide some hardness and elasticity and, (iii) cannot crack even in thicker layers. Moreover, it can act as a protective (not showing combustibility) and insulating (sound and heat) material.

For aesthetic purposes, colour, design, gloss rating, and finish texture have to be taken in account. In this way the dyes and pigment industry spends much effort studying new products or improving those already commercialized to meet the customer's needs. Among the properties of interest, the colour properties are the most important and, among these, lightfastness is a fundamental one [26]. In contrast to the latter, the term photochromism implies the reversibility of colour and has been observed for a variety of inorganic materials (e.g., MoO_3 [28-32], WO_3 [35-38, 41, 115], WO_3-TiO_2 [34, 42, 93, 114], photochromic glasses [43, 44], $BiVO_4$ [26, 27, 45] and others [46-55].

Despite the fact that most of the work reported in the literature (~90%) concerns organic materials, in this work it was decided to explore the use of inorganic photochromic materials due to the fact that most organic materials might degraded, due to the high pH values of the fresh mortar pastes.

3.1.2 Photochromism

Photochromism is the reversible transformation of a chemical species between two forms by the absorption of electromagnetic radiation, where the two forms have different absorption spectra [56]. Trivially, this can be described as a reversible change of colour upon exposure to light.

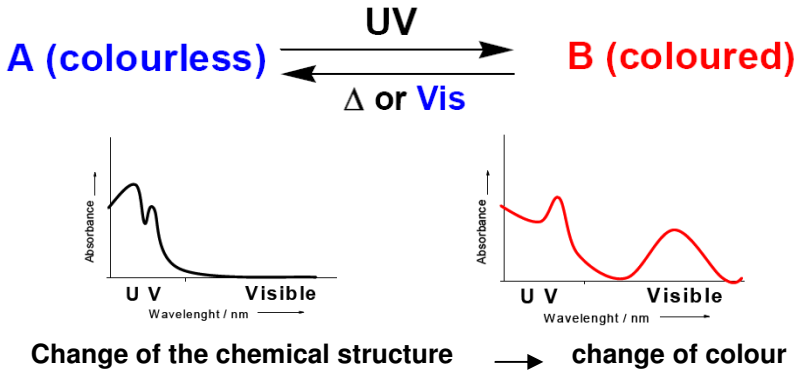

Fig. 3.1 - Schematic of an hypothetical photochromic material [125].

The phenomenon was discovered in late 1880s, including the work by Markwald, who studied the reversible change of colour of 2,3,4,4-tetrachloronaphthalen-1(4H)-one in the solid

state. He labelled this phenomenon "phototropy", and this name was used until the 1950s when Yehuda Hirshberg, of the Weizmann Institute of Science in Israel proposed the term "photochromism". Photochromism can take place in both organic and inorganic materials, and also has its place in biological systems (for example the retina in the vision process) [57].

Some of the most common processes involved in photochromism are pericyclic reactions, cis-trans isomerizations, intramolecular hydrogen transfer, intramolecular group transfers, dissociation processes and electron transfers (oxidation-reduction).

Another somewhat arbitrary requirement of photochromism is that it requires the two states of the molecule to be thermally stable at ambient conditions for a reasonable time.

There is therefore a close relationship between photochromic and thermochromic materials. The timescale of thermal back-isomerization is important for applications, and may be molecularly engineered [58].

Since photochromic chromophores are dyes, and operate according to well-known reactions, their molecular engineering to fine-tune their properties can be achieved relatively easily using known design models, quantum mechanics calculations, and experimentation. In particular, the tuning of absorbance bands to particular parts of the spectrum and the engineering of thermal stability have received much attention [58].

In photochromic materials, fatigue resistance refers to the loss of reversibility by processes such as photodegradation, photobleaching, photooxidation, and other side reactions. All photochromics suffer fatigue to some extent, and its rate is strongly dependent on the activating light and the conditions of the sample.

In order to incorporate photochromic material in working systems, the same issues as those found with other dyes have to be dealt with. These materials are often charged in one or more states, and their photochromic response may involve large changes in polarity. They also often contain large conjugated systems that limit their solubility. Reversible photochromics are also found in applications such as toys, cosmetics, clothing and industrial applications. If necessary, they can be made to change between desired colours by combination with a permanent pigment [40].

As mentioned before, in this work, special attention will be given to the photochromism of the inorganic materials.

3.1.2.1 Silver Chlorides

Silver chloride (AgCl) is a white crystalline solid which is well known for its low solubility in water. Upon exposure to light it becomes deep greyish blue due to its decomposition in metallic silver and atomic chloride. This light-sensitive behaviour is the basis of the photographic processes. AgCl occurs naturally as a mineral chlorargyrite. The solid adopts the fcc NaCl structure, in which each Ag^+ ion is surrounded by an octahedron of six chloride ligants. One of the most famous reversible photochromic applications is the sunglasses [87]. The switching

speed of photochromic dyes is highly sensitive to the rigidity of the environment around the dye. As a result, they switch most rapidly in solution and slowest in the rigid environment like a polymer lense.

3.1.2.2 Tungsten Oxide (WO_3) and mixtures of Tungsten Oxide with Titanium oxide (WO_3-TiO_2)

Tungsten (VI) oxide, also known as tungsten trioxide (WO_3) is one of the important chromogenics that can continuously switch between two optical states, and which shows many potential applications such as in "smart windows", large area displays, automatic glare control in automotive rear-view mirrors, and erasable optical storage for example. So, extensive research studies have been carried out since Deb first reported its colouration phenomena at room temperature [93]. With the advent of research on colloidal semiconductors, He et al have published two particularly interesting papers regarding the photochromic behaviour of colloids of WO_3 and of WO_3-TiO_2. [93, 114] According to these authors, WO_3 has the band structure illustrated in Figure 3.2 and when electrons are added, they can occupy the t_{2g} band yielding W^{5+} therefore, WO_3 becomes coloured. In turn, when the electrons are removed, WO_3 recovers its original transparency as the band gap becomes wider. Moreover, these authors have also shown that the use of a photoresponsive semiconductor material such as TiO_2 (which has a different energy-band structure – see Fig. 3.3) in the presence of oxygen, enhances the optical properties of WO_3. This is thought to be due to the increase of electrons generated in the system and subsequent suppression of the recombination process of photogenerated carriers. In fact, they have actually shown that the photochromic properties of WO_3 can be tuned by adequately adjusting the proportions of tungsten oxide to titanium oxide.

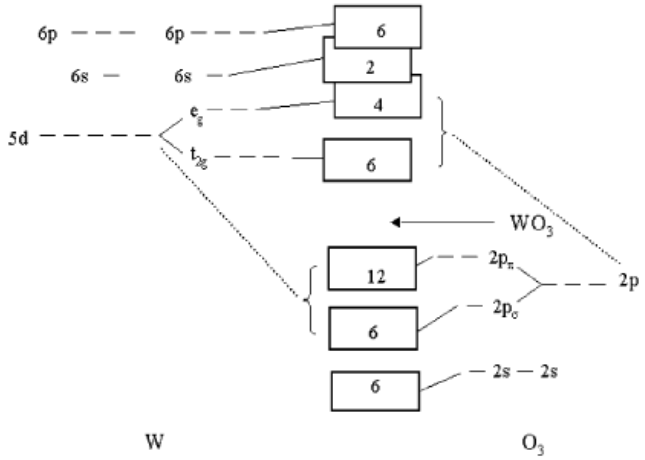

Fig. 3.2 - Schematic band structure for the WO_3 [93].

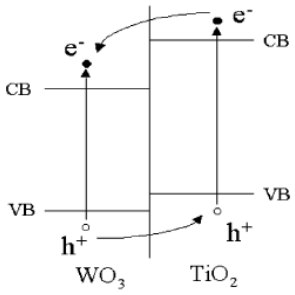

Fig. 3.3 – Energy diagram for WO_3-TiO_2 composite system [93].

3.1.3 Colorimetry

Colorimetry is the science used to quantify and describe what the human perceives. The basis for this science was established in 1931 by CIE (Commission Internationale de l' éclairage) [89]. Despite of its apparent trivial nature, colorimetry is a rather complex science, similar to spectrophotometry but its spectra are reduced to tristimulus values. According to CIE accurate specification of object colours and colour differences should be based on the three dimensional uniform colour spaces – CIELAB and CIELUV in 1976.

Tristimulus values of a colour are the quantities of the three primary colours in any three-component additive colour model used to match a colour [126]. In CIELAB space, L shows the lightness, and (a, b) the colour as shown in Fig. 3.4. The three coordinates of CIELAB represent the lightness of the colour (L, L = 0 yields black and L = 100 indicates diffuse white; specular white may be higher), its position between red/magenta and green (a, negative values indicate green while positive values indicate magenta) and its position between yellow and blue (b, negative values indicate blue and positive values indicate yellow) (See Figs. 3.4 and 3.5) [91].

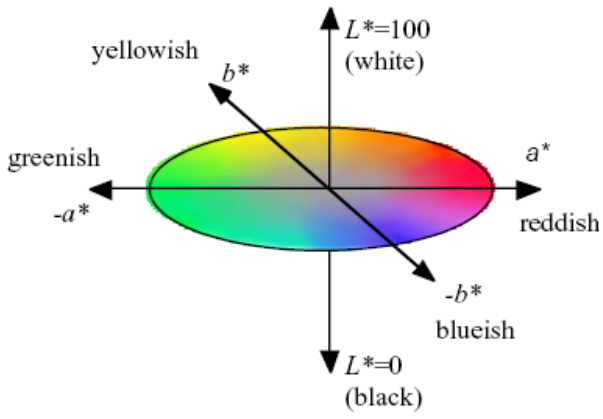

Fig. 3.4 – CIELAB colour space in 2D [26].

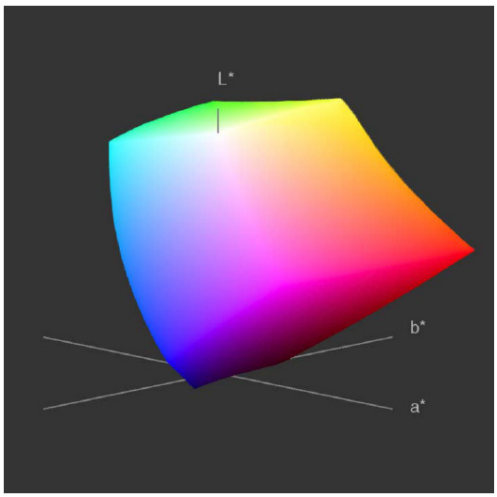

Fig. 3.5 - CIELAB colour space in 3D [91].

Several standard illuminants have been defined, e.g., standard illuminant A for incandescent light or D65 for natural daylight at a colour temperature of 6504 K. Moreover, as the geometry of the object is a crucial aspect, CIE recommends the use of one of four standard geometries – 45º/normal (45/0), normal/45º (0/45), diffuse/normal (d/0), and normal/diffuse (0/d) [89].

In this work colorimetry was used to monitor colour changes and/or changes in colour shade. This was done using the CIELAB Colour System was which is widely applied in industrial tests including at Weber Cimenfix. For most industrial purposes, colour differences are calculated from the reflectance spectra (RS). The difference of two such spectra obtained from an illuminated and non-illuminated sample, the ‘‘difference reflectance spectrum’’ (DRS), is automatically calculated by the colorimeter, as the Euclidean distance between the points in this three-dimensional space, according to the equation below. [89]

$$\Delta E^*ab = [(\Delta L^*)^2+(\Delta a^*)^2+(\Delta b)]^2$$

In this work notice should be made that the term reflectance spectra used in the context of colorimetry refers exclusively to relations between tristimulus values. Moreover, in our case we called DRS to the difference between the parameters measured L, a and b before and after the sunlight exposure in order to determined if the colour of the samples were changing, and if so, which parameters were actually changing (i.e. black to white, green to red and/or blue to yellow). As opposed to the values determined automatically by the instrument, the procedure described above provided further information regarding the photochromic processes involved.

The L, a and b values were measured for each sample before and after exposure to light and the difference between such parameters calculated and compared to those obtained for a standard sample. When the difference between any of the parameters was above one order of magnitude it was considered a “positive result”, i.e. the phtochromic effect of the additive used was detected.

3.2 Experimental

3.2.1 Addition of Halides (silver chloride)

AgCl powder was purchased from Acros Organics (purity >90%). In this work the halide compound was mechanically mixed with the semi-finished decorative mortar. Upon one day of drying in a curing room colorimetry, measurements were made before an after exposure to light.

3.2.1.1 Preparation of specimens

Two different sets of specimens have been prepared: one using a decorative mortar containing TiO_2 dye (to provide a white colour to the mortar) and another without it. For each set a standard product (0% of AgCl) was also prepared for comparison. The composition of the semi-finished product can be found in 5.2.2.

The silver chloride powder was added to the decorative mortar in the following concentrations (by weight of semi-finished product):

- 0,01%;
- 0,02%;
- 0,04%;
- 0,10%.

For 100 gram of semi-finished cement mortar the silver chloride powder was added according of the concentrations cited above. The paste was manually mixed until homogenization and then applied on the surface of a white panel for further visualization.

3.2.1.2 Results and Discussion

3.2.1.2.1 Colorimetry

Upon one day in a curing room (when the specimens were dry) the panels were kept in a dark room for 30 minutes prior to testing. Figs. 3.6 and 3.7 show the panels containing the samples prepared.

Colorimetry analyses were carried out under a fluorescent lamp considered as standard. Each specimen was measured three times. Then, the panel was kept under sunlight exposure for 1 hour and the same colorimetric analysis was carried out. The results from the reflectance spectra (RS) of the samples before and after sunlight exposure are summarized in Tables 3.1 and 3.2. Table 3.3 shows the difference reflectance spectra (DRS) of the samples before and after sunlight exposure.

Fig. 3.6 – Effect of silver chloride on DCM with white dye. STD sample (left), 0,05%, 0,10%, 0,20%, 0,40% and 1% (right).

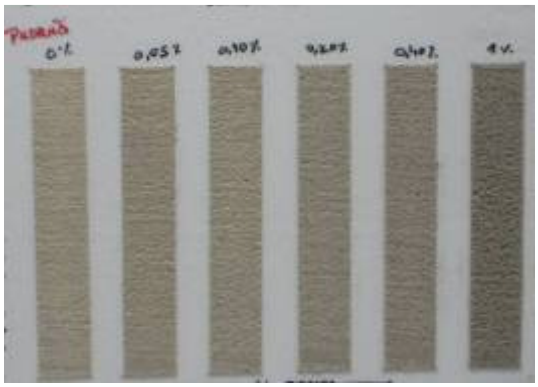

Fig. 3.7– Effect of silver chloride on DCM without white dye. STD sample (left), 0,05%, 0,10%, 0,20%, 0,40% and 1% (right).

Table 3.1 – RS results of DCM without TiO_2 before sunlight exposure.

RS of the samples before sunlight exposure						
Average	**0%**	**0,05%**	**0,10%**	**0,20%**	**0,40%**	**1%**
L	66,8	63	63,9	62,4	61,1	55,9
a	1,3	1,8	1,4	1,7	1,8	1,5
b	10,2	9,7	9	8,7	8	6,1

Table 3.2 - RS results of DCM without TiO_2 after sunlight exposure.

RS of the samples after sunlight exposure (1 hour)						
Average	**0%**	**0,05%**	**0,10%**	**0,20%**	**0,40%**	**1%**
L	66,4	62,9	63	61,9	59,7	52,6
a	1,2	1,3	1,9	1,2	0,7	1,5
b	10,5	9,9	9,1	7,7	7,8	5,9

Table 3.3 – DRS results of DCM without TiO_2.

DRS of the samples						
Average	**0%**	**0,05%**	**0,10%**	**0,20%**	**0,40%**	**1%**
ΔL	-0,4	-0,1	-0,9	-0,5	-1,4	-3,3
Δa	-0,1	-0,5	0,5	-0,5	-1,1	0
Δb	0,3	0,2	0,1	-1,0	-0,2	-0,2

As it can be seen on Table 3.3, the DRS of the samples (without white dye) were not expressive. These differences in the colour cannot be distinguished visually and even the DRS values are too similar (or smaller) to the standard sample.

The same procedure was followed for the samples using white dye. The results from the reflectance spectra (RS) of the samples before and after sunlight exposure are summarized in Tables 3.4 and 3.5. Table 3.6 shows the difference reflectance spectra (DRS) of the samples before and after sunlight exposure.

Table 3.4 – RS results of DCM with TiO_2 before sunlight exposure.

RS of the samples before sunlight exposure						
Average	**0%**	**0,05%**	**0,10%**	**0,20%**	**0,40%**	**1%**
L	78	78	76,9	76,9	77,3	75,8
a	-0,3	-0,3	-0,3	-0,3	-0,4	-0,4
b	2,7	2,6	2,8	2,9	2,5	2,1

Table 3.5 - RS results of DCM with TiO_2 after sunlight exposure.

RS of the samples after sunlight exposure (1 hour)						
Average	**0%**	**0,05%**	**0,10%**	**0,20%**	**0,40%**	**1%**
L	77	78	77,3	76,9	76,7	76,2
a	-0,9	-1,3	-1,3	-1,2	-1,5	-1,2
b	3,1	2,2	2,4	2,6	2,1	1,6

Table 3.6 – DRS results of DCM with TiO_2.

DRS of the samples						
Average	**0%**	**0,05%**	**0,10%**	**0,20%**	**0,40%**	**1%**
ΔL	-1,0	0	0,4	0	-0,6	0,4
Δa	-0,6	-1,0	-1,0	-0,9	-1,1	-0,8
Δb	0,4	-0,4	-0,4	-0,3	-0,4	-0,5

As it can be seen on Table 3.6, the DRS of the samples (with white dye) were also not expressive. As in the previous case these differences on the colour cannot be distinguished visually or and even the DRS values are too similar (or smaller) to the standard sample.

Upon light exposure AgCl turns to greyish or purplish colouration due its conversion to silver in chloride [58]. In fact, due to its high sensitive to oxidation by atmospheric oxygen AgCl may also undergo oxidation during the preparation of the mortar paste. Possible reasons for the poor results obtained are probably due chemical reaction between the components of the cement paste and the silver chloride resulting in the oxidation of the latter. Moreover the concentration of the halide compound might not be enough to be detected. However, bearing in mind the high price of AgCl the use of higher concentrations would result in commercially unviable DCM.

Having checked the literature, another cause for the results obtained may be related to the fact that the photochromic effect is highly sensitive to the rigidity of the environment around the dye. Therefore, it is possible that due the rigid structure of the cement mortar after cure ageing it may not be possible for the AgCl structure to expand after light exposure hence, not achieving the colour change. Another reason, possibly the most probable, for the poor results obtained in this work was the fact that copper chloride (CuCl) crystals were not added together with the AgCl as it is done in the case of the photogrey lenses. In fact it has been reported that CuCl is responsible for the reverse photochromic effect of the AgCl [92]. Unfortunately, this information

was only found when this thesis was being written. The main mechanism of the susceptibility to oxidation and reduction of the AgCl by light is described below:

$$Cl^- \xrightarrow{\text{oxidation}} Cl + e^-$$

$$Ag^+ + e^- \xrightarrow{\text{reduction}} Ag$$

The chloride ions are oxidized to produce chlorine atoms and an electron. The electron is then transferred to the silver ions to produce silver atoms. These atoms cluster together and block the transmittance of light, causing the lenses to darken [92].

The net effect of these reactions is that the lenses become transparent again as the silver and chloride atoms are converted to their original oxidized and reduced states. In this way when the lenses are removed from light the presence of copper chloride reverses the darkening process as illustrated in the following scheme:

$$\underset{\text{oxidizing agent}}{Cl} + \underset{\text{reducing agent}}{Cu^+} \longrightarrow \underset{\text{oxidized species}}{Cu^{+2}} + \underset{\text{reduced species}}{Cl^-}$$

The chlorine atoms formed upon exposure to light are reduced by the copper ions, preventing their escape as gaseous atoms from the matrix [92]. The (+1) ion copper is oxidized to produce copper (+2) ions, which then react with the silver atoms as shown below:

$$\underset{\text{oxidizing agent}}{Cu^{+2}} + \underset{\text{reducing agent}}{Ag} \longrightarrow \underset{\text{reduced species}}{Cu^{+1}} + \underset{\text{oxidized species}}{Ag^+}$$

Probably the AgCl was oxidized during the preparation of the sample and could not act in the reverse way due to the absence of CuCl.

3.2.2 Addition of Halides (milled photochromic lenses containing silver chloride)

As the use of the AgCl powder did not provide satisfactory results it was decided to try the use of photogrey lenses. In this case the photochromic filler can be provided at a low cost or even no-cost from the eyeglass industry, as was in our case.

The use of milled lenses may act in a different way because the halides are dispersed in the glass in pre-tested concentrations and approved for commercial uses. Furthermore the lenses may act as a reinforcement material for the mortar due to the presence of SiO_2.

3.2.2.1 Preparation of specimens

The photochromic eyeglass lenses were kindly given by the company IOLA - SOLA Optical Portugal that produces lenses using glass and polycarbonate materials. As the main composition of glasses is SiO_2 and it can be used in mortars as fillers providing enhancement of the mechanical properties, glass-based lenses were chosen to be used in this work instead of the polymeric ones. Besides, glass is easier to be milled when compared to polycarbonate. Moreover, in this case the AgCl is dispersed in the entire material (glass lenses) while in polymer based ones just a thin film is used.

For industrial and commercial purposes, the company did not provide the composition of the lenses. The lenses were milled until a uniform size of the particle was reached. The milling procedure of the lenses is described in the 5.2.7.

Two different sets, one using decorative mortar containing TiO_2 dye (to provide a white colour to the mortar) and another decorative mortar without TiO_2 dye, were prepared in each case a standard product (0% of milled lenses) was used for comparison.

For 100 gram of semi-finished cement mortar the milled lenses powder was added according of the concentrations cited below:

- 0,01%;
- 0,02%;
- 0,04%;
- 0,10%.

The paste was manually mixed until homogenization and then applied on the surface of a white panel for further visualization.

3.2.2.2 Results and Discussion

3.2.2.2.1 Inductively coupled plasma mass spectrometry (ICP-MS) of the milled lenses

A sample of the milled eyeglass lenses was analysed by ICP-MS in order to determine its elemental composition (especially the Ag concentration). Table 3.7 shows the concentrations of the ions obtained:

Table 3.7 – Elemental analysis of the photochromic eyeglass lenses.

B	Mg	Na	Si	K	Ag	Cd	Ba	Pb
µg/g	µg/g	% (m/m)	µg/g	µg/g	µg/g	µg/g	µg/g	µg/g
<30	99,4	10,8	<500	2050	25,1	0,32	4130	1090

As it can be seen the concentration of Ag in the sample was high confirming the presence of the AgCl. The other components are common in the composition of the glasses used to produce this kind of lenses.

3.2.2.2.2. Size Dispersion

The average size and dispersion of the lenses' particles was carried out using a Zeta Size equipment. Fig. 3.8 shows the size distribution of the particles and Table 3.8 summarizes the average distribution of the particles.

Table 3.8 - Average distribution of the particles from the eyeglass lenses.

Size (nm)	Mean (Intensity %)
712	3,4
825	9,6
955	16,3
1110	20,7
1280	20,7
1480	16,4
1720	9,6
1990	3,2

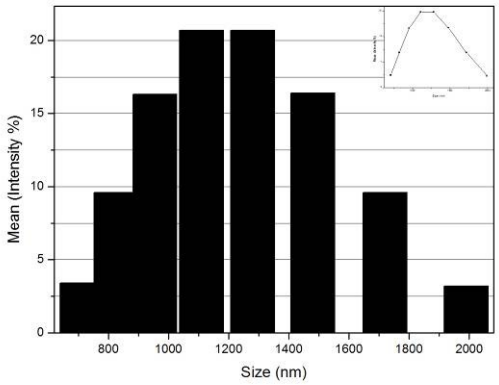

Fig. 3.8 - Average distribution of the particles from the eyeglass lenses.

As can be seen the average size of the particles was around 1110 and 1280 nanometres. The sample showed a broad distribution which is good for its dispersion in the mortar.

3.2.2.2.3 Colorimetry

Upon one day in the curing room (when the specimens were dry) the panel was kept in a dark room for 30 minutes to avoid any light exposure. Colorimetry analyses were carried out under a fluorescent lamp considered as standard. Each specimen was measured three times. Then, the panel was kept upon sunlight exposure for 1 hour and the same colorimetric analysis was carried out. The results from the reflectance spectra (RS) of the samples before and after sunlight exposure are summarised in Tables 3.9 and 3.10. Table 3.11 shows the difference reflectance spectra (DRS) of the samples before and after sunlight exposure. Figs. 3.9 and 3.10 show the panels containing the samples prepared.

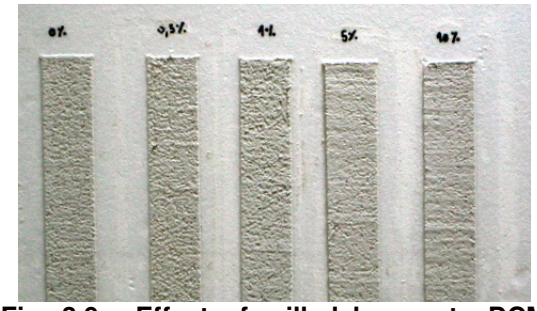

Fig. 3.9 - Effect of milled lenses to DCM with TiO_2. STD (left), 0,05%, 0,10%, 0,20%, 0,40% and 1% (right).

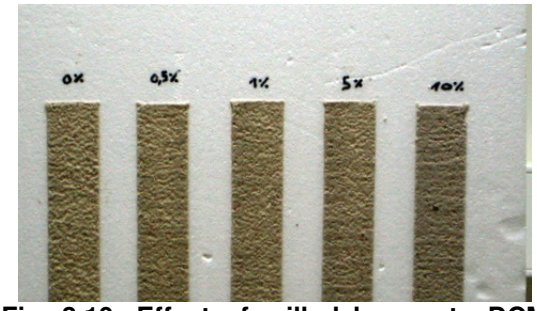

Fig. 3.10- Effect of milled lenses to DCM without TiO_2. STD (left), 0,05%, 0,10%, 0,20%, 0,40% and 1% (right).

Table 3.9 – RS results of DCM without TiO_2 before sunlight exposure.

RS of the samples before sunlight exposure					
Average	**0%**	**0,50%**	**1%**	**5%**	**10%**
L	63,30	64,17	64,40	64,30	63,77
a	1,87	1,40	1,40	2,13	1,73
b	10,87	11,10	10,70	10,70	9,20

Table 3.10 - RS results of DCM without TiO_2 after sunlight exposure.

RS of the samples after sunlight exposure (1 hour)					
Average	**0%**	**0,50%**	**1%**	**5%**	**10%**
L	64,33	63,47	64,13	64,20	63,83
a	1,33	1,60	1,47	1,50	1,47
b	11,03	11,23	10,87	10,27	8,73

Table 3.11 – DRS results of DCM without TiO_2.

DRS of the samples					
Average	**0%**	**0,50%**	**1%**	**5%**	**10%**
ΔL	1,03	-0,70	-0,27	-0,10	0,07
Δa	-0,53	0,20	0,07	-0,63	-0,27
Δb	0,17	0,13	0,17	-0,43	-0,47

As it can be seen on Table 3.11, the DRS of the samples without the white dye were not expressive as the differences in the colour cannot be distinguished visually and even the DRS values are too similar (or smaller) to the standard sample. The possible reasons for the negative results are the same as explained previously for AgCl.

The same procedure was applied for the samples using white dye. The results from the reflectance spectra (RS) of the samples before and after sunlight exposure are summarised in Tables 3.12 and 3.13. Table 3.14 shows the difference reflectance spectra (DRS) of the samples before and after sunlight exposure.

Table 3.12 – RS results of DCM with TiO_2 before sunlight exposure.

RS of the samples before sunlight exposure					
Average	**0%**	**0,50%**	**1%**	**5%**	**10%**
L	76,73	76,23	75,37	77,50	75,67
a	-0,10	-0,10	-0,53	-0,30	-0,03
b	3,43	3,63	3,37	3,50	3,53

Table 3.13 - RS results of DCM with TiO_2 after sunlight exposure.

RS of the samples after sunlight exposure (1 hour)					
Average	**0%**	**0,50%**	**1%**	**5%**	**10%**
L	77,03	76,47	76,07	76,83	75,77
a	-0,43	-0,33	-0,83	-0,30	-0,23
b	3,63	3,77	3,60	3,60	3,40

Table 3.14 - DRS results of DCM with TiO_2.

DRS of the samples					
Average	**0%**	**0,50%**	**1%**	**5%**	**10%**
ΔL	0,30	0,23	0,70	-0,67	0,10
Δa	-0,33	-0,23	-0,30	0,00	-0,20
Δb	0,20	0,13	0,23	0,10	-0,13

As can it be seen on the Table 3.14 the variation on the colorimetry results of the samples (with white dye) were not significant. These differences on the colour cannot be distinguished visually and even the DRS values are too similar (or smaller) to the standard sample. The possible reasons for these results are the same as explained previously for AgCl.

As regards the concentration of milled lenses it was not increased due the negative effects that it might cause on the physical and mechanical properties of the DCM. Another possible reason for the results obtained is probably the concentration of the AgCl in the milled lenses. According to the ICP-MS results, the concentration of the Ag (from AgCl) in the lenses was 25 µg/g (by weight of glass); probably not enough for the photochromic effect to be detected in the composite. Notice should be made that copper was not analysed by the ICP-MS because at that time we did not know about its effect on the lenses' photochromism. However, as the lenses showed positive photochromic effect after being exposed to the sunlight in this case, the poor results obtained were not related to the eventual absence of copper.

3.2.3 Addition of Tungsten Oxide (WO_3)

Taking in account the poor results regarding the use of halides (AgCl and milled lenses), a new approach was studied. Is known from the literature [35-38, 41, 115] that materials based on WO_3 exhibit photochromic effects upon sunlight exposure. Moreover, further to He et al works, which have already been briefly discussed in 3.1.2 this material was also used in combination with TiO_2.

3.2.3.1 Preparation of the DCM-WO_3 specimens

Specimens have been prepared using decorative mortar containing TiO_2 dye. A standard product (0% of WO_3) was prepared for comparison.

For 100 gram of semi-finished cement mortar the tungsten oxide powder was added according of the concentrations cited below:

- 0,5%;
- 1,0%;
- 2,5%

The paste was manually mixed until homogenization and then applied on the surface of a white panel for further visualization.

3.2.3.2 Results and Discussion

3.2.3.2.1 Colorimetry

Upon one day in the curing room (when the specimens were dry) the panel was kept in a dark room for 30 minutes to avoid any light exposure. After this time, colorimetry analyses were carried out under a fluorescent lamp considered as standard. Each specimen was measured three times. Then, the panel was kept upon sunlight exposure for 1 hour and the same colorimetric analysis was carried out. The results from the reflectance spectra (RS) of the samples before and after sunlight exposure are summarized in Tables 3.15 and 3.16. Table 3.17 shows the difference reflectance spectra (DRS) of the samples before and after sunlight exposure.

Figure 3.11 shows the panel containing the samples after one day in the curing room.

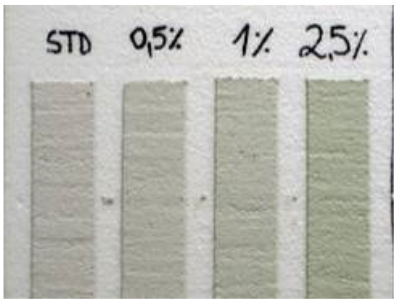

Fig. 3.11 - Effect of WO_3 on DCM. From left to right, STD, 0,5%, 1,0% and 2,5% of WO_3.

Table 3.15 – RS results of DCM with TiO_2 before sunlight exposure.

RS of the samples before sunlight exposure				
Average	**STD**	**0,50%**	**1,00%**	**2,50%**
L	78,63	77,60	76,33	74,10
a	-0,50	-2,43	-3,60	-5,43
b	3,27	4,40	5,17	6,40

Table 3.16 - RS results of DCM with TiO_2 after sunlight exposure.

RS of the samples after sunlight exposure (1 hour)				
Average	**STD**	**0,50%**	**1,00%**	**2,50%**
L	78,47	76,43	74,97	71,37
a	-0,60	-2,90	-4,03	-5,83
b	3,17	3,57	3,77	4,40

Table 3.17 – DRS results of DCM with TiO_2.

DRS of the samples				
Average	**STD**	**0,50%**	**1,00%**	**2,50%**
ΔL	-0,17	-1,17	-1,37	-2,73
Δa	-0,10	-0,47	-0,43	-0,40
Δb	-0,10	-0,83	-1,40	-2,00

From the tables above it is possible to observe that the results of the samples were expressive. The samples after 1 hour of sunlight exposure became a little bit darker, greener and bluer.

The parameter "**L**", related to the lightness, tends to decrease upon sunlight exposure when the concentration of WO_3 powder is increased. The parameter "**a**", related to the green-red colour, was reduced but the value was kept constant even when the concentration of the WO_3 powder was increased. The parameter "**b**", related to the blue-yellow colour, also decreased upon with sunlight exposure when the concentration of WO_3 powder was increased.

The colours from the sample (before and after sunlight exposure) containing 2,5% of WO_3 powder (sample with the highest differences on the results of the colorimetry, DRS) were simulated on the Abobe Photoshop program using real parameters (L, a and b from Cielab space) and shown on Figs. 3.12 and 3.13.

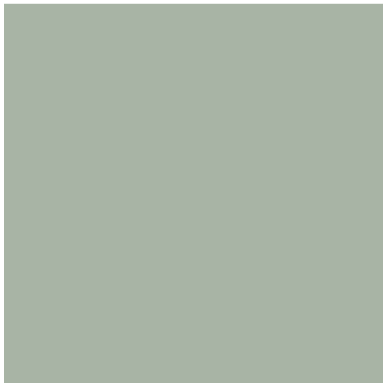

Fig. 3.12 – Colour (simulated on Abobe Photoshop) of the sample before sunlight exposure.

Fig. 3.13 - Colour (simulated on Abobe Photoshop) of the sample after sunlight exposure.

Fig. 3.14 – Possible colour (simulated on Adobe Photoshop) using the DRS extrapolated values of the samples containing WO_3 powder.

These differences are still not easily distinguished by naked eye after sunlight exposure and cannot still be used for commercial purposes. However, this material may have commercial applications in the future with further study on enhancement of its photochromic effect.

Fig. 3.14 shows a colour simulated on Adobe Photoshop using the DRS values calculated for the sample prepared using 2,5% of WO_3 which were multiplied by 10. This exercise was done to have an idea of the colour that might be obtained if the photochromic effect of the DCM would be increased by 10 fold. As it can be seen in the Fig. 3.14 using extrapolated values, the colour tends to be darker and bluer after sunlight exposure.

3.2.4 Addition of tungsten oxide mixed with titanium oxide nanoparticles (WO_3-TiO_2)

Taking into account the promising results regarding the use of WO_3 powder though not very significant, mixtures of this material with TiO_2 were studied aiming at improving the photochromism effect. As referred in the introduction the use of WO_3 combined with TiO_2 nanoparticles is known to enhance the photochromic effects upon sunlight exposure. [34, 42, 93, 114] Based on He et al. work [114] who obtained positive results using WO_3-TiO_2 colloids synthesized via the forced hydrolysis technique, in this work mixtures of commercial powders of WO_3 and TiO_2 were tested. The reasons for this option were due to the time necessary for the preparation of the colloids and the fact that, the semi-finished mortar should no longer had any addition of water.

In order to assess the effect of the ratio between the two components two composites have been tested. Composite 4026 WT was produced using the molar ratios 0,40 M (WO_3): 0,26 M (TiO_2) while composite 02363 WT was produced using the molar ratios 0,023 M (WO_3): 0,063 M (TiO_2). These ratios were the same as those tested by He et al using colloids.

3.2.4.1 Preparation of DCM-4026 WT and DCM-02363 WT specimens

Composites WO_3-TiO_2, called in this work 4026 WT and 02363 WT depending on the molar ratios were prepared using WO_3 and TiO_2 nanoparticles purchased from Degussa. For 4026 WT the molar ratio was 0,40M (WO_3) : 0,26 M (TiO_2). For 02363 WT the molar ratio was 0,023 M (WO_3): 0,063 M (TiO_2). Both components were weighted and mixed manually. Neither water nor any other dispersant was used.

The quantities used for each case, based on 100 gram of semi-finished mortar with TiO_2 dye, were:

For DCM-4026 WT:

- 0,85%;
- 1,70%;
- 3,4%.

And for DCM-02363 WT

- 1,03%;
- 2,6%;
- 4,12%.

The paste was manually mixed until homogenization and then applied on the surface of a white panel for further visualization. A standard product (0% of WO_3-TiO_2 compound) was prepared for comparison.

3.2.4.2 Results and Discussion of DCM-4026 WT

3.2.4.2.1 Colorimetry

Upon one day in the curing room (when the specimens were dry) the panel was kept in a dark room for 30 minutes to avoid any light exposure. After this time, colorimetry analyses were carried out under a fluorescent lamp considered as standard. Each specimen was measured three times. Then, the panel was kept under sunlight exposure for 1 hour and the same colorimetric analysis was carried out. The results from the reflectance spectra (RS) of the samples before and after sunlight exposure are summarised in Tables 3.18 and 3.19. Table 3.20 shows the difference reflectance spectra (DRS) of the samples before and after sunlight exposure.

Figure 3.15 shows the panel containing the samples after one day in the curing room.

Fig. 3.15 - Effect of 4026 WT on DCM. From left to right, STD, 0,5%, 1,0% and 2,5% of 4026 WT.

Table 3.18 – RS results of DCM-4026 WT before sunlight exposure.

RS of the samples before sunlight exposure				
Average	**STD**	**0,85%**	**1,70%**	**3,40%**
L	78,90	77,13	74,83	72,27
a	-0,57	-2,97	-4,27	-5,83
b	3,23	4,73	5,37	5,70

Table 3.19 – DRS results of DCM-4026 WT after sunlight exposure.

RS of the samples after sunlight exposure (1 hour)				
Average	**STD**	**0,85%**	**1,70%**	**3,40%**
L	78,77	75,73	72,33	69,63
a	-0,63	-3,53	-4,93	-6,37
b	3,20	3,53	3,40	3,27

Table 3.20 – DRS of the DCM-4026 WT samples.

DRS of the samples				
Average	**STD**	**0,85%**	**1,70%**	**3,40%**
ΔL	-0,13	-1,40	-2,50	-2,63
Δa	-0,07	-0,57	-0,67	-0,53
Δb	-0,03	-1,20	-1,97	-2,43

From the tables above it is possible to confirm that the results of the samples were expressive. The results were still better than those obtained using just WO_3 as it can be compared from Tables 3.15 and 3.16.

The samples after sunlight exposure became a little bit darker, greener and bluer. The parameter "**L**" tends to decrease upon sunlight exposure even when the 4026 WT is increased. The parameter "**a**" was reduced but the value was kept constant even when the concentration of the 4026 WT was increased. The parameter "**b**" also tends to decrease upon sunlight exposure when the concentration of 4026 WT powder was increased.

The colours from the sample (before and after sunlight exposure) containing 3,4% of 4026 WT powder (sample with highest differences of DRS) were simulated on the program Abobe Photoshop using real parameters (L, a and b from Cielab scale) and are shown on Figs. 3.1 and 3.17.

Fig. 3.18 shows a colour simulated on Adobe Photoshop using the DRS values calculated for the sample prepared using 3,4% of 4026 WT powder which were multiplied by 10. This exercise was done to have an idea of the colour that may be achieved in the future if the photochromic effect of the DCM is increased the same trend.

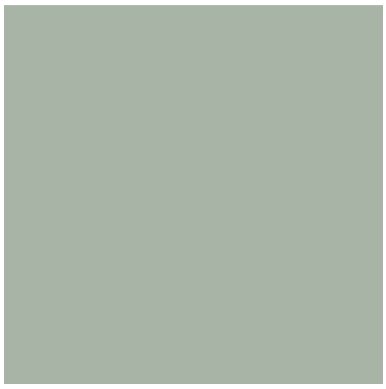

Fig. 3.16 – Colour (simulated on Abobe Photoshop) of the sample before sunlight exposure.

Fig. 3.17 - Colour (simulated on Abobe Photoshop) of the sample after sunlight exposure.

As it can be seen in the Fig. 3.18 using extrapolated values, the colour tends to be darker and bluer after the sunlight exposure when the concentration of 4026 WT powder is increased.

These differences are still hard to distinguish by the naked eye after sunlight exposure and still cannot be used for commercial purposes. This material may have commercial applications in the future after further studies on the enhancement of its photochromic effect.

Fig. 3.18 – Possible colour (simulated on Adobe Photoshop) using the DRS extrapolated values of the samples containing 4026 WT powder.

3.2.4.3 Results and Discussion of DCM-02363 WT

3.2.4.3.1 Colorimetry

Upon one day in the curing room (when the specimens were dry) the panel was kept in a dark room for 30 minutes to avoid any light exposure. After this time, colorimetry analyses were carried out under a fluorescent lamp considered as standard. Each specimen was measured three times. Then, the panel was kept upon sunlight exposure for 1 hour and the same colorimetric analysis was carried out. The results from the reflectance spectra (RS) of the samples before and after sunlight exposure can be seen on Tables 3.21 and 3.22. Table 3.23 the difference reflectance spectra (DRS) of the samples before and after sunlight exposure.

Figure 3.19 shows the panel containing the samples after one day in the curing room.

Fig. 3.19 - Effect of 02363 WT on DCM. From left to right, STD, 1,03%, 2,6% and 4,12% of 02363 WT.

Table 3.21 – RS results of DCM-02363 WT before sunlight exposure.

RS of the samples before sunlight exposure				
Average	**STD**	**1,03%**	**2,60%**	**4,12%**
L	78,50	76,90	74,53	72,90
a	-0,47	-2,60	-4,50	-5,37
b	3,27	4,37	5,20	5,33

Table 3.22 - RS results of DCM-02363 WT after sunlight exposure.

RS of the samples after sunlight exposure (1 hour)				
Average	**STD**	**1,03%**	**2,60%**	**4,12%**
L	78,03	75,33	72,07	69,63
a	-0,73	-3,20	-5,13	-1,97
b	3,53	3,33	3,17	2,80

Table 3.23 – DRS of the DCM-02363 WT samples.

DRS of the samples				
Average	**STD**	**1,03%**	**2,60%**	**4,12%**
ΔL	-0,47	-1,57	-2,47	-3,27
Δa	-0,27	-0,60	-0,63	3,40
Δb	0,27	-1,03	-2,03	-2,53

From the tables above it is possible to confirm that the results of the samples were also significant. The results were still better than those obtained for composite 4026 WT.

The parameter "**L**" tends to decrease upon sunlight exposure when the concentration of 02363 WT is increased.

Different from the specimens prepared with WO_3 and 4026 WT, for the sample containing 4,12% of 02363 WT the values of the "a" parameter increased considerably (instead of decreasing) tending to the colour red against what was expected. In all samples tested before the values for that parameter decreased to greener values. These results are quite important commercially, opening possibilities for the mortar to change colour instead of just changing its shade.

The parameter "**b**" related to the blue-yellow colour also tends to decrease upon sunlight exposure when the concentration of 02363 WT powder was increased. The samples after sunlight exposure became a little bit darker, less green (tending to red) and bluer.

The colours from the sample (before and after sunlight exposure) containing 4,12% of 02363 WT (sample with highest DRS) were simulated on the program Abobe Photoshop using real parameters (L, a and b from Cielab scale) which are shown on the Figs. 3.20 and 3.21.

Fig. 3.22 shows a colour simulated on Adobe Photoshop using the DRS values calculated for the sample prepared using 4,12 % of 02363 WT powder which were multiplied by 10. This

exercise was done to have an idea of the colour that may be achieved in the future if the photochromic effect of the DCM is increased in the same trend.

Fig. 3.20 - Colour (simulated on Abobe Photoshop) of the sample before sunlight exposure.

Fig. 3.21 - Colour (simulated on Abobe Photoshop) of the sample after sunlight exposure.

Fig. 3.22 – Possible colour (simulated on Adobe Photoshop) using the DRS extrapolated values of the samples containing 4,12 % of 02363 WT powder.

As it can be seen in the Fig. 3.22 using extrapolated values, the colour tends to be purple after sunlight exposure when the concentration of 02363 WT powder is increased.

These differences are still hard to distinguish by the naked eye after sunlight exposure and still cannot be used for commercial purposes. This material may have commercial applications in the future after further studies on the enhancement of its photochromic effect.

The improvement on the photochromic effect registered resulting from the addition of TiO_2 seems to be explained by the argument proposed by He et al for colloidal suspensions of these materials. As discussed earlier in 3.1.2, the TiO_2 seems to be responsible for the increase of photogenerated electrons that participate in the colouration process for the same concentration of WO_3 [114]. Considering the simplicity of the procedure followed in this study and the fact that commercial WO_3 particles were used, the results obtained are particularly promising.

This material may have commercial applications in future though further studies regarding the enhancement of its photochromic effect are still necessary.

3.2.5 - Reinforced Decorative Mortar (DCM-MWCNT)

As DCM are used to cover walls, floors and grounds and they are always related to aesthetical purposes, the objective of this work was to test the possibility of using CNTs in DCM to increase the mechanical properties without changing the aesthetics of the product i.e. the texture of the mortar, agglomerates and etc…).

Different from the previous studies, no colorimetry or mechanical/physical properties were carried out. Assessments were simply made by visual inspection to detect the presence of agglomerates.

Taking in account that the DCM is a semi-finished product (i.e. already contains water) the CNTs had to be added almost directly to the mortar without any previous dispersion. Different amounts of MWCNT and MWCNT-oxy have been tested.

3.2.5.1 Addition of MWCNT to DCM

DCM-MWCNT was prepared via manual mixture. For 100 gram of semi-finished mortar with TiO_2 dye, MWCNT were added according of the concentrations cited below:

- 0,10% with dispersion in water (**Dwt**);
- 0,10% with dispersion in water and Triton X405 (**Dt**);
- 0,10% with dispersion in water, Triton X405 and poly(acrylic acid) (**Da**) ;
- 0,25% using dry mixture (**Dd**);
- 0,30% using dry mixture (**Dd**).

The paste was manually mixed until homogenization and then applied on the surface of a white panel for further visualization. A standard product (0 w% of MWCNT) was prepared for comparison.

As it can be seen in Fig. 3.23 all samples had aggregates of CNT. In samples where the concentration of CNTs was higher (0,25% and 0,30% of CNT) the addition was almost impossible due to the high amount of agglomerates formed during the trowelling. As a result the workability of the mortars decreased with the use of the MWCNTs. In conclusion, it is impossible to use neat MWCNT in any concentration as the formation of agglomerates significantly changes the workability and aesthetics of the original product.

Fig. 3.23 - Effect of addition of MWCNT in different concentrations and dispersion methods. Left to right side: (i) STD, (ii) 0,10% of CNT (Dt), (iii) 0,10% of CNT Dwt, Da and, (iv) 0,25% CNT Dd, (v) 0,30% CNT (Dd).

3.2.5.2 – Addition of MWCNT-oxy to DCM

Next, the effect of MWCNT-oxy was tested using 0,10 w%. From the visual inspection it is possible to conclude that it is possible to use MWCNT-oxy in DCM. The MWCNT-oxy were well dispersion in the DCM resulting in a product without agglomerates. The colour of the DCM with the nanotubes became greyish due the good dispersion of the nanotubes. The changing of the colour is a good indicative that the nanotubes were well dispersed in the material. Fig. 3.24 shows the panel where the samples were applied.

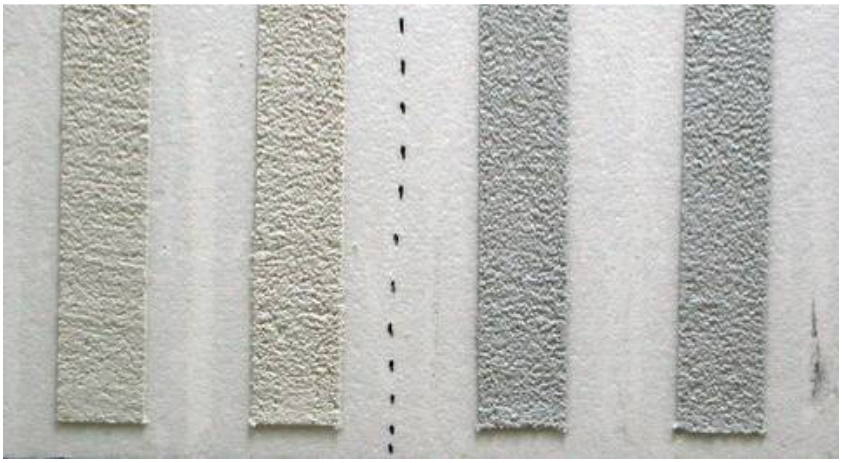

Fig. 3.24- Effect of MWCNT-oxy on DCM. STD sample (left side) and right side (DCM with MWCNT-oxy).

The workability of the DCM decrease a little bit with the addition of the MWCNT-oxy when compared to the standard product but the trowelling process occurred normally.

The use of oxidized MWCNT is possible due to the good affinity of the nanotubes to the semi-finished product.

3.3 Conclusions

The industry of pigments as well as researchers are investing time and new technologies to produce materials that present photochromic behaviour for applications in a wide variety of areas but it is still difficult to find materials that may act efficiently in DCM. DCM with photochromic materials have a particularly potential for some niches of the market if their effects can be detected by naked eye after some exposure to sunlight. This work showed that photochromic materials may in future be possible candidates to enhance aesthetical properties of decorative mortars.

Regarding the materials tested during this work, the use of the silver chloride did not result in positive effects of photochromism on the decorative mortar (with or without the presence of the TiO_2 dye). Possible reasons may include (i) its oxidation when in contact of the oxygen from the atmosphere air, (ii) some chemical reaction with the components of the fresh mortar paste, (iii) the stiffness of the cement mortar after curing blocking the free movements of the Ag and Cl and, (iv) the fact that copper chloride was not added to the samples resulting in this way in a irreversible photochromic effect.

Regarding the use of the milled lenses, its addition did not result in positive effects of photochromism on the decorative mortar (with or without the presence of the TiO_2 dye). Possible reasons may include the concentration of milled lenses used in this work which possibly did not match the necessary percentage to yield some photochromic effect or even the quality of the lenses. The increase of this percentage becomes impossible due to the possible changes on the mechanical properties of the decorative mortar

Addition of the WO_3 powder resulted in positive effects of photochromism on the decorative mortar but cannot be used commercially due its low photochromism effect. From the DRS values of the CIELAB Colour System it is possible to affirm that the colour of the sample tends to become darker and bluer when the concentration of the WO_3 powder is increased. Upon sunlight exposure the samples presented changes related to the colour shade.

Addition of 4026 WT resulted in positive effects of photochromism on the decorative mortar but still cannot be used commercially due its low photochromism effect. From the DRS values of the CIELAB Colour System it is possible to affirm that the colour of the sample tends to become darker and bluer when the concentration of the 2640 WT is increased. Upon sunlight exposure the samples presented changes related to the colour shade.

Addition of 02363 WT resulted in positive effects of photochromism on the decorative mortar but cannot be used commercially due its low photochromism effect. From the DRS values of the CIELAB Colour System it is possible to affirm that the colour of the sample become darker, tending to the purple colour (mixture of the red and blue) when the concentration of the 02363 WT is increased. Upon sunlight exposure the samples presented changes related to the colour. The enhancement of photochromism effect obtained can be

explained by the combination of TiO_2 and WO_3 that according to He et al results from the fact that the total quantity of electrons originally generated in the system increases after the combination of the TiO_2 (photoresponsive semiconductor) with the WO_3.

As mentioned before these materials using WO_3 and TiO_2 still cannot be used commercially, but they are very promising materials in the future when their photochromic properties will be enhanced.

As a suggestion for further works, the use of different methods of mixing the materials as colloids or gel-sol solutions [93, 114] and even thermal treatments [27, 41] should be considered. The use of different materials such as bismuth vanadate [27, 45], Ni-Al [46], $Tb_3Ga_{12}O_{12}$ [52], POM [47, 49, 51], SiO_2-TiO_2 [55] Cu [53] as well as Co-Fe [54] are also promising materials that might be worth investigating.

For the colorimetry analyses it is suggested the use of an UV-lamp that simulates the sunlight exposure. The use of this lamp will provide the same irradiation on the samples and the analyses can be carried out using different exposure times.

Finally, although the use of these DCM with addition of photochromic materials still cannot be used commercially due its low photochromism effect it was proven they are promising materials to be used in the future.

As regards the effect of MWCNT, the use of MWCNT without any surface modification is not possible also in DCM just like it was verified for SCM. The products have shown the presence of agglomerates for all concentrations and methods of dispersion tested. The workability of the product decreased during the trowelling process hence its application becomes almost impossible. However, the use of MWCNT-oxy yielded good results and no agglomerates were detected. The workability was inferior to the standard product but can be used without problems. These nanotubes have shown good affinity to the DCM resulting in a greyish homogenous product.

Chapter 4 - Conclusions

This study has shown that it is possible to distribute CNT across cement grains using oxidation and dispersion in a titanium oxide suspension techniques. The key for the improvement of the SCM's mechanical properties is the homogeneous dispersion of the nanotubes in the cement matrix. The answer to provide a good interaction between the reinforcement and the matrix is the affinity of the CNT towards polar media, in particular water.

The use of neat MWCNT did not yield good results due its bad dispersion in the cement paste resulting in aggregates and a non-uniform distribution of the bundles within the matrix which led to a decrease in the mechanical properties. The optimum concentration of CNT seems to be 0,10% (wt %) of the cement powder. However, it is suggested that further studies should be aimed at establishing the optimum concentrations for carbon nanotubes oxidized and dispersed in titanium oxide suspensions to confirm this value.

Dispersion experiments with oxidized carbon nanotubes showed that the surface treatment using HNO_3 gave to the nanotubes a good affinity to water. The same behaviour was found using MWCNT-TiO_2.

Nanotube pull-out from the matrix is possibly the predominant mode of overload failure. This seems reasonable because the interfacial (MWCNT-cement mortar) shear strength is believed to be less than the nanotubes tensile strength.

The use of MWCNT-TiO_2 is the most promising when compared with all other samples tested in this work due to the easy of preparation and time consumed for dispersion. Furthermore this dispersion method can be easily adapted for industrial production scale.

DCM with photochromic materials have a particularly potential for some niches of the market if their effects can be detected by naked eye after some exposure to sunlight. This work showed that photochromic materials may in future be possible candidates to enhance aesthetical properties of decorative mortars.

Regarding the materials prepared during this work, the use of silver chloride and of milled photochromic eyeglass lenses did not promote any effects on the decorative mortar (with or without TiO_2 dye).

Addition of WO_3 powder and of mixtures of WO_3 and TiO_2 (2640 WT and 02363 WT) resulted in positive effects but cannot be used commercially due to the low photochromism effect. DRS values of the CIELAB Colour System regarding the WO_3 powder or 2640 WT samples showed that the colour of the sample tends to become darker and bluer when the concentration of the WO_3 powder or of 2640 WT is increased. The same analysis for the sample prepared with 02363 WT showed that the colour of the sample become darker, tending to the purple colour when the concentration of 02363 WT is increased moreover, upon sunlight exposure these samples presented colour changes.

Regarding the addition of MWCNT (neat) to DCM the products obtained have shown the presence of agglomerates in any concentration and methods of dispersion used. The workability of the product decreased during the trowelling process becoming difficult its application. The use of MWCNT-oxy has shown good results since no agglomerates were observed. The workability was inferior to that of the standard product but still can be used without problems. These nanotubes have shown good affinity to the DCM, resulting in a greyish homogeneous product.

Chapter 5 – Materials and Methods

5.1 Materials

All raw materials used to produce the cement mortars in this work were provided by Weber Cimenfix and the samples were prepared there. Specimens were maintained inside a curing room at least for 28 days at 55% relative humidity (RH) at 23 ºC and demolded after 24 hours after preparation.

5.1.1 Carbon Nanotubes

The MWCNT used in the present work were supplied by Nanocyl Co. The properties specified by the company can be seen below in Table 1. The purification and oxidation were done at the Chemistry Department in collaboration with Madhu Phani.

Table 5.1 - Properties of MWCNT.

Characteristics	MWCNT
External diameter	<10nm, 10-20nm, 10-30 nm, 20-40 nm, 40-60 nm e 60-100 nm.
Purity	≥95%
Amorphous carbon	2%
Ash	≤0,2W%
Length	5-15μm(tipo L); 1-2(tipo S)
Special surface area	40-300 m^2/g
Shells distance	0,8 cm^3/g
Electrical Conductivity	300W/mK
Temperature (º C)	>550 (air) e 3500 (inert atmosphere or vacuum)

5.1.2 Silver chloride (AgCl)

The AgCl used in the present work was supplied by Acros Organics with purity >99% extra pure and Mw = 143.82 AgCl.

5.1.3 Tungsten oxide (WO_3)

The WO_3 (Tungsten(VI) oxide), CAS number 1314-35-8, used in the present work was purchased from Fluka with purity >99,99%.

5.1.4 Triton X 450

The Octylphenol Ethoxylate (nonionic surfactant) dispersant Triton X405 4-$(C_8H_{17})C_6H_4(OCH_2CH_2)_nOH$ was supplied by DOW with pH 7.

5.1.5 Polyacrylic acid sodium salt

Polyacrylic acid sodium salt $(C_3H_3NaO_2)_n$ used as dispersant was retrieved from commercial nappies.

5.1.6 Nitric acid sodium salt

Nitric acid used to oxidize the MWCNT was purchased from Acros Organics with purity > 99 %.

5.1.7 Titanium oxide (TiO_2)

The titanium oxide (TiO_2), was purchases from Degussa. P25 TiO_2 is mostly in the form of anatase and has a BET surface area of 50m^2/g, corresponding to a mean particle size of 30 nm.

5.2 General sample preparation

5.2.1 Composition of structural cement mortars

Sets of samples were prepared according to the European standard EN12004 (2004) under 55% relative humidity at 23 ºC.

A commercial general cement mortar composition was used (See Table 5.2).

Table 5.2 - Typical structural cement mortar composition.

Wt.%	Component	Term used
~15	Ordinary Portland cement	Cement
~10	Calcium Carbonate	Carbonate
~ 75	Silica	Silica
~1%	Additives	Additives

5.2.2 Decorative Mortars

Sets of samples were prepared according to the European standard EN12004 under 55% relative humidity at 23 ºC.

A commercial mortar composition was used (See Table 5.3).

Table 5. 3 - Typical composition of the decorative mortars.

Wt.%	Component	Term used
~ 7	Acrylic-styrene resin	Resin
~ 50	Calcium Carbonate	Carbonate
~ 25	Quartz - Silica	Silica
~1	Additives	Additives

5.2.3 Dispersion of the CNT

CNT were added to a beaker containing 100 ml of deionised water. The mixture was stirred for 15 minutes. Two drops of Triton X405 (nonionic surfactant) dispersant were added to the mixture which was kept stirring for 10 minutes more (See Fig 5.1).

Fig. 5.1 – Dispersion of CNT in water.

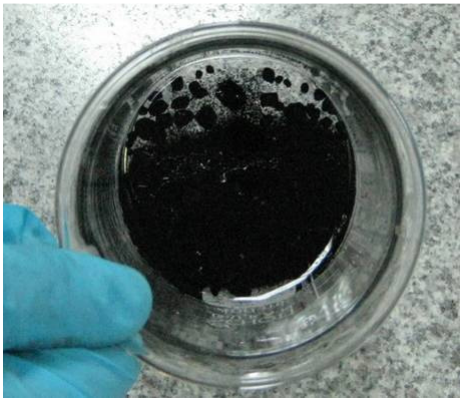

Fig. 5.2 - Presence of bundles after dispersion with or without triton dispersant.

The presence of bundles was observed after the dispersion of CNT due to its hydrophobicity (Fig. 5.2).

5.2.4 Cement paste preparation and moulding

One kilogram of cement was weighted. CNT suspension was transferred into an open plastic container (Fig 5.3) and additional water (the concentration may vary according to the sample, normally 80 to 90 ml ~ 8 to 9%) was used to wash the beaker. The cement was added to the container to form a cement paste (Fig 5.4) and then it was stirred by hand till the CNT were homogeneously dispersed (about 2 min).

A rotary mixer with a flat beater (Fig. 5.5) was used for mixing the paste for 30 s at 62 RPM. The CNT paste was manually mixed for 2 more minutes. The mixture was left resting for 10 minutes. In all the pastes prepared the formation of bundles of CNT was noticed. Additional manual mixture was tried to reduce these aggregates but did not bring any improvements.

After this step, the density and workability of the cement paste were evaluated to decide **i**f water was necessary. The specimens were prepared using a mould of silicon (See Fig 5.7).

Fig. 5.3 - Mixture (water + CNT + dispersant) addition to an open plastic container.

Fig. 5.4 – Bundles of CNT present in the cement paste.

Fig. 5.5 - Rotary mixer with a flat beater.

Fig. 5. 6 – Cement paste ready for use, with some CNT bundles.

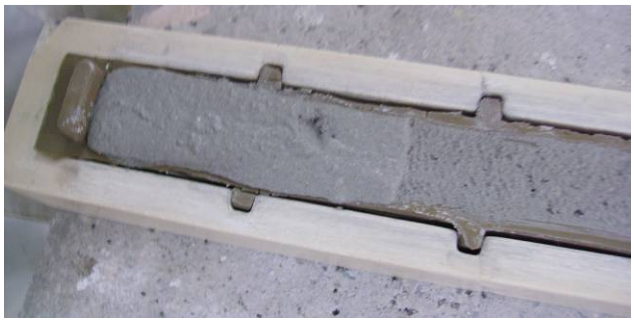

Fig. 5.7 – Moulding of specimen.

5.2.5 Dispersion of MWCNT using poly(acrylic acid)

Poly(acrylic acid) was used in order to improve the dispersion of MWCNT. When the stirring was stopped, the CNT decanted and aggregates were formed. This polymer became a gel when in contact with water with the MWCNT were homogeneously dispersed inside it. Figs. 5.9 and 5.10 show pictures of this process.

Fig. 5.8 - mechanical mixing machine.

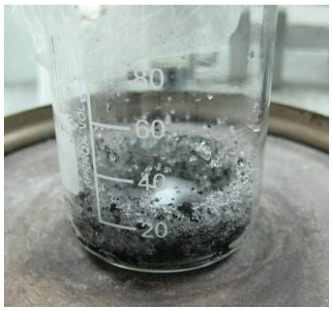

Fig. 5.9 - Addition of poly(acrylic acid) to CNT suspension.

Fig. 5.10 – Poly(acrylic acid) gel with CNT dispersed.

5.2.6 Dispersion of MWCNT in a suspension with titanium oxide

Typically the dispersion of MWCNT in a TiO_2 suspension involved the fallowing sequence of steps:

(i) addition of 1 g TiO_2 to a beaker containing 100 grams of deionised water;

(ii) Magnetic stirring for 10 minutes;

(iii) addition of 1 g of MWCNT

(iv) sonication for 10 minutes in a ultrasound both;

(v) Magnetic stirring of the suspension for 10 hours.

After 90 minutes it was possible to see a good dispersion of the MWCNT.

5.2.7 Milling of Photochromic lenses

The lenses were ground manually using first a hammer to break them in small parts. After that, the material was milled using a "ball mill" with 50% of the volume of balls for 1 hour until a uniform powder was obtained. The average particle size was 1100 and 1280 μm.

5.3 Methods and characterisation

5.3.1 Solubility Tests

This test was carried out to asses the polarity of the neat and functionalised nanotubes. For this purpose a small quantity of CNT was introduced into vials and water was added. Each vial was sonicated for 5 minutes and left standing for 30 minutes before been visually analysed.

5.3.2 Scanning Electron Microscopy

A FEG-SEM Hitach 4100S scanning electron microscope (SEM) equipped with an energy-dispersive X-ray analyzer (EDS RONTEC) was used for the surface investigation. Samples were prepared in two ways: (i) a piece of cement mortar was ground and (ii) a piece of cement mortar was broken to analyze the surface of the cement mortar. All samples were covered by a thin carbon layer.

5.3.3 Compression Testing/ Bending Test

The compression and bend tests were performed in a Universal tensile tester CONTROLS model 65-L1860. The speed of applied deformation was 3 mm/min (according to EN 1015-11:1999/A1) using a 5 KN force transducer at room temperature. The strain was recorded by a position encoder.

5.3.4 Colorimetry Analysis

The analyses of colorimetry were conducted using a MINOLTA Instruments model CR-10. The measurements were made 3 times at a different place in the same specimen for the parameters a, b and L. An average value for 3 measurements was made which were compared to those of a standard specimen. The measurements were carried out in a curing room under a fluorescent lamp considered as standard (Fig. 5.11).

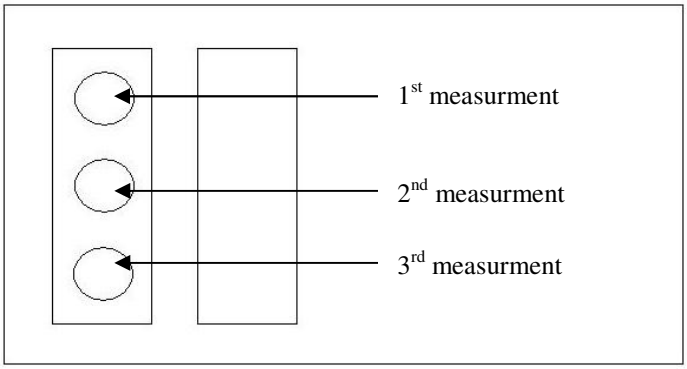

Fig. 5.11 – Place where the colorimetry measurements were realized

5.3.5 Modulus of Elasticity Test

The modulus of elasticity was determined in an equipment consisting of:

(i) function generator Good Will Instruments model GFG-8019-G,

(ii) electromagnetic vibrator model LING DYNAMICS SYSTEM model V-201 with frequencies between 5-1300 Hz,

(iii) Amplifier Dytran Instruments model 4102,

(iv) Osciloscope Hameg model 203-7.

5.3.6 Capillarity Test

The capillarity test was performed in an homemade equipment consisting of a plastic container with dimensions of 330 x 330 x 5,3150 which was kept in a curing room at 23º C ± 2ºC. Zinc sulphate solution (1500 g/l of water) was added 24 hours before the test to keep the humidity of the container high (90 % ± 5%). The amount of zinc sulphate was sufficient to cover 1 cm of the height of the container walls (See Fig. 5.12). Inside the higher container, small containers were put, each one containing its own sponge (made of polyurethane) covered by water at a height of 5 mm (See Fig. 5.13). The samples were previously lightly embedded with water and weighted. After 10 and 90 minutes, the specimens were withdrawn from the container, mopped with a dry paper and weighted. The result is the difference between the initial and final weight expressed in $g/dm^2.min^{-1/2}$.

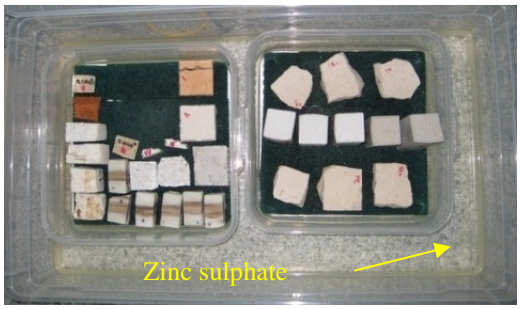

Fig. 5.12 - Plastic container with zinc sulphate solution and 2 small containers where the specimens were placed.

Fig. 5.13 - Specimens on the sponge embedded with water inside the small container.

5.4 Surface modification of MWCNT (oxidation)

The MWCNT were treated with nitric acid. The suspension was first sonicated for 35 minutes at 40 ºC using an ultrasound bath, and then heated under reflux for 4 hours (80 ºC) under nitrogen atmosphere. After the oxidation the reaction mixture was neutralised. The sample was divided in two batches. NaOH 2M was added carefully added to the mixture (about 3 ml each time) using an ice bath until pH 5. (See Fig. 5.15). The excess solution was removed trough decantation. The solids were dispersed in water and filtered. This was repeated several times up to pH 7. (See Fig. 5.16). The resultant “pulp” was dried for 24h in an oven at 100 ºC.

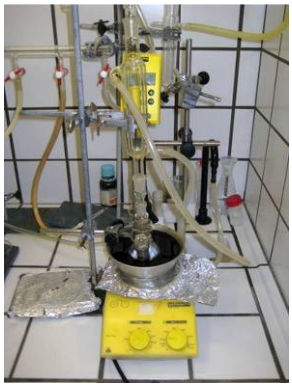

Fig. 5.14 - Oxidation process of the MWCNT on oil bath at 40 ºC for 35 min.

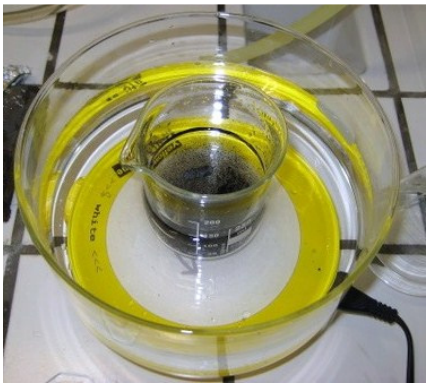

Fig. 5.15 - Neutralisation process of the MWCNT under continuous stirring.

Fig. 5.16 - Filtration of the MWCNT under vacuum before drying.

Chapter 6 – References

[1] Li, G. Y., Wang,P. M., Zhao, X. (2007). "Pressure-sensitive properties and microstructure of carbon nanotube reinforced cement composites." Cement and Concrete Composites 29(5): 377-382.

[2] Li, G. Y., Wang, P. M., Zhao, X. (2005). "Mechanical behavior and microstructure of cement composites incorporating surface-treated multi-walled carbon nanotubes." Carbon 43(6): 1239-1245.

[3] Nanoarchitecture.net. Retrieved on November, 26 2007 – from http://www.cement.org/basics/concretebasics_history.asp

[4] Maggos, T., Plassais A., Bartzis, J. G., Vasilakos, C., Moussiopoulos, N. Bonafous, L. (2008). "Photocatalytic degradation of NOx in a pilot street canyon configuration using TiO_2-mortar panels." Environmental Monitoring and Assessment 136(1-3): 35-44.

[5] Yuranova, T., Sarria V., Jardim, W., Rengifo, J., Pulgarin, C., Trabesinger, G., Kiwi, J., (2007). "Photocatalytic discoloration of organic materials on outdoor building cement panels modified by photoactive coatings." Journal of Photochemistry and Photobiology a-Chemistry 188(2-3): 334-341.

[6] Retrieved on September, 13 2007 – from http://www2.unine.ch/webdav/site/surfchem/shared/documents/swdc.pdf

[7] National Research Council Canada. Retrieved on January, 22 2008 – from http://irc.nrc-cnrc.gc.ca/pubs/fulltext/nrcc46618/

[8] Elsen, J. (2006). "Microscopy of historic mortars - a review." Cement and Concrete Research 36(8): 1416-1424.

[9] Hendry, E. A. W. (2001). "Masonry walls: materials and construction." Construction and Building Materials 15(8): 323-330.

[10] Kanagaraj, S., Varanda F. R., Zhil'tsova, T. V., Oliveira, M. S. A., Simoes, J. A. O., (2007). "Mechanical properties of high density polyethylene/carbon nanotube composites." Composites Science and Technology 67(15-16): 3071-3077.

[11] Prato, M., Tasis, D., Tagmatarchis, N., Georgakilas, V., , (2003). "Soluble carbon nanotubes." Chemistry-a European Journal 9(17): 4001-4008.

[12] Banerjee, S., M. G. C. Kahn, Wong, S. S., (2003). "Rational chemical strategies for carbon nanotube functionalization." Chemistry-a European Journal 9(9): 1899-1908.

[13] Bahr, J. L. & Tour, J. M. (2002). "Covalent chemistry of single-wall carbon nanotubes." Journal of Materials Chemistry 12(7): 1952-1958.

[14] Shaffer, M. S. P. & Koziol, K. (2002). "Polystyrene grafted multi-walled carbon nanotubes." Chemical Communications(18): 2074-2075.

[15] Holzinger, M., Vostrowsky, O., Hirsch, A., Hennrich, F., Kappes, M., Weiss, R., Jellen, F., (2001). "Sidewall functionalization of carbon nanotubes." Angewandte Chemie-International Edition 40(21): 4002.

[16] Yan, X. B., Tay, B. K., Yang, Y., (2006). "Dispersing and functionalizing multiwalled carbon nanotubes in TiO_2 sol." Journal of Physical Chemistry B 110(51): 25844-25849.

[17] Seo, J. W., Couteau, E., Umek, P., Hernadi, K., Marcoux, P., Lukic, B., Miko, C., Milas, M., Gaal, R., Forro, L. (2003). "Synthesis and manipulation of carbon nanotubes." New Journal of Physics 5.

[18] Retrieved on October, 15 2007 – from http://en.wikipedia.org/wiki/Carbon_nanotube

[19] Bayer, Retrieved on August, 12 2007 – from http://www.research.bayer.com/edition_17/Nanotubes.aspx

[20] Springer Handbook of Nanotechnology. Bhushan, Bharat (Ed.) 2nd rev. and extended ed., 2007, XLIV, 1916 p. 1593 illus. in color.

[21] Retrieved on August, 13 2007 – from http://www.rpi.edu/dept/phys/ScIT/FutureTechnologies/nano/images/nanocutoways.jpg

[22] Retrieved on April 22 2008 – from http://www.ks.uiuc.edu/Research/nanotube/lattice_combine.jpg

[23] Minerals commodity summary - cement - 2007 (2007-06-01). Retrieved on 2008-01-16.

[24] de Ibarra, Y. S., Gaitero, J. J., Erkizia, E., Campillo, I., (2006). "Atomic force microscopy and nanoindentation of cement pastes with nanotube dispersions." Physica Status Solidi a-Applications and Materials Science 203(6): 1076-1081.

[25] Marrs, B., Andrews, R., Rantell, T., Pienkowski, D., (2006). "Augmentation of acrylic bone cement with multiwall carbon nanotubes." Journal of Biomedical Materials Research Part A 77A(2): 269-276.

[26] Tucks, A. & Beck, H. P. (2005). "The photochromic effect of bismuth vanadate pigments. Part I: Synthesis, characterization and lightfastness of pigment coatings." Journal of Solid State Chemistry 178(4): 1145-1156.

[27] Tucks, A. & Beck, H. P. (2007). "The photochromic effect of bismuth vanadate pigments: Investigations on the photochromic mechanism." Dyes and Pigments 72(2): 163-177.

[28] Pathan, H. M., Min, S. K., Jung, K. D., Joo, O. S., (2006). "Electrosynthesis of molybdenum oxide thin films onto stainless substrates." Electrochemistry Communications 8(2): 273-278.

[29] Okumu, J., Koerfer, F., Salinga, C., Pedersen, T. P., Wuttig, M., (2006). "Gasochromic switching of reactively sputtered molybdenumoxide films: A correlation between film properties and deposition pressure." Thin Solid Films 515(4): 1327-1333.

[30] Cui, L. F., Li, D. M., Wu, J. F., Cui, X. B., Wang, T. G., Xu, J. Q., (2006). "Synthesis, structural determination and photochromism characterization of two

complexes with [$MO_2(O_2CCOPh_2)(2)$](2-) cores [M = Mo or W]." Journal of Molecular Structure 797(1-3): 34-39.

[31] Mohamed, S. H. & Venkataraj S. (2007). "Thermal stability of amorphous molybdenum trioxide films prepared at different oxygen partial pressures by reactive DC magnetron sputtering." Vacuum 81(5): 636-643.

[32] Yao, J. N., Yang Y. A., Loo, B. H. (1998). "Enhancement of photochromism and electrochromism in MoO3/Au and MoO3/Pt thin films." Journal of Physical Chemistry B 102(11): 1856-1860.

[33] Katayama, S., Yamada, N., Kikuta, K., Awano, M. (2006). "Synthesis and photochromism of organosiloxane-based organic/inorganic hybrid containing an inorganic component derived from tungstic acid." Journal of the Ceramic Society of Japan 114(1325): 114-119.

[34] Wang, S. J., Cheng, G., Jiang, X. H., Li, Y. C., Huang, Y. B., Du, Z. L. (2006). "Direct observation of photoinduced charge redistribution of WO_3-TiO_2 double layer nanocomposite films by photoassisted Kelvin force microscopy." Applied Physics Letters 88(21).

[35] Wang, S. T., Feng, X. J., Yao, J. N., Jiang, L. (2006). "Controlling wettability and photochromism in a dual-responsive tungsten oxide film." Angewandte Chemie-International Edition 45(8): 1264-1267.

[36] Galvão, J. R. & Scarminio J. (2003). "Fotocromismo em filmes finos de óxidos de tungstênio de diferentes composições." Química Nova 26: 488-492.

[37] Poirier, G., Nalin, M., Cescato, L., Messaddeq, Y., Ribeiro, S. J. L. (2006). "Bulk photochromism in a tungstate-phosphate glass: A new optical memory material?" Journal of Chemical Physics 125(16).

[38] He, T. & Yao, J. N. (2007). "Photochromic materials based on tungsten oxide." Journal of Materials Chemistry 17(43): 4547-4557.

[39] dos Santos, P. V., Carvalho, J. F., Frejlich, J. (2007). "Photochromism, bleaching and photorefractive recording in undoped $Bi_{12}TiO_{20}$ crystals in the visible and near infrared wavelength range." Optical Materials 29(5): 462-467.

[40] Goliath business knowledge on demand: Retrieved on March, 13 2007 – from http://goliath.ecnext.com/coms2/gi_0199-3767300/Photochromic-effects-Hans-Elzbieta-Brand.html

[41] Nogueira, H. I. S., Cavaleiro, A. M. V., Rocha, J., Trindade, T., de Jesus, J. D. P. (2004). "Synthesis and characterization of tungsten trioxide powders prepared from tungstic acids." Materials Research Bulletin 39(4-5): 683-693.

[42] He, T., Ma, Y., Cao, Y., Liu, H. M., Yang, W. S., Yao, J. N. (2004). "Comparison between the effects of TiO2 synthesized by photoassisted and conventional sol-gel methods on the photochromism of WO_3 colloids." Journal of Colloid and Interface Science 279(1): 117-123.

[43] Seitz, F. (1951). "Speculations on the properties of the silver halide crystals." Reviews of Modern Physics 23(4): 328-352.

[44] Shalem, S., German, A., Barkay, N., Moser, F., Katzir, A. (1997). "Mechanical and optical properties of silver-halide infrared transmitting fibers." Fiber and Integrated Optics 16(1): 27-54.

[45] Xu, G., Guo, G. C., Wang, M. S., Zhang, Z. J., Chen, W. T., Huang, J. S. (2007). "Photochromism of a methyl viologen bismuth(III) chloride: Structural variation before and after UV irradiation." Angewandte Chemie-International Edition 46(18): 3249-3251.

[46] Wei, M., Xu, X. Y., Wang, X. R., Li, F., Zhang, H., Lu, Y. L., Pu, M., Evans, D. G. Duan, X. (2006). "Study on the photochromism of Ni-Al layered double hydroxides containing nitrate anions." European Journal of Inorganic Chemistry(14): 2831-2838.

[47] Xu, B. B., Xu, L., Gao, G. G., Jin, Y. N. (2007). "Nanosized multilayer films with concurrent photochromism and electrochromism based on Dawson-type polyoxometalate." Applied Surface Science 253(6): 3190-3195.

[48] Gavrilyuk, A. I. & Lanskaya, T. G. (2006). "Photochromism in $RbAg_4I_5$ thin films enhanced by hydrogen photosensitization simultaneous to illumination." Thin Solid Films 515(4): 2337-2341.

[49] Pang, Y. H., Pang, Y. H., Feng, W., Chen, J., Liu, Y., Cai, W. M. (2007). "Controlled microstructure and photochromism of inorganic-organic thin films by ultrasound." Journal of Materials Science & Technology 23(4): 477-480.

[50] Tatsuma, T. & Suzuki, K. (2007). "Photoelectrochromic cell with a Ag-TiO_2 nanocomposite: Concepts of drawing and display modes." Electrochemistry Communications 9(4): 574-576.

[51] He, T. & Yao, J. N. (2006). "Photochromism in composite and hybrid materials based on transition-metal oxides and polyoxometalates." Progress in Materials Science 51(6): 810-879.

[52] Dachraoui, H., Rupp, R. A., Lengyel, K., Ellabban, M. A., Fally, M., Corradi, G., Kovacs, L., Ackermann, L. (2006). "Photochromism of doped terbium gallium garnet." Physical Review B 74(14).

[53] Liang, Z., Liu, Z. L., Jiang, L., Gao, Y. H. (2007). "A new fluorescent chemosensor for copper(II) and molecular switch controlled by light." Tetrahedron Letters 48(9): 1629-1632.

[54] Shimamoto, N., Ohkoshi, S., Sato, O., Hashimoto, K. (2000). "Photochromic behavior based on spin transition on a cobalt-iron polycyanide." Molecular Crystals and Liquid Crystals 344: 95.

[55] Caseri, W. R. (2006). "Nanocomposites of polymers and inorganic particles: preparation, structure and properties." Materials Science and Technology 22(7): 807-817.

[56] Grofcsik, A., Baranyai, P., Bitter, I., Grün, A., Köszegi, É., Kubinyi, M., Pál, K., Vidóczy, T. (2002). "Photochromism of a spiropyran derivative of 1,3-calix[4]crown-5." Journal of Molecular Structure 614(1-3): 69-73.

[57] Retrieved on November, 25 2007 – from http://www.weizmann.ac.il/ICS/booklet/17/pdf/abstracts.pdf

[58] Chemeurope Retrieved on November, 25 2007 – from: http://www.chemeurope.com/lexikon/e/Photochromism

[59] Beni, A., Carbonera, C., Dei, A., Letard, J. F., Righini, R., Sangregorio, C., Sorace, L. (2006). "Optically induced valence tautomeric interconversion in cobalt dioxolene complexes." Journal of the Brazilian Chemical Society 17(8): 1522-1533.

[60] Berthet, J., Micheau, J. C., Lokshin, V., Vales, M., Samat, A., Vermeersch, G., Delbaere, S. (2007). "Photoreversible cyclisation of a 3-(2-benzylbenzoyl)-quinolinone: A highly efficient photochromic compound." Journal of Photochemistry and Photobiology a-Chemistry 187(2-3): 269-274.

[61] Born, R., Fischer, W., Heger, D., Tokarczyk, B., Wirz, J. (2007). "Photochromism of phenoxynaphthacenequinones: diabatic or adiabatic phenyl group transfer?" Photochemical & Photobiological Sciences 6(5): 552-559.

[62] Choi, D. H., Ban, S. Y, Kim, J. H. (2003). "Stability of photochromism in new bifunctional copolymers containing spiropyran and chalcone moiety in the side chain." Bulletin of the Korean Chemical Society 24(4): 441-445.

[63] Coelho, P. J. (2006). "Estudo do comportamento fotocrómico de um naftopirano: uma experiência simples ilustrativa do fotocromismo." Química Nova 29: 607-610.

[64] Coue, V., Dessapt, R., Bujoli-Doeuff, M., Evain, M., Jobic, S. (2006). "Synthesis and characterization of two new photochromic organic-inorganic hybrid materials based on isopolyoxomolybdate: (HDBU)(3)(NH4)[beta-Mo8O26] center dot H2O and (HDBU)(4)[delta-Mo8O26]." Journal of Solid State Chemistry 179(12): 3615-3627.

[65] Fridman, N., Kaftory, M., Eichen, Y., Speiser, S. (2007). "Spectroscopy, photophysical and photochemical properties of bisimidazole derivatives." Journal of Photochemistry and Photobiology a-Chemistry 188(1): 25-33.

[66] Fukaminato, T., Umemoto, T., Iwata, Y., Yokojima, S., Yoneyama, M., Nakamura, S., Irie, M. (2007). "Photochromism of diarylethene single molecules in polymer matrices." Journal of the American Chemical Society 129(18): 5932-5938.

[67] Fukuda, H., Amimoto, K., Koyama, H., Kawato, T. (2003). "Crystalline photochromism of N-salicylidene-2,6-dialkylanilines: advantage of 2,6-dialkyl substituents of aniline for preparation of photochromic Schiff base crystals." Organic & Biomolecular Chemistry 1(9): 1578-1583.

[68] Gorodetsky, B. & Branda, N. R. (2007). "Bidirectional ring-opening and ring-closing of cationic 1,2-dithienylcyclopentene molecular switches triggered with light or electricity." Advanced Functional Materials 17(5): 786-796.

[69] Irie, M., Sakemura, K., Okinaka, M., Uchida, K. (1995). "Photochromism of dithienylethenes with electron-donating substituents." Journal of Organic Chemistry 60(25): 8305-8309.

[70] Jimenez, A., Pinheiro, C., Parola, A. J., Maestri, M., Pina, F. (2007). "The chemistry of 6-hydroxyflavylium: zwitterionic base and p-quinoidal chalcones. A multiswitchable system operated by proton, electron and photon inputs." Photochemical & Photobiological Sciences 6(4): 372-380.

[71] Kuhni, J. & Belser, P. (2007). "Gated photochromism of 1,2-diarylethenes." Organic Letters 9(10): 1915-1918.

[72] Li, Y. L., He, B., Zhang, J. L. (2007). "Synthesis and photochromic properties of 9-(4-substituted)phenoxy-naphthaceno[5,6-bc]pyran-2,8-diones derived from phenoxynaphthacenequinones." Dyes and Pigments 75(1): 111-115.

[73] Matsubara, Watanabe, M., Takeoka, Y. (2007). "A thermally adjustable multicolor photochromic hydrogel." Angewandte Chemie-International Edition 46(10): 1688-1692.

[74] Moorthy, J. N., Venkatakrishnan, P., Samanta, S. (2007). "Novel photochromism of differently-linked bis-benzopyrans." Organic & Biomolecular Chemistry 5(9): 1354-1357.

[75] Ortica, F., Smimmo, P., Zuccaccia, C., Mazzucato, U., Favaro, G., Impagnatiello, N., Heynderickx, A., Moustrou, C. (2007). "Photobehaviour of diarylethenes with thiophenes as aryl groups and dithiole-2-thione and dithiole-2-one at the ethenic bond." Journal of Photochemistry and Photobiology a-Chemistry 188(1): 90-97.

[76] Pina, F., Parola, A. J., Melo, M. J., Laia, C. A. T., Afonso, C. A. M. (2007). "Photochromism of 7-(N, N-diethylamino) 4 '-hydroxyflavylium in a water-ionic liquid biphasic system." Chemical Communications(16): 1608-1610.

[77] Pu, S. Z., Liu, G., Shen, L., Xu, J. K. (2007). "Efficient synthesis and properties of isomeric photochromic diarylethenes having a pyrrole unit." Organic Letters 9(11): 2139-2142.

[78] Sobolewski, A. L. & Domcke, W. (2007). "Photophysics of eumelanin: Ab initio studies on the electronic spectroscopy and photochemistry of 5,6-dihydroxyindole." Chemphyschem 8(5): 756-762.

[79] Sriprom, W., Neel, M., Gabbutt, C. D., Heron, B. M., Perrier, S. (2007). "Tuning the color switching of naphthopyrans via the control of polymeric architectures." Journal of Materials Chemistry 17(19): 1885-1893.

[80] Takami, S. & Irie, M. (2007). "Photochromic properties of diarylethenes having 2,4-diphenylphenyl substituents in the amorphous and PMMA films." Journal of Photochemistry and Photobiology a-Chemistry 187(2-3): 202-208.

[81] Takami, S., Kuroki, L., Irie, M. (2007). "Photochromism of mixed crystals containing bisthienyl-, bisthiazolyl-, and bisoxazolylethene derivatives." Journal of the American Chemical Society 129(23): 7319-7326.

[82] Takeshita, M., Tanaka, A., Hatanaka, T.. (2007). "Photoreversible refractive index change of [2.2]metacyclophan-1-ene in PMMA film." Optical Materials 29(5): 499-502.

[83] Tan, T. F. (2007). "Crystal structure and photochromism in paint of 1,3,3-trimethyl-6 '-dihydro-indolinyl-spiro[2,3 '-[3H]-naphtho[2,1-b] [1,4]]oxazine." Chinese Journal of Structural Chemistry 26(5): 572-574.

[84] Yamada, S., Ishii, E., Konno, T., Ishihara, T. (2007). "Reaction of perfluorocyclopentene with various carbon nucleophiles - heteroaromatic lithium reagents, enolate and phosphonium ylide." Organic & Biomolecular Chemistry 5(9): 1442-1449.

[85] Yildiz, I. & Raymo, F. M. (2006). "Photochromic nanocomposites of bipyridinium dications and semiconductor quantum dots." Journal of Materials Chemistry 16(12): 1118-1120.

[86] Zhao, W. L. & Carreira, E. M. (2007). "Oligothiophene-linked bisnaphthopyrans: Sequential and temperature-dependent photochromism." Chemistry-a European Journal 13(9): 2671-2685.

[87] Nature Materials. 2005, 4, 249-253; Macromolecules, 2006, 39, 1391-1396; Australian Journal of Chemistry, 2005, 58, 825-830.

[88] Wikipedia: Retrieved on November, 26 2007 – from http://en.wikipedia.org/wiki/Photochromism

[89] Ohno, Yoshi (Oct. 16-20 2000). "CIE Fundamentals for Color Measurements" in *IS&T NIP16 Conference*. *Vancouver, Canada*: 540-545.

[90] Wikipedia. Retrieved on November, 26 2007 –from http://en.wikipedia.org/wiki/Tristimulus#Tristimulus_values

[91] Cielab. Retrieved on November, 25 2007 – 20:15hs from: http://www.fho-emden.de/~hoffmann/cielab03022003.pdf

[92] Photo oxidation: Retrieved on November, 26 2007 – from http://library.kcc.hawaii.edu/external/chemistry/everyday_photo_oxid.html

[93] He, Y. P., Z. Y. Wu, Fu, L. M., Li, C. R., Miao, Y. M., Cao, L., Fan, H. M., Zou, B. S. (2003). "Photochromism and size effect of WO_3 and WO_3-TiO_2 aqueous sol." Chemistry of Materials 15(21): 4039-4045.

[94] An, G. M., Ma, W. H., Sun, Z. Y., Liu, Z. M., Han, B. X., Miao, S. D., Miao, Z. J. Ding, K. L. (2007). "Preparation of titania/carbon nanotube composites using supercritical ethanol and their photocatalytic activity for phenol degradation under visible light irradiation." Carbon 45(9): 1795-1801.

[95] Banerjee, S., Kahn, M. G. C., Wong, S. S. (2003). "Rational chemical strategies for carbon nanotube functionalization." Chemistry-a European Journal 9(9): 1899-1908.

[96] Brock Marrs, Andrews, R., Rantell, T., Pienkowski, D. (2006). "Augmentation of acrylic bone cement with multiwall carbon nanotubes." Journal of Biomedical Materials Research Part A 77A(2): 269-276.

[97] Hart, A. J. & Slocum, A. H. (2006). "Rapid growth and flow-mediated nucleation of millimeter-scale aligned carbon nanotube structures from a thin-film catalyst." Journal of Physical Chemistry B 110(16): 8250-8257.

[98] Hart, A. J. and A. H. Slocum (2006). "Rapid growth and flow-mediated nucleation of millimeter-scale aligned carbon nanotube structures from a thin-film catalyst." Journal of Physical Chemistry B 110(16): 8250-8257.

[99] Kanagaraj, S., Varanda, F. R., Zhil'tsova, T. V., Oliveira, M. S. A., Simoes, J. A. O. (2007). "Mechanical properties of high density polyethylene/carbon nanotube composites." Composites Science and Technology 67(15-16): 3071-3077.

[100] Kumar, M. K., Reddy, A. L. M., Ramaprabhu, S. (2008). "Exfoliated single-walled carbon nanotube-based hydrogen sensor." Sensors and Actuators B-Chemical 130(2): 653-660.

[101] Lee, G. W., Jagannathan, S., Chae, H. G., Minus, M. L., Kumar, S. (2008). "Carbon nanotube dispersion and exfoliation in polypropylene and structure and properties of the resulting composites." Polymer 49(7): 1831-1840.

[102] Luo, D. M., Wang, W. X., Takao, Y. (2007). "Effects of the distribution and geometry of carbon nanotubes on the macroscopic stiffness and microscopic stresses of nanocomposites." Composites Science and Technology 67(14): 2947-2958.

[103] Monthioux, M. & Kuznetsov, V. L. (2006). "Who should be given the credit for the discovery of carbon nanotubes?" Carbon 44(9): 1621-1623.

[104] Nicolosi, V., Cathcart, H., Dalton, A. R., Aherne, D., Dieckmann, G. R., Coleman, J. N. (2008). "Spontaneous exfoliation of single-walled carbon nanotubes dispersed using a designed amphiphilic peptide." Biomacromolecules 9(2): 598-602.

[105] Oh, W. C. & Chen, M. L. (2008). "Synthesis and characterization of CNT/TiO_2 composites thermally derived from MWCNT and titanium(IV) n-butoxide." Bulletin of the Korean Chemical Society 29(1): 159-164.

[106] Oliveira, Nogueira, R. F. P., Gomes Neto, J. A., Jardim, Wilson F., Rohwedder, J. (2001). "Sistema de injeção em fluxo espectrofotométrico para monitorar peróxido de hidrogênio em processo de fotodegradação por reação foto-Fenton." Química Nova 24: 188-190.

[107] Romero, J. G. V., Luengo, C. A., Huber, J. G., Rosolen, J. M. (2002). "Síntese de nanotubos de carbono de parede simples por sublimação de grafite em atmosfera de hélio." Química Nova 25: 59-61.

[108] Seo, J. W., Couteau, E., Umek, P., Hernadi, K., Marcoux, P., Lukic, B., Miko, C., Milas, M., Gaal, R., Forro, L. (2003). "Synthesis and manipulation of carbon nanotubes." New Journal of Physics 5: 120.2-120.22

[109] Shafir, I., Gayer, O., Nagli, L., Shalem, S., Katzir, A. (2007). "Middle-infrared luminescence of Nd ions in silver halide crystals." Journal of Luminescence 126(2): 541-546.

[110] Wansom, S., Kidner, N. J., Woo, L. Y., Mason, T. O. (2006). "AC-impedance response of multi-walled carbon nanotube/cement composites." Cement & Concrete Composites 28(6): 509-519.

[111] Xia, X. H., Jia, Z. H., Yu, Y., Liang, Y., Wang, Z., Ma, L. L. (2007). "Preparation of multi-walled carbon nanotube supported TiO2 and its photocatalytic activity in the reduction of CO_2 with H_2O." Carbon 45(4): 717-721.

[112] Xue, C. H., Shi, M. M., Yan, Q. X., Shao, Z., Gao, Y., Wu, G., Zhang, X. B., Yang, Y., Chen, H. Z., Wang, M. (2008). "Preparation of water-soluble multi-walled carbon nanotubes by polymer dispersant assisted exfoliation." Nanotechnology 19(11).

[113] Armstrong, J. A. & Weller, M. T. (2006). "Structural observation of photochromism." Chemical Communications(10): 1094-1096.

[114] He, T., Ma, Y., Cao, Y., Hu, X., Liu, H., Zhang, G., Yang, W., Yao, J. (2002). "Photochromism of WO_3 colloids combined with TiO_2 nanoparticles." Journal of Physical Chemistry B 106(49): 12670-12676.

[115] He, T. & Yao, J. N. (2007). "Photochromic materials based on tungsten oxide." Journal of Materials Chemistry 17(43): 4547-4557.

[116] Lampert, C. M. (1992). "Smart windows switch on the light." Ieee Circuits and Devices Magazine 8(2): 19-26.

[117] Van Gemert, B. (2000). "The commercialization of plastic photochromic lenses: A tribute to John Crano." Molecular Crystals and Liquid Crystals 344: 57-62.

[118] LQES - Laboratório de Química do Estado Sólido – Instituto de Química – UNICAMP: Retrieved on February, 15 2008 – from http://lqes.iqm.unicamp.br/images/vivencia_lqes_monografias_odair_nanotubos_carbono.pdf

[119] Science Magazzine: Retrieved on February, 15 2008 – from http://www.sciencemag.org/sciext/globalvoices/bai/images/nanotubes.jpg

[120] Springer Handbook of Nanotechnology. Bhushan, Bharat (Ed.) 2nd rev. and extended ed., 2007, XLIV, 1916 p. 1593 illus. in color.

[121] Helland, A., P. Wick, Koehler, A., Schmid, K., Som, C. (2007). "Reviewing the environmental and human health knowledge base of carbon nanotubes." Environmental Health Perspectives 115(8): 1125-1131.

[122] Kohler, A. R. & Som, C. (2008). "Environmental and health implications of nanotechnology - Have innovators learned the lessons from past experiences?" Human and Ecological Risk Assessment 14(3): 512-531.

[123] Helland, A., M. Scheringer, Siegrist, M., Kastenholz, H. G., Wiek, A.,Scholz, R. W (2008). "Risk assessment of engineered nanomaterials: A survey of industrial approaches." Environmental Science & Technology 42(2): 640-646.

[124] O'Brien, N. & Cummins, E. (2008). "Recent developments in nanotechnology and risk assessment strategies for addressing public and environmental health concerns." Human and Ecological Risk Assessment 14(3): 568-592.

[125] The University of Hull - Department of Chemistry: Retrieved on January, 12 2008 – from http://chemistry.hull.ac.uk/lectures/ghm/06547-2006.pdf

[126] Hunt, R. W. (1998). Measuring colour, 3rd edition, Fountain Press, England

[127] Technimind.org: Retrieved on March 3, 2008 – from http://www.techmind.org/colour/

[128] NIST National Institute of Standards and Technology: Retrieved on January, 13 2008 – from http://physics.nist.gov/Divisions/Div844/facilities/photo/Publications/OhnoNIP16-2000.pdf

[129] Wikipedia.org: Retrieved on March 7, 2008 – from http://en.wikipedia.org/wiki/Beam_(structure)

[130] Sriyai, M. Master Thesis, Technische Universität Hamburg-Harburg, Germany (2008).

[131] Ghislandi, M. G., Master Thesis, Technische Universität Hamburg-Harburg, Germany (2007).

[132] howstuffworks.com: Retrieved on March 9, 2008 – from http://static.howstuffworks.com/gif/nanotechnology-6.gif

[133] Wikipedia.org: Retrieved on March 6, 2008 – from http://en.wikipedia.org/wiki/Carbon_nanotubes

[134] Yan, X. B., Tay, B. K., Yang, Y. (2006). "Dispersing and functionalizing multiwalled carbon nanotubes in TiO2 sol." Journal of Physical Chemistry B 110(51): 25844-25849.

[135] Geng, J., Jiang, Z., Wang, Y., Yang, D.(2008). "Carbon-modified TiO_2 nanotubes with enhanced photocatalytic activity synthesized by a facile wet chemistry method." Scripta Materialia 59(3): 352-355.

[136] Wang, W., Serp, P., Kalck, P., Silva, C., Faria, J. (2008). "Preparation and characterization of nanostructured MWCNT-TiO_2 composite materials for photocatalytic water treatment applications." Materials Research Bulletin 43(4): 958-967.

[137] Liu, B. and H. C. Zeng (2008). "Carbon nanotubes supported mesoporous mesocrystals of anatase TiO_2." Chemistry of Materials 20(8): 2711-2718.